TALLINN UNIVERSITY OF TECHNOLOGY
SCHOOL OF ENGINEERING
Department of Electrical Power Engineering and Mechatronics

DEVELOPMENT OF ENERGY MANAGEMENT STRATEGIES TO INCREASE THE ECONOMIC FEASIBILITY OF URBAN MICROGRIDS

ENERGIAHALDUSE STRATEEGIATE ARENDAMINE MIKROVÕRKUDE MAJANDUSLIKU TASUVUSE SUURENDAMISEKS

MASTER'S THESIS

Student: Daniel Stich

Student code: 225246AAAM

Supervisor: Prof. Dr. Sc. Eng. Argo Rosin

Co-supervisor: Prof. Dr.-Ing. Dr. h.c. Helmuth Biechl

Tallinn, 2022

Author's declaration

Hereby I declare, that I have written this thesis independently. No academic degree has been applied for based on this material. All works, major viewpoints and data of the other authors used in this thesis have been referenced.

"......" 2022

Author: ....
            (Signature)

Thesis is in accordance with terms and requirements

"......" 2022

Supervisor: ....
                (Signature)

Accepted for defence

"......" 2022

Chairman of theses defence commission: ....
                                                    (Name and signature)

Non-exclusive licence for publication and reproduction of graduation thesis[1]

I, Daniel Stich, herby

1. grant Tallinn University of Technology (TalTech) a non-exclusive license for my thesis

   "Development of energy management strategies to increase the economic feasibility of urban microgrids",

   supervised by Prof. Dr. Sc. Eng. Argo Rosin,

   1.1 reproduced for the purposes of preservation and electronic publication, incl. to be entered in the digital collection of TalTech library until expiry of the term of copyright;

   1.2 published via the web of TalTech, incl. to be entered in the digital collection of TalTech library until expiry of the term of copyright.

   1.3 I am aware that the author also retains the rights specified in clause 1 of this license.

2. I confirm that granting the non-exclusive license does not infringe third persons' intellectual property rights, the rights arising from the Personal Data Protection Act or rights arising from other legislation.

_____ (date)

---

[1] The non-exclusive licence is not valid during the validity of access restriction indicated in the student's application for restriction on access to the graduation thesis that has been signed by the school's dean, except in case of the university's right to reproduce the thesis for preservation purposes only. If a graduation thesis is based on the joint creative activity of two or more persons and the co-author(s) has/have not granted, by the set deadline, the student defending his/her graduation thesis consent to reproduce and publish the graduation thesis in compliance with clauses 1.1 and 1.2 of the non-exclusive licence, the non-exclusive license shall not be valid for the period

ABSTRACT

Author: Daniel Stich	Type of the work: Master's thesis

Title: Development of energy management strategies to increase the economic feasibility of urban microgrids

Date: 21.12.2022	114 pages

University: Tallinn University of Technology

School: School of Engineering

Department: Department of Electrical Power Engineering and Mechatronics

Supervisor(s) of the thesis: Prof. Dr. Sc. Eng. Argo Rosin, Prof. Dr.-Ing. Dr. h.c. Helmuth Biechl

Consultant(s): Tarmo Korõtko, Freddy Plaum, Vahur Maask

Abstract:

The thesis consists of 114 pages, it contains 46 figures, 27 tables, 6 algorithms, 43 equations and 64 references.

The transition of energy supply from fossil fuels to renewable energies is driven by financial, political, and environmental reasons. Renewable energy sources (RESs) in form of distributed generation (DG) and novel electric vehicle (EV) charging services introduce new challenges to power quality, especially in urban distribution grids. Instead of reinforcing the existing infrastructure along with significant costs, capacity reserves of street lighting systems can be used to deploy a grid-tied microgrid (MG) with energy storage and photovoltaic (PV). Energy management is part of tertiary-level control, responsible for the economic operation of the MG. This thesis proposes three different energy management strategies to increase the economic feasibility of urban MGs. A simulation case study is performed on an Estonian pilot site in the city of Tartu, which involves multiple owners. Component models are developed for the battery energy storage system (BESS), PV and street lighting system. For EV chargers, a measurement-based modelling approach is introduced. Economic feasibility is evaluated based on a peer-to-peer (P2P) trading market and a collective revenue sharing (CRS) market. The first strategy is developed to establish a simple and robust baseline. The second strategy includes decisions based on the market price signal and the third strategy uses an optimisation technique to schedule power setpoints that are dispatched by the controller. Results show that the second strategy increases economic feasibility the most while proving the best EV charging service. Nevertheless, estimations of payback periods (PBPs) unveil that none of the proposed strategies and markets could generate enough profit to make investments attractive.

Keywords: Microgrids, energy management, urban distribution grids, battery energy storage systems, electric vehicles, peer-to-peer trading.

LÕPUTÖÖ LÜHIKOKKUVÕTE (ABSTRACT IN ESTONIAN)

Autor: Daniel Stich	Lõputöö liik: Magistritöö

Töö pealkiri: Energiahalduse strateegiate arendamine mikrovõrkude majandusliku tasuvuse suurendamiseks

Kuupäev: 21.12.2022	114 lk

Ülikool: Tallinna Tehnikaülikool

Teaduskond: Inseneriteaduskond

Instituut: Elektroenergeetika ja mehhatroonika instituut

Töö juhendaja(d): Prof. Dr. Sc. Eng. Argo Rosin, Prof. Dr.-Ing. Dr. h.c. Helmuth Biechl

Töö konsultant (konsultandid): Tarmo Korõtko, Freddy Plaum, Vahur Maask

Sisu kirjeldus:

Lõputöö koosneb 114 lehest ning sisaldab 46 joonist, 27 tabelit, 6 algoritmi, 43 võrrandit ja 64 viited.

Energiavarustuse üleminekut fossiilsetelt kütustelt taastuvenergiale ajendavad rahalised, poliitilised ja keskkonnaalased põhjused. Taastuvate energiaallikate hajutatud tootmise ja uute elektrisõidukite (EV) laadimisteenuste näol tekivad uudsed probleemid elektrienergia kvaliteedis, eriti linnade jaotusvõrkudes. Teine strateegia seisneb reeglipõhises juhtimis vastavalt päev ette elektri turuhindadele. Kolmas strateegia loob mikrovõrgu seadmete optimeeritud juhtimisplaani kasutades optimeerimise algoritmi koos päev ette (PV) tootmise ennustusega. Energiahaldus on osa kolmanda tasandi juhtimisest, mis vastutab mikrovõrgu majandusliku toimimise eest. Käesolevas lõputöös pakutakse välja kolm erinevat energiahaldusstrateegiat, et suurendada linnas asuvate mikrovõrkude majanduslikku tasuvust. Simulatsioonil põhinev uuring viiakse läbi Tartu linnas oleva pilootprojekti alusel, mis hõlmab mitut omanikku. Komponentide mudelid töötati välja aku energiasalvestussüsteemi, PV ja tänavavalgustussüsteemi jaoks. EV-laadiate puhul kasutati mõõtmistel põhinevat modelleerimist. Majanduslikku tasuvust hinnati vastastikuse kauplemise (*peer-to-peer*, P2P) turu ja ühise tulude jagamise turu (*collective revenue sharing*, CRS) alusel. Esimene strateegia töötati välja lihtsa ja usaldusväärse baasstsenaariumi saamiseks. Teine strateegia seisneb reeglipõhises juhtimis vastavalt päev ette elektri turuhindadele. Kolmas strateegia loob mikrovõrgu seadmete optimeeritud juhtimisplaani kasutades optimeerimise algoritmi koos päev ette PV tootmise ennustusega. Kasumi analüüs näitab, et teine strateegia on majanduslikult kõige tasuvam, pakkudes samaaegselt parimat EV laadimisteenust. Tasuvusaegade analüüs näitas, et ükski pakutud strateegiatest ja turgudest ei tooda piisavalt kasumit, et investeerimine oleks atraktiivne.

Märksõnad: Mikrovõrgud, energiahalduse, linnade jaotusvõrgud, akuenergiasalvestid, elektrisõidukid, peer-to-peer kauplemine.

THESIS TASK

Thesis title:	**Development of energy management strategies to increase the economic feasibility of urban microgrids**
Student:	**Daniel Stich, 225246AAAM**
Programme:	**Energy Conversion and Control Systems**
Type of work:	**Master's thesis**
Supervisor of the thesis:	**Prof. Dr. Sc. Eng. Argo Rosin**
Co-supervisor of the thesis:	**Prof. Dr.-Ing. Dr. h.c. Helmuth Biechl**
(company, position and contact)	**University of Applied Sciences Kempten, Head of Programme Electrical Engineering, biechl@hs-kempten.de**
Validity period of the thesis task:	**2022/2023 – 2022/2023 Autumn**
Submission deadline of the thesis:	**21.12.2022**

_____	_____	_____
Supervisor (signature)	Student (signature)	Head of programme (signature)

_____
Co-supervisor (signature)

1. Reasons for choosing the topic

Cities are anticipating increased supply requirements for electricity distribution infrastructure due to the rising popularity of electric vehicles (EVs). Connection capacity is a major barrier to the provision of novel e-mobility services. Increasing connection points usually goes hand in hand with additional costs. While renewable energy sources (RESs) like photovoltaic (PV) deployed as distributed generation (DG) can support the distribution grid and the environmentally friendly integration of EV charging, their stochastic nature introduces new challenges. Disruptions and outages due to power quality can lead to significant economic losses. Microgrids (MGs) with energy storage systems (ESSs) pose an alternative to costly infrastructure enhancements. One of the key features of MG control is energy management. Apart from increasing the power supply reliability, it can provide an economically beneficial way of operating the distribution grid. This, in turn, helps such MGs find favour, which makes them attractive in other locations, where they can help to further reduce costs.

This thesis will contribute to the FinEst project "Reducing energy supply requirements using microgrids and energy storage" at TalTech and to the existing research in the field of microgrid modelling and control.

2. Thesis objective

The aim of this thesis is to develop energy management strategies for urban microgrids with the intention of increasing their economic feasibility.

3. List of sub-questions:

- How can MGs be classified in general?
- What role does energy management play in hierarchical MG control?
- Which models of what MG components are required to simulate energy management strategies for the pilot site?
- What are possible market models for energy trading in multi-ownership MGs?
- How should battery storage and EV chargers be controlled to increase the economic feasibility of urban MGs?
- Which of the developed energy management strategies increases MG's economic feasibility the most?

4. Basic data:

- PV generation data from photovoltaic geographical information system (PVGIS)
- On-site power consumption metering data of street lighting system
- Power consumption metering data of an EV fast charger
- Charging characteristics from an online EV database
- Datasheets and manuals from manufacturers
- Data from project reports

5. Research methods

The research of this work is based on the analysis of literature and simulations. The models are developed in Matlab/Simulink. Model data is obtained from databases, measurements, literature and datasheets. Simulation scenarios are defined and simulation results are analysed and evaluated according to the thesis objective.

6. Graphical material

Graphical materials like explanatory drawings, schematics and tables are used in the theoretical part. The practical part includes also data plots, pseudo code, charts and comprehensive schematics. Appendices list figures and tables of detailed simulation data.

7. Thesis structure

Introduction

1 State of the art analysis

2 Modelling of microgrid

3 Development of business models

4 Development of energy management strategies

5 Discussion on simulation results

Summary

8. References

Types of sources used in this thesis are books, research papers, websites, newspaper articles, project reports, datasheets, etc. Some examples are listed below.

M. A. Hossain *et al.*, "Evolution of microgrids with converter-interfaced generations: Challenges and opportunities", *International Journal of Electrical Power & Energy Systems*, vol. 109, pp. 160–186, 2019, ISSN: 01420615. DOI: *10.1016/j.ijepes.2019.01.038*

Y. Zhou and C. Ngai-Man Ho, "A review on Microgrid architectures and control methods", in *2016 IEEE 8th International Power Electronics and Motion Control Conference (IPEMC-ECCE Asia)*, (Hefei, China), IEEE, 2016, pp. 3149–3156, ISBN: 978-1-5090-1210-7. DOI: *10.1109/IPEMC.2016.7512799*

A. Ahmad Khan *et al.*, "A compendium of optimization objectives, constraints, tools and algorithms for energy management in microgrids", *Renewable and Sustainable Energy Reviews*, vol. 58, pp. 1664–1683, 2016, PII: S1364032115016421, ISSN: 13640321. DOI: *10.1016/j.rser.2015.12.259*

S. Ishaq *et al.*, "A review on recent developments in control and optimization of micro grids", *Energy Reports*, vol. 8, pp. 4085–4103, 2022, PII: S2352484722000804, ISSN: 23524847. DOI: *10.1016/j.egyr.2022.01.080*

9. Thesis consultants

Tarmo Korõtko, Freddy Plaum, Vahur Maask

10. Work stages and schedule:

- Literature research (14.05.2022)
- State of the art analysis (30.06.2022)
- Modelling of MG components and setup of Matlab/Simulink simulation (22.07.2022)
- Development of energy trading markets (29.07.2022)
- Development and implementation of energy management strategies (22.09.2022)
- Simulation of scenarios and compilation of results (30.09.2022)
- Evaluation of simulation results (28.10.2022)
- Conclusion of thesis (30.11.2022)
- Final version of thesis (15.12.2022)

CONTENTS

PREFACE

The present thesis was prepared at Tallinn University of Technology (TalTech) in the department of Electrical Power Engineering and Mechatronics within the frame of my double degree studies. It is part of my study programme Electrical Engineering at the University of Applied Sciences Kempten (UAS Kempten) and Energy Conversion and Control Systems at TalTech.

I would like to thank my co-supervisor at the UAS Kempten, Prof. Dr.-Ing. Dr. h.c. Helmuth Biechl, for offering me the opportunity to study abroad in Estonia and to obtain a master's degree from both universities in Kempten and Tallinn based on the international cooperation agreement. I would also like to thank Tobias Häring for coordinating everything.

The topic was initiated by my consultant and researcher Tarmo Korõtko to contribute to the ongoing research within the FinEst project "Reducing energy supply requirements using microgrids and energy storage".

A sincere thank you goes to Tarmo Korõtko for providing me with information and assistance to complete this work. I appreciate the unique opportunity to gain experience in the field of power engineering and microgrids. Further, I want to thank my supervisor Prof. Dr. Sc. Eng. Argo Rosin for supporting me during my time at TalTech.

At this point, I want to thank everyone in the Microgrids and Metrology research group, in particular my other consultants and PhD students Freddy Plaum and Vahur Maask, as well as the nice people I met here for helping me with advice and making me feel welcome.

I also want to especially thank my family and friends, who have supported me throughout my studies.

Tallinn, 21.12.2022

Daniel Stich

Application in English

From: Daniel Stich (225246AAAM)

To: Toomas Vaimann

I, Daniel Stich, would like to request permission to write this master's thesis in English due to the following reasons.

This thesis is prepared to obtain a dual master's degree from the University of Applied Sciences Kempten and Tallinn University of Technology based on the international co-operation agreement between those two universities.

I, as an Erasmus student from Germany, am not sufficiently educated in Estonian to write a master's thesis in the Estonian language. Furthermore, this thesis must also be submitted to my home university in English.

Thank you for your understanding.

Tallinn, 21.12.2022

Daniel Stich

LIST OF ABBREVIATIONS AND SYMBOLS

Abbreviations

AI   Artificial Intelligence
API   Application Programming Interface
BESS   Battery Energy Storage System
CapEx   Capital Expenditure
CB   Circuit Breaker
CDG   Closed Distribution Grid
CDS   Closed Distribution System
CO   Charger Operator
CO_2 Carbon Dioxide
CoE   Centre of Excellence
CRS   Collective Revenue Sharing
DE   Diesel Engine
DG   Distributed Generation
DLC   Direct Load Control
DLVS   Digital Low-Voltage Substation
DoD   Depth of Discharge
DR   Demand Response
DSO   Distribution System Operator
DSOS   Distribution System Operating System
EFC   Equivalent Full Cycle
EMS   Energy Management System
EP   Electricity Provider
ESS   Energy Storage System
ETP   Effective Total Profit
EV   Electric Vehicle
FC   Fuel Cell
GHG   Greenhouse Gas
HV   High-Voltage
HVDC   High-Voltage DC
ICT   Information and Communication Technologies
IoT   Internet of Things
IPCC   Intergovernmental Panel on Climate Change
LEC   Local Energy Community
LED   Light-Emitting Diode
Li   Lithium
LUT   Lookup Table
LV   Low-Voltage
MG   Microgrid
MGCC   Microgrid Central Controller
MGN   Microgrid Network
MILP   Mixed-Integer Linear Programming
MT   Micro Turbine

MV	Medium-Voltage
NMC	Lithium Nickel Manganese Cobalt Oxide
NPS	Nord Pool Spot Market
OpEx	Operational Expenditure
OPF	Optimal Power Flow
OS	Operating System
P2G	Power-to-Gas
P2P	Peer-to-Peer
P2X	Power-to-X
PBP	Payback Period
PCC	Point of Common Coupling
PV	Photovoltaic
PVGIS	Photovoltaic Geographical Information System
PWM	Pulse-Width Modulation
RCD	Residual-Current Device
REG	Renewable Energy Generation
RES	Renewable Energy Source
RT	Real-Time
SMG	Smart Microgrid
SoC	State of Charge
STC	Standard Test Conditions
TC	Tartu City
ToU	Time of Use
UC	Unit Commitment
V2G	Vehicle-to-Grid
VAT	Value-Added Tax
WT	Wind Turbine

Symbols

C_{CO}	Total cost of CO (optimisation expression for scheduling)
C_{LEC}	Total cost of LEC (optimisation expression for scheduling)
$\cos\varphi$	Power factor
C_{SL}	Operational cost of street lighting system
C_{TC}	Total cost of TC (optimisation expression for scheduling)
$\Delta E_{min,idle}$	Threshold for minimum EV energy reference per hour
$\Delta E_{min,sh}$	Threshold for minimum EV energy reference of single hour consumption periods
DoD_{BESS}	DoD of BESS
$\Delta SoC_{EV,min}$	Minimum SoC difference of target-based EVs
ΔT	Simulation timestep
ΔT_{ch}	Planned charging time of time-based EVs
$\Delta T_{ch,max,AC}$	Maximum charging time of EVs at AC chargers
$\Delta T_{ch,max,DC}$	Maximum charging time of EVs at DC charger
$\Delta T_{ch,min}$	Minimum charging time of time-based EVs
$\Delta T_{horizon}$	Timestep of optimisation horizon (parameter for scheduling)

E	Active energy
E_{BESS}	Gross energy capacity of BESS
$\eta_{BESS,ch}$	Charging efficiency of BESS
$\eta_{BESS,dis}$	Discharging efficiency of BESS
$E_{EV,ch}$	Total charged energy given by EV dataset
EFC	EFCs of BESS
ETP	ETP of energy management strategy in P2P trading market
FC_{CO}	Fixed cost of CO per timestep
FC_{LEC}	Fixed cost of LEC per timestep
FC_{TC}	Fixed cost of TC per timestep
FR_{CO}	Fixed revenue of CO per timestep
FR_{LEC}	Fixed revenue of LEC per timestep
FR_{TC}	Fixed revenue of TC per timestep
I	Current
i	Index for interpolated EV dataset
I_n	Nominal current
$I_{PCC,r}$	Rated current of PCC circuit breaker
I_{sc}	Rated short-circuit current
k	AC charger number/index
m_{LEC}	Price margin specified by LEC
$M_{LEC,exp}$	Maximum power export of LEC to TC (big-M parameter for scheduling)
$M_{LEC,imp}$	Maximum power import of LEC from TC (big-M parameter for scheduling)
m_{TC}	Price margin specified by TC
$M_{TC,exp}$	Maximum power export of TC to main grid (big-M parameter for scheduling)
$M_{TC,imp}$	Maximum power import of TC from main grid (big-M parameter for scheduling)
$N_{occ,AC}$	Number of occupied AC chargers
$N_{occ,DC}$	Number of occupied DC chargers
OCC_{AC}	Binary/boolean status signals (occupied) of AC chargers
OCC_{DC}	Binary/boolean status signal (occupied) of DC charger
P	Active power
$P_{AC,avg}$	Peak charging hours of AC chargers (average consumption based on one year's data)
$P_{AC,dem}$	Power demand of AC chargers
$P_{AC,r}$	Rated power of AC charger
$P_{AC,sched}$	Scheduled power available for all AC chargers (optimisation variable for scheduling)
$P_{AC,set}$	Power limit setpoints of AC chargers
$P_{BESS,ch}$	Charging power of BESS
$P_{BESS,ch,avail}$	Available charging power of BESS according to SoC
$P_{BESS,ch,max}$	Maximum charging power of BESS
$P_{BESS,ch,res}$	Available power reserve for BESS charging in case of no EV charging
$P_{BESS,ch,sched}$	Scheduled charging power of BESS (auxiliary optimisation variable for scheduling)
$P_{BESS,dis}$	Discharging power of BESS
$P_{BESS,dis,avail}$	Available discharging power for BESS according to SoC
$P_{BESS,dis,max}$	Maximum discharging power of BESS

$P_{BESS,dis,res}$	Available power reserve for BESS discharging in case of no EV charging
$P_{BESS,dis,sched}$	Scheduled discharging power of BESS (auxiliary optimisation variable for scheduling)
$P_{BESS,meas}$	Measured power at BESS connection point
$P_{BESS,sched}$	Scheduled power of BESS (optimisation variable for scheduling)
$P_{BESS,set}$	Power setpoint of BESS
PBP	PBP of owner's capital investment
$P_{charger,r}$	Rated power of considered EV charger (for EV charger modelling)
$P_{DC,avg}$	Peak charging hours of DC charger (average consumption based on one year's data)
$P_{DC,dem}$	Power demand of DC charger
$P_{DC,r}$	Rated power of DC charger
$P_{DC,sched}$	Scheduled power available for DC charger (optimisation variable for scheduling)
$P_{DC,set}$	Power limit setpoint of DC charger
$P_{EV,ch}$	Charging power of EV
$P_{EV,dem}$	Power demand of all EV chargers
$P_{EV,res}$	Available power reserve for all EV chargers
$P_{LEC,exp}$	Power export of LEC to TC (auxiliary optimisation variable for scheduling)
$P_{LEC,imp}$	Power import of LEC from TC (auxiliary optimisation variable for scheduling)
$P_{PCC,max}$	PCC power capacity
$P_{PCC,meas}$	Measured power at PCC
$P_{PV,excess}$	Available PV excess power
$P_{PV,gen}$	Power generation of PV system
$P_{PV\text{-}inv,r}$	Rated power of PV inverter
$P_{PV,peak}$	Peak power of PV system
$P_{PV,pred}$	Predicted/forecasted power generation of PV system over optimisation horizon (parameter for scheduling)
Pr_{AC}	Charging tariff of AC charger
Pr_{DC}	Charging tariff of DC charger
Pr_{EP}	Profit margin specified by EP
Pr_{exp}	Price for exporting energy to main grid
$Pr_{grid,fix}$	Fixed part of grid tariff
$Pr_{grid,var}$	Variable part of grid tariff
Pr_{imp}	Price for importing energy from main grid
Pr_{NPS}	NPS day-ahead price
$Pr_{NPS,avg}$	Average NPS day-ahead price
$P_{SL,dem}$	Total street lighting power demand
$P_{TC,exp}$	Power export of TC to main grid (auxiliary optimisation variable for scheduling)
$P_{TC,imp}$	Power import of TC to main grid (auxiliary optimisation variable for scheduling)
Q	Reactive power
R_{CO}	Total revenue of CO (optimisation expression for scheduling)
R_{LEC}	Total revenue of LEC (optimisation expression for scheduling)
R_{TC}	Total revenue of TC (optimisation expression for scheduling)
SoC_{BESS}	SoC of BESS

$SoC_{BESS,init}$	Initial SoC of BESS at simulation start
$SoC_{BESS,max}$	Upper SoC limit of BESS
$SoC_{BESS,min}$	Lower SoC limit of BESS
$SoC_{BESS,start}$	SoC of BESS at start of optimisation horizon (parameter for scheduling)
$SoC_{BESS,th}$	SoC reserve threshold for EV charging support
SoC_{EV}	SoC of EV battery
$SoC_{EV,arr}$	SoC of EV battery on arrival at charger
$SoC_{EV,max}$	Defined upper limit for SoC of EV battery
$SoC_{EV,min}$	Defined lower limit for SoC of EV battery
$SoC_{EV,tgt}$	Targeted SoC of target-based EVs
t	Time (variable or discrete index)
$T_{horizon}$	Number of forecasting horizon timesteps (parameter for scheduling)
TP	Total profit of MG (objective function for scheduling)
V	Voltage
V_n	Nominal grid voltage
$w_{TC,C}$	Weight factor for cost carried by TC (parameter for scheduling)
$w_{TC,R}$	Weight factor for revenue generated by TC (parameter for scheduling)
Y_{LEC}	Indicator for power import or export of LEC (binary optimisation variable for scheduling)
Y_{TC}	Indicator for power import or export of TC (binary optimisation variable for scheduling)

LIST OF FIGURES

LIST OF TABLES

LIST OF ALGORITHMS

INTRODUCTION

Background

Reliable energy supply is an integral part of life in our modern society. Many sectors such as electricity, heating, transport and industry need energy to function on daily basis. As of right now, a major part of the primary energy demand is satisfied with fossil energy resources like coal, oil and natural gas [1]. But the request for clean energy is constantly rising. There are numerous reasons for this development.

The awareness of the necessity for the change in energy supply can be dated back to the oil crisis in 1973 when the production of oil was artificially depressed [2]. This awareness is a consequence of economic and political reasons. The current war led by Russia in Ukraine shows that the same problems still exist. While Estonia plans to stop importing gas from Russia by the end of 2022, Germany has built up a strong dependency on fossil fuels by relying on gas imports from Russia and the new Nord Stream 2 pipeline [3, 4].

The environmental impact of the combustion of fossil energy resources is the biggest problem on a global scale, especially in the long run. This fact was once again highlighted by the latest Intergovernmental Panel on Climate Change (IPCC) report 2022. "Global warming, reaching 1.5 °C in the near term, would cause unavoidable increases in multiple climate hazards and present multiple risks to ecosystems and humans" [5]. Further, the impact of fossil fuels on the local environment is causing concerns. One example is the damaged oil rig Deepwater Horizon (2010). The same goes for nuclear power and the disasters at Chernobyl (1986) and Fukushima (2011) [6].

The most important mean of fighting climate change is the reduction of greenhouse gas (GHG) emissions, especially carbon dioxide (CO_2). The Paris Agreement signed in 2015 and the European Green Deal presented in 2019 marked the start of major changes in the energy supply [7, 8]. Electricity will play a key role in this change due to its flexibility. Electric heat pumps can efficiently provide heat to buildings and factories. The transport sector sees a vast increase in electric vehicles (EVs) starting with individual mobility. Sectors that are difficult to transform to electricity-based energy supply will benefit from power-to-gas (P2G) and other power-to-X (P2X) technologies [9].

The share of renewable energy sources (RESs) will have to be increased to ideally 100 % not only for electricity but for primary energy [10]. Other resources like nuclear fusion are still in their infancy and cannot be considered as an alternative in the next decades [11]. This transition is fuelled by the constantly decreasing costs of RESs, while fossil fuels are becoming more and more expensive due to their inherent depletion and economic as well as political reasons [12]. RESs introduce new problems to the conventional electricity grid, especially when connected to the distribution system as distributed generation (DG). The classical and strongly hierarchical electricity grid was designed to transmit energy from large centralised fossil fuel power plants to consumers [13]. Due to the increasing demand, amongst other things, caused by the rising popularity of EVs, the historical AC grid is outdated and will reach its limits. This was illustrated by the blackout, which happened in Germany in the year 2006 [14]. It pointed out the fragility

of the current grid structure. The problem becomes more challenging when considering the fluctuating availability of RESs which makes it difficult to satisfy classical load demand patterns and balance the grid. Therefore, the German grid operator Tennet builds with its SuedLink project high-voltage DC (HVDC) lines to transport wind energy from the north of Germany to the south where solar generation is more prolific [15]. Though, the project is accompanied by protests criticising area consumption and its impact on the landscape [16].

Microgrids (MGs) are meant to solve many of these problems. MGs are closed distribution systems (CDSs) with (controllable) loads, DG and energy storage systems (ESSs). Hereby, the grid is transformed from a centralised grid towards a decentralised topology. The MGs' off-grid capability increases supply security in case of failures. But this approach does not only benefit the utility, it also allows customers to participate in the electricity market and to provide ancillary services like demand response (DR) or (virtual) inertia [15, 17].

FinEst Centre

The FinEst projects under the organisation of Tallinn University of Technology focus on the transformation of cities towards smart cities. The project "Reducing energy supply requirements using microgrids and energy storage" tries to tackle the following two problems identified by the Smart City Centre of Excellence (CoE) (see also [18, 19]).

- Energy supply infrastructure for industrial development is low
- Energy production is too carbon-intensive

Municipalities often have limited means of influence on the supply infrastructure. Bureaucracy slows down development even when demand is urgent. On the other side, distribution system operators (DSOs) cannot handle individual requests by single clients. On top of that, expenses for enhancing the infrastructure are mostly carried by the end users. Consequently, industries are likely to settle at sites where the required infrastructure is already available. The problems related to carbon-intensive energy production have been already mentioned.

According to the project description, the solution approach intends a closed distribution grid (CDG) inside an electrical MG. The grid is formed by digital low-voltage substations (DLVSs) with smart measuring and control functionalities complemented by ESSs. RESs as a mean to implement DG, which can be logically distinguished from larger grids, have the chance to increase economic feasibility by maximising self-consumption and minimising fossil energy consumption. Therefore the main goals are to have DG that can be easily integrated into existing grids and also to reduce supply requirements.

The project aims to develop open software and hardware for a so-called distribution system operating system (DSOS) to maximise the use of locally generated energy. The general design was inspired by operating systems (OSs) for PCs where the OS interacts with the underlying hardware so that software applications can be built on top via application programming interfaces (APIs). It should enable various ownership scenarios

and provide targeted services with the goal to include the private sector into sustainable energy transition. The following three research branches are described.

- Cyber-security in cyber-physical systems
- Power quality of MGs
- Energy policies and local energy markets

Besides the already mentioned power quality issues in conventional grids, security in terms of computer technologies and the legal frame are challenges to take on.

The project plans to establish two pilot sites with individual objectives for demonstration purposes. The industrial park PAKRI at Lääne-Harju Parish and the pilot site at the city of Tartu. The latter describes an urban setting where a MG will operate in a given low-voltage (LV) AC infrastructure with additional EV charging opportunities.

In consideration of the aforementioned, this thesis focuses on the energy management of urban MGs to increase their economic feasibility. It involves power quality aspects as well as economics in the form of local energy markets. The MG pilot site in Tartu is a suitable research subject for this purpose. In this thesis, chapter 1 covers MGs and their control in general. Chapter 2 gives an overview of the pilot site and the modelling of the MG is described. Chapter 3 deals with the economic aspects of the MG. The development of suitable energy management strategies and the investigation of the simulation results is discussed in chapter 4 and 5 respectively. The summary finally summarises the findings and presents possibilities for future work.

Keywords: Microgrids, energy management, urban distribution grids, battery energy storage systems, electric vehicles, peer-to-peer trading.

1 STATE OF THE ART ANALYSIS

The rapidly developing economy and society make energy and environmental issues the most important socioeconomic issues. The combustion of fossil fuels results in severe energy and environmental pollution problems [20].

This chapter gives a short overview of the current electricity grid and the impact of introducing large-scale RESs. The transition to a decentralised grid in the form of MGs plays an important role in solving those issues. Therefore, MGs and their typical classification criteria are investigated. The advantages, possible problems, and challenges of MGs are stated. Further, the concept of hierarchical control is explained, which enables the efficient operation of MGs.

1.1 Existing grid

The first generation of electricity grids had production near to the consumption. Since then, the grid has been based on AC voltage. Transformers used to be the only option to step up or step down the voltage since suitable power electronics did not exist yet [21]. With the increasing demand, centralised power systems developed. Before the 1990s, power plants were located near fuel sources and remote locations due to logistics and the advantage of increased safety. Generated electricity was transmitted via high-voltage (HV) and then distributed via medium-voltage (MV) and LV systems. The grid today is still strongly hierarchical. CO_2 emissions, energy deficiency, and the lack of supply security made changes necessary. Since the 1990s, incentives for small-scale RESs were introduced. These RESs are connected to the distribution grid (DG units) and thus altered the power flow from unidirectional to bidirectional [13, 15]. Figure 1.1 illustrates the transition process.
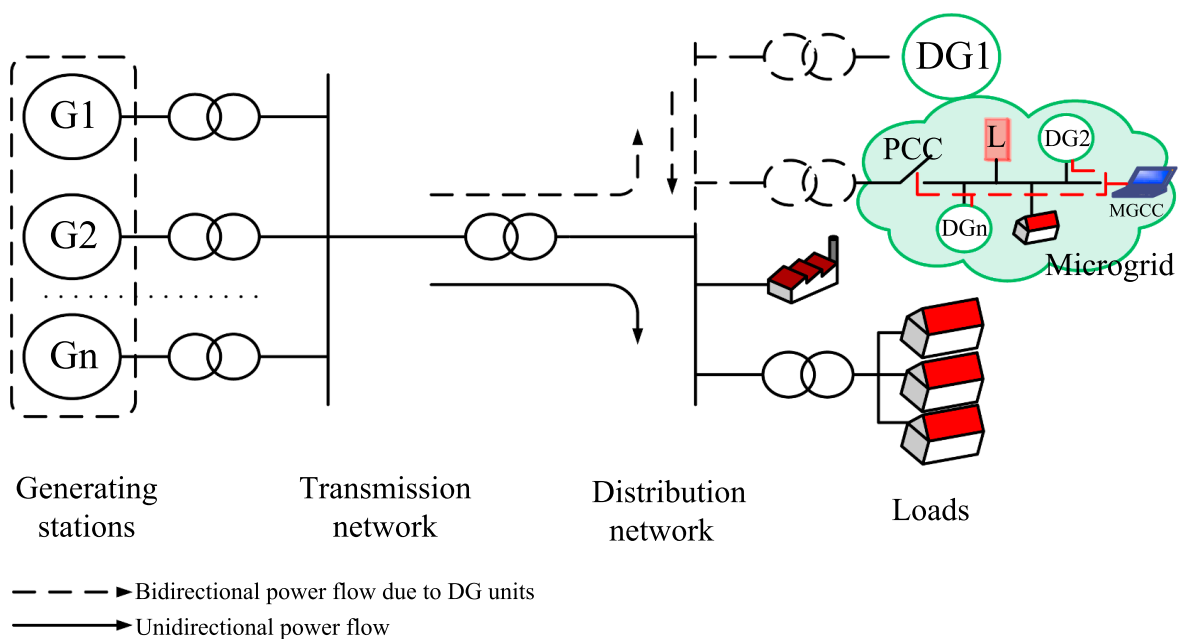
Figure 1.1: Transition from centralised to decentralised electricity grid [13]

DG has the potential to improve supply reliability since failures have less impact on the power system. Further, transmission losses are reduced by placing generation units near demand. There is no need in enhancing feeder capacity because less energy needs to be imported. But the biggest advantage of DG is the possibility to integrate RESs [13, 20].

RESs are essential for promoting (local) development in an economic and socially sustainable manner and for mitigating the effects of climate change and energy crises. The shift to RESs is driven on the one hand by the drawbacks of fossil fuels like coal, gas and oil. The gradual depletion and stricter emission policies make them unattractive [13, 22]. On the other hand, RESs offer the advantage of low environmental pollution. In addition, associated technologies get cheaper which makes them a viable option for satisfying the steadily increasing demand. Small-scale distributed RESs can be installed flexibly and therefore provide higher transmission efficiency with fewer investments in new infrastructure [20, 23].

DG units also introduce new challenges. Power quality is a major concern. The inverse power flow changes the network from passive to active, which makes protection more difficult [23]. Also, converter-fed DG has low or zero inertia characteristics which affect frequency stabilisation. In addition, most of the RESs depend on the weather. They have stochastic and discontinuous behaviour. Further, they cannot be dispatched and need to be curtailed without proper control [13, 20]. It can be said that DG implemented with RESs add complexity to the currently existing power system.

1.2 Microgrids

MGs are meant to cope with the problems and complexity of the power system while exploiting the advantages of DG and RESs [13]. They foster the idea of decentralised generation by combining DG with loads and ESSs in one small closed power distribution system usually sited on the LV level [20]. The MG's connection with the main grid is called the point of common coupling (PCC) which allows the MG to operate off-grid in case of failures. Besides the components, the control aspect is a key idea.

The concept of MGs was first introduced in 2001 by [24] and has evolved over time. There is no standardised definition of MGs to date, but in [13] the following is proposed.

Definition (Microgrid). *A microgrid (consisting of small-scale emerging generators, loads, energy storage elements and a control unit) is a controlled small-scale power system that can be operated in an islanded and/or! grid-connected mode in a defined area to facilitate the provision of supplementary power and/or maintain a standard service.*

With the ongoing digitalisation, integration of internet of things (IoT) devices and artificial intelligence (AI) technologies, smart metering, cloud services and computing, and real-time (RT) data collection, MGs converge towards smart microgrids (SMGs) [21, 23, 25]. Aside from the advantages of DG and RESs, MGs and their smart control add more benefits. They enhance the distribution system further through intelligent energy management and a fast restoration from physical/cyber attacks. In addition, they enable the

environmentally friendly integration of EVs and promote customers to participate [22, 26].

MGs can be classified according to the type of components, their voltage type (topology and voltage level), and operation mode. But there are also other criteria like ownership or the application of MGs [22].

1.2.1 Components

A MG consists of several components. The main components are DG units, loads and ESSs. Aside from that, distribution facilities, protection, and load monitoring devices are part of the system [20].

Distributed generation is usually referred to as small-scale on-site generation units. It is vaguely defined in [27] as follows.

Definition (Distributed generation)**.** *An electric power generation unit that is connected directly to the distribution network or on the customer side of the meter.*

DG units can be either classically fuel-powered like diesel engines (DEs) or micro turbines (MTs). Fossil fuels can be considered always available, which is beneficial for a secure power supply [21]. Emissions are their major drawback. But RESs have the potential to provide cheap and clean energy for the MG. Typical renewables include photovoltaic (PV), wind turbines (WTs), hydro, tidal waves, geothermal, fuel cells (FCs), and generators powered by renewable fuels like biomass and gas [20, 21]. This makes RESs the preferable choice. RESs provide cheap energy and therefore are normally not curtailed [23, 25]. Commonly, renewable energy is exploited as much as possible. Though, the current electricity market structure is a burden for integrating RESs [25].

Loads can be classified as deferrable and interruptible, deferrable and non-interruptible, and non-deferrable and non-interruptible [20]. Figure 1.2 illustrates these load types in the context of household appliances. Deferrable means that the start time of the load demand can be postponed for a certain number of time windows. Interruptible means that loads can be switched off for a certain number of time windows and switched on again later until the demand is met. Inelastic, non-controllable or sensitive loads like street lighting need to be supplied immediately while controllable or elastic loads can provide flexibility (e.g. DR) [25]. Also, large-scale EV charging and possibly discharging will affect the grid's stability [20]. Thus, controllable loads are interesting for energy management systems (EMSs).
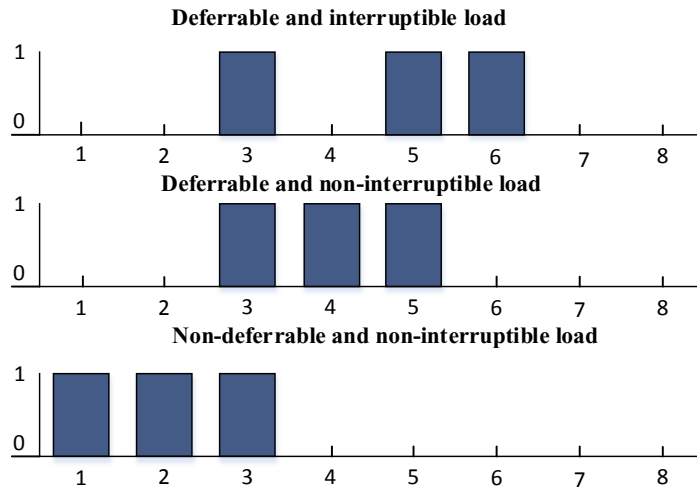
Figure 1.2: Classification of loads, horizontal axis: time windows, vertical axis: status of load (0: off, 1: on) [20]

Energy storage systems can be seen as prosumers that either function as loads or generators. They are not a mandatory part of MGs but often enable MGs to operate efficiently. Storages can be used for peak shaving or valley filling to increase stability. The exploitation of storages usually reduces the costs of MGs. Therefore, ESS control is usually the main feature of an EMS [20, 25]. Besides control, optimal sizing and the lifetime of ESSs are major concerns [13]. Figure 1.3 gives an overview of storage types that can be applied in MGs. In the future, EVs equipped with vehicle-to-grid (V2G) technology can provide additional storage capacities to the MG [20].
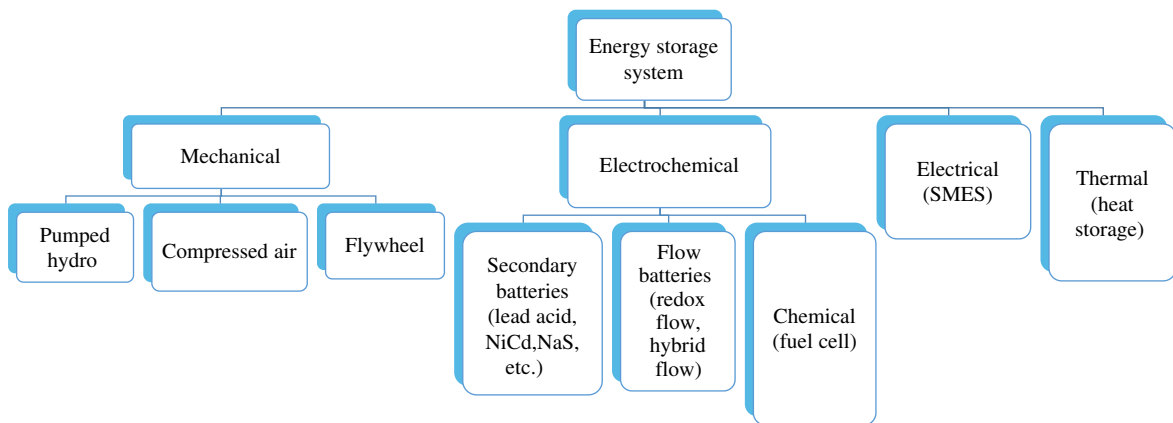
Figure 1.3: Classification of ESSs [28]

1.2.2 Topologies

MG infrastructure can be divided into three topologies namely AC, DC, and hybrid. The topology is one of the main classification criteria. Each topology has its advantages and drawbacks which are discussed in the following sub-section. Since most MGs are based on LV systems, the voltage level is not considered here.

AC microgrid topology is the most common type of topology since the electrical grid has been historically based on AC and protective devices are cheap and reliable. Therefore, this topology is often applied in existing (urban) distribution systems [21]. Figure 1.4 illustrates such a MG. The AC bus is directly connected to the main/utility grid via the PCC. Classical AC loads and DG units can be easily connected to the bus either directly or via AC/AC converters. DC DG units like PV need to be interfaced via DC/AC converters. ESSs like a battery require bidirectional converters for the connection to the AC bus [29]. A major drawback of this topology is the need for synchronisation of voltage and frequency to the main grid. Besides active power control also reactive power control is necessary to maintain nominal voltage [21].
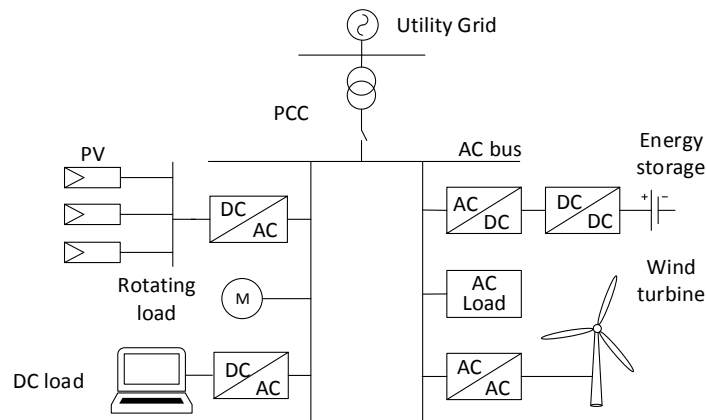
Figure 1.4: AC MG topology [29]

DC microgrid topology and DC power systems in general have gained popularity due to the fast development of power electronics in recent years [13]. DC power systems bypass problems like power quality and synchronisation that still exist in AC systems. Figure 1.5 shows an example of a DC MG topology. This MG requires a main converter at the PCC to connect to the main grid. The DC bus provides an easy way to integrate the rising number of DC generators and loads like EVs and light-emitting diode (LED) street lighting, which reduces the complexity [21]. AC equipment requires DC/AC converters [29]. In DC MGs only active power needs to be controlled [21]. Difficulties arise when there is already an existing AC grid that is meant to be repurposed. Also, protective gear is less developed and standardised than its AC counterpart [13].

Hybrid microgrid approach links the AC and the DC sub-MGs with an AC/DC converter while only the AC bus is connected to the main grid [21, 29]. The hybrid topology is depicted in figure 1.6. This approach combines the simplicity of DC buses with the flexibility and reliability of AC buses [25]. Control in this case is more complex compared to the other two topologies.
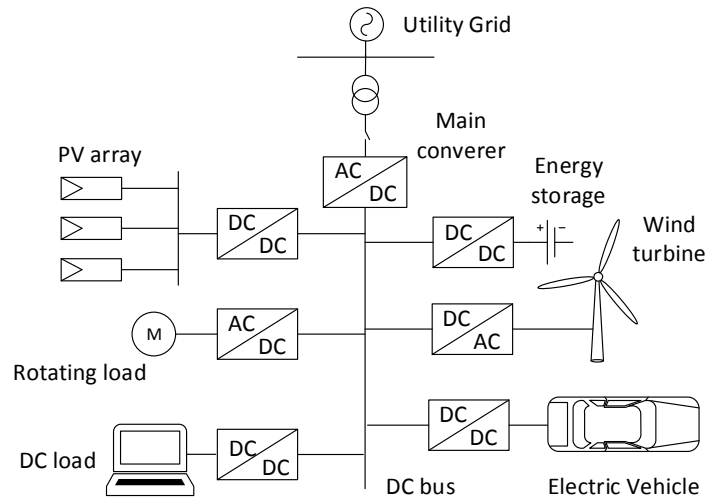
Figure 1.5: DC MG topology [29]
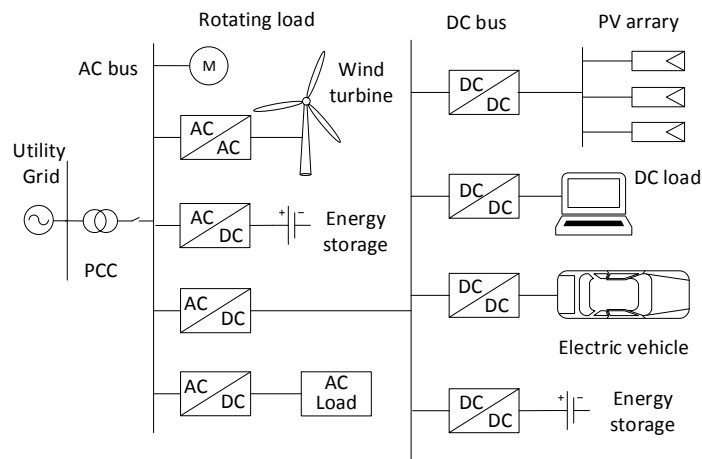
Figure 1.6: Hybrid MG topology [29]

1.2.3 Operation modes

In general, MGs operate in one of two modes, the on-grid or off-grid mode. The switching of operation mode depends on various factors. Two special cases of MGs exist. First, grid-tied MGs that only operate in on-grid mode. They can be usually found in urban environments where the infrastructure is already well established. Second, standalone MGs can only operate in off-grid mode. This type of MG can be applied in rural areas where the distribution system is weak or non-existing [22].

On-grid/grid-connected   operation means the MG is connected to the main grid. This implies that there is no fault in the grid. Here, the main grid sets the voltage and frequency. Thus, grid-following inverters can be used. The main grid supports the MG, which makes active and reactive power control easier than in off-grid operation [21].

Off-grid/islanding   operation mode is especially beneficial in areas where supply se-curity is weak. Voltage sags or frequency deviations might cause failures of the grid but

MGs with islanding capability can disconnect from the main grid in such cases. DG and ESSs then support the closed system and ensure a reliable power supply [29]. Since there is no voltage and frequency set by the main grid, grid-forming inverters are required [21].

1.3 Hierarchical control

The control system allows MGs to manage resources in an intelligent way. MGs can pursue different goals. Control can contribute and support to achieve the goals. Some of them are listed in table 1.1 [20–22, 25].

Table 1.1: MG goals

Decrease/minimise	Increase/maximise
• Operation costs	• Efficiency
• Maintenance costs	• Exploitation of RESs
• Energy purchase	• Reliability of power supply
• Fuel consumption	• Power quality
• Environmental pollution	• Cyber-security of power supply
• Peak load	
• Load shedding	
• RESs curtailment	
• Transmission/power losses	
• Main grid dependency	

These goals are settled on different levels and can be achieved through different approaches. Therefore, MG control has many different tasks that need to be dealt with on different timescales. Thus, it is logical to separate control into different layers to make it more robust. This concept is called hierarchical control. Hierarchical control is defined vaguely since the type of MG (e.g. residential or rural) has an impact on the control approaches. Figure 1.7 shows one possible approach. Different tasks are assigned to different layers. Each layer has typical timescales that are getting longer towards the higher control levels [25].

Control also relies on the flow of information based on information and communication technologies (ICTs). Thus, control levels can be implemented on different spatial levels which impact the amount of communication required. Mainly three types are distinguished: centralised, distributed/hybrid and decentralised [22, 25]. Figure 1.8 illustrates these structures and the information flows.
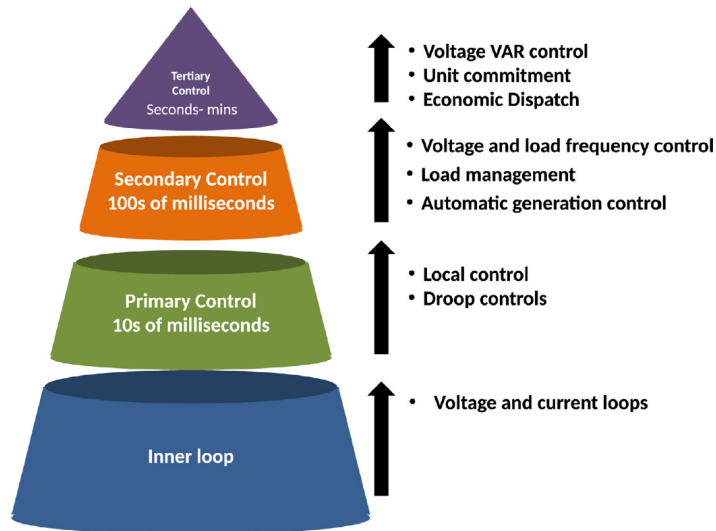
Figure 1.7: Hierarchical control pyramid [21]
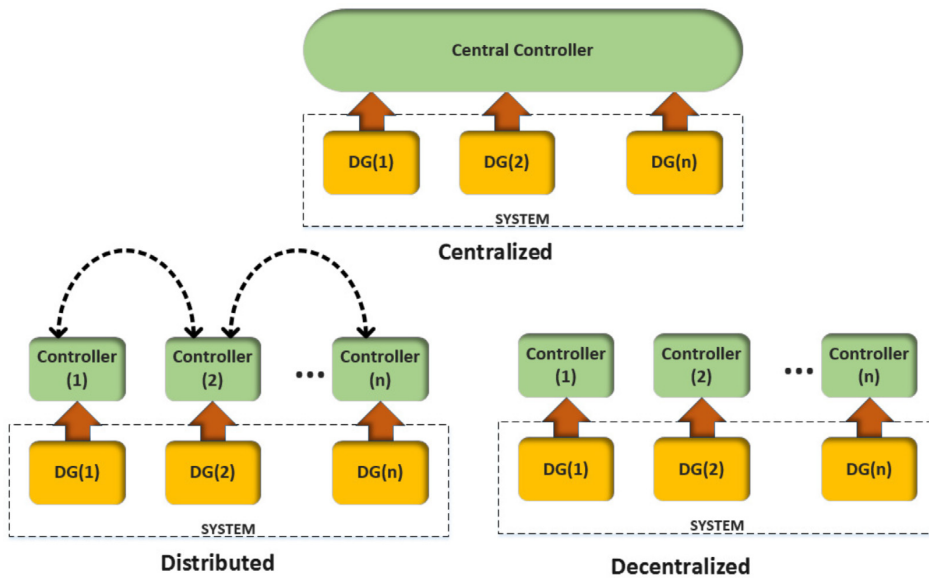
Figure 1.8: MG control structures, dashed arrows: limited communication [21]

1.3.1 Primary-level

Primary-level control is usually implemented with distributed local controllers based on local measurements to provide fast response times of $1\,\mathrm{ms}$ to $100\,\mathrm{ms}$ [25]. It directly interacts with the power converters (inner loop) by providing either P/Q or I/V setpoints. In rare cases, primary control can directly generate pulse-width modulation (PWM) signals for power hardware. It is designed to be dependent only on minimum and/or low-bandwidth communication. In addition, an emergency control mode is implemented that provides a minimum of functionality in the event of a communication failure. Typical tasks are balancing out overcurrents, stabilising local voltage and frequency and ensuring safe and correct power sharing, but also islanding detection. The timescale of some tasks can go up to $1\,\mathrm{s}$. Droop control is a popular control strategy [21, 25].

1.3.2 Secondary-level

Secondary-level control is also known as the supervisory control system. It can be seen as the moderator between the primary and tertiary controllers [25]. It is implemented either as a centralised or distributed controller. Reaction times start from 100 ms and go up to 1 min [21]. In the first place, voltage and frequency deviations inside the MG are kept to zero. Further, this layer is supposed to correct mismatches between upper-level references and feasible setpoints in the lower level. Therefore, a redundant optimisation layer is implemented with a focus on power quality instead of economics [21, 25].

1.3.3 Tertiary-level

Tertiary-level control is usually implemented as a central controller. The timescale ranges from 1 min to 1 h [25]. The main task of this control layer is to provide economic-oriented energy management (optimal P/Q setpoints for the secondary controller). Besides economic power dispatch, the tertiary controller also does other tasks like energy marketing, exchanging energy with the main grid or providing ancillary services like spinning reserve or frequency and voltage regulation. If a microgrid network (MGN) is present, another task is the coordination between the individual MGs [21, 25].

Figure 1.9 shows an example of how the control can be structured and how the control layers are assigned. The so-called microgrid central controller (MGCC) takes over tertiary-level control tasks. The primary-level control tasks are assigned to local controllers and the distributed secondary-level controller moderates between the MGCC and the local controllers.
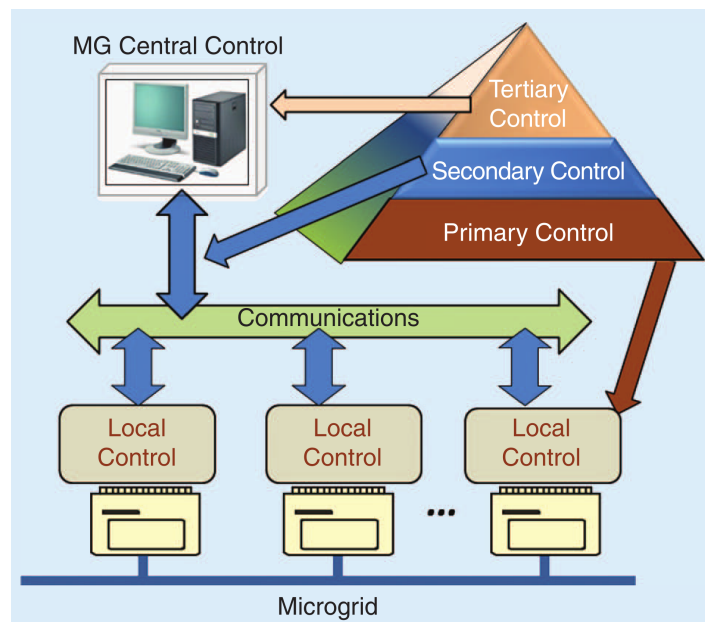
Figure 1.9: Example of hierarchical control layers and structures [17]

Energy management approaches can be divided into supply-side and demand-side management. The individual control approaches depend on the structure and communication, operation mode, components, etc. [21, 22]. On the supply side, unit commitment (UC) and economic (load) dispatch are common approaches. UC seeks startup-shutdown schedules for power plants and economic dispatch arranges the generation outputs and the transmission between the MG and main grid. These problems are also known as optimal power flow (OPF) problems. Demand-side management means influencing load demand which is often done by price-based (e.g. time of use (ToU) pricing) or incentive-based (e.g. direct load control (DLC)) DR [20].

For optimal energy management, accurate forecasting of load demand, generation, and market prices is crucial. Forecast horizons have been divided in [13] into very short-term (1 min to 1 h), short-term (1 h to 1 week), medium-term (1 month to 1 year), and long-term (1 year and above). Day-ahead (24 h) horizons are common for tasks related to energy management [21, 25]. Stochastics in load demand and renewable energy generation (REG), and eventually unpredictable tariffs make this task challenging [26]. The energy management problem can have one or more objectives (compare table 1.1). Most of them can be translated into cost. Energy management problem costs have been categorised in [22] as follows.

- Environmental cost (costs related to carbon emissions, …)
- Capital and operational costs (fuel, maintenance, …)
- Energy storage cost (battery, …)
- Miscellaneous (load shedding costs, cost of power losses, …)

Multiple stakeholders complicate the formulation of objectives [20]. Energy management is restricted to different constraints, which can be categorised as follows [22].

- Generation (minimum and maximum power output limits, …)
- Loads (operating limits like consumption and load constraints, …)
- Storage devices (limits of charge and discharge rate, limit of discharge, …)
- Operational constraints (spinning, non-spinning reserves, ramping limits, and start-up and shut-down rates of generating elements, …)

1.4 Conclusion

The rest of this thesis focuses on the economic energy management aspect of tertiary-level control. Thus, a centralised control approach is pursued. Energy management usually relies on an accurate forecast of load demand and generation. Since small-scale EV charging is highly stochastic, classic optimisation-based methods cannot be applied. Therefore, simplified energy management strategies need to be developed taking into account the stochastic nature while ensuring safe operation. For the chosen pilot site, DLC of EV chargers and ToU tariffs can be applied. The EV chargers are not intended to provide V2G services. Another open research topic is energy management with multiple stakeholders, which is also an issue of the MG in Tartu.

2 MODELLING OF MICROGRID

When developing energy management strategies for urban MGs, their impact on the economic feasibility of the MG needs to be verified through simulations. Therefore, a model of the pilot site at the city of Tartu is developed. The next section gives an overview of the pilot site and its classification. Hereafter, the pilot site top-level model and its component-level models are introduced. This chapter focuses on the technical part of modelling. The economic aspects are investigated and modelled in the subsequent chapter 3.

2.1 Pilot site

The physical structure of the distribution grid at the pilot site is given in appendix A.1. Highlighted components have not yet been installed at the pilot site, but are planned to be included. Apart from small consumers like a bicycle charging station and an advertisement display panel at a bus stop, the distribution grid is mainly used for street lighting. The grid is based on LV AC (400 V phase-to-phase) as is typical for existing distribution systems in Europe. None of the components that already exist, or will be built, use grid-forming inverters, which makes this MG grid-tied without islanding capability. The pilot site, therefore, represents a typical urban street lighting distribution grid suitable as a case study for the simulation of energy management strategies according to the thesis task.

The PCC is rated at 40 A and the cables are all designed for nominal currents of 69 A and 100 A. Street lights consume in total around 4 kW (compare measurement data in subsection 2.4.3). This indicates a low usage rate of the existing electricity infrastructure. The project report states a utilisation rate below 35 % related to the PCC size and 5 % related to the cable dimensions. The upcoming demand for EV charging poses challenges to the urban electricity infrastructure [30]. The capacity needs to be increased which translates into high cost for grid enhancements. The idea of the MG is to use the capacity reserves to provide the novel service of EV charging stations in the urban environment without building new infrastructure or extending the capacity of the connection point.

The integration of DG in form of a PV system and a battery energy storage system (BESS) together with the controller will support the MG. Figure 2.1 shows the planned carport with chargers and rooftop PV. All EV chargers come without V2G functionality. For MG control, a mobile container will be installed at the PCC. This container accommodates the MGCC as well as metering equipment and the BESS.

The system, given in detail in appendix A.1, consists of the main bus that is connected to the main grid via the PCC. The main bus supplies several smaller consumption units. These are the control cabinet directly at the PCC with self-consumption sockets, the bicycle and e-scooter charging station, and the advertisement display panel. Due to the size of the units, they are not part of the modelling. The main load is the 50 kW DC fast charger for EVs (in the following referred to as DC charger). A 100 kWh BESS and a 30 kWp PV system are connected as well. The PCC capacity is an important constraint
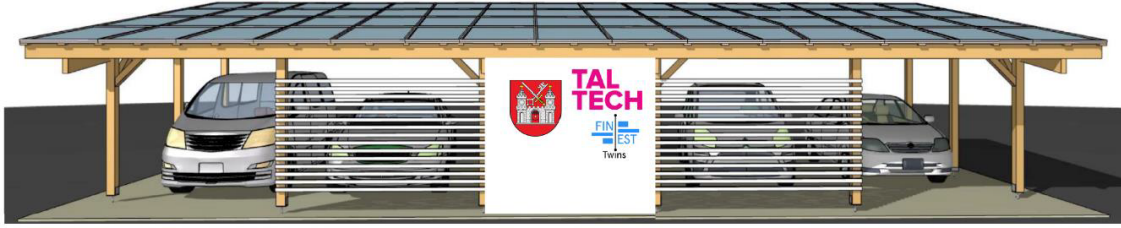
Figure 2.1: Illustration of carport at pilot site

for the safe operation of the MG. Consequently, the maximum allowed power through-put needs to be calculated. Table 2.1 lists the relevant parameters. Since there is no

Table 2.1: PCC parameters

Parameter	Value
$I_{PCC,r}$	40 A
V_n	400 V
$\cos \varphi$	0.9

information available for the power factor in the grid, a constant value of 0.9 at the PCC is assumed. A value close to 1 can be expected since all the considered units are inter-faced with power electronics that can control the power factor. With that information, a bidirectional power capacity of around 25 kW is determined (see equation (2.1)).

$$P_{PCC,max} = \sqrt{3} \cdot V_n \cdot I_{PCC,r} \cdot \cos \varphi \approx 24.94 \, \text{kW} \tag{2.1}$$

The street lighting system at the pilot site has its own bus which is connected to the main bus via a circuit breaker. While the connection power of the PCC is fixed, the circuit breaker rating for the street lighting bus can be increased according to the limits of the cables. Each of the three streets has its own feeder. The lights are distributed to the three phases. Feeder 2 is additionally supplying four 22 kW AC chargers for EV slow charging (in the following referred to as AC chargers).

Small MGs, which can be for instance found on the household level, often have a single owner. The MG at the pilot site has multiple owners. This is important for the financial aspect of energy management. In the case of the pilot site, three owners are present. Firstly, the Tartu municipality, hereafter referred to as Tartu city (TC); secondly, the local energy community (LEC); and thirdly, the charger operator (CO). Table 2.2 shows which of the assets belong to what owner. It also indicates which assets are considered in the pilot site model.

Table 2.2: Ownership of assets

TC	LEC	CO
Grid	BESS	4 AC chargers
Street lighting	PV	1 DC charger

2.2 Top-level model

Accurate modelling is important to get reliable simulation results. The following sections introduce the chosen modelling approaches for the MG and its components. Matlab/Simulink is used as a simulation environment. Simulink offers an easy-to-use graphical interface for modelling purposes. Matlab, though, offers a flexible programming language. Matlab system blocks combine the advantages of both worlds and are a good choice for modelling on the component level. More information about Matlab system blocks can be found in [31].

Figure 2.2 gives a top-level overview of the MG model. The top-level model specifies the grid structure, which is replicated graphically in Simulink. For the sake of simplicity, the
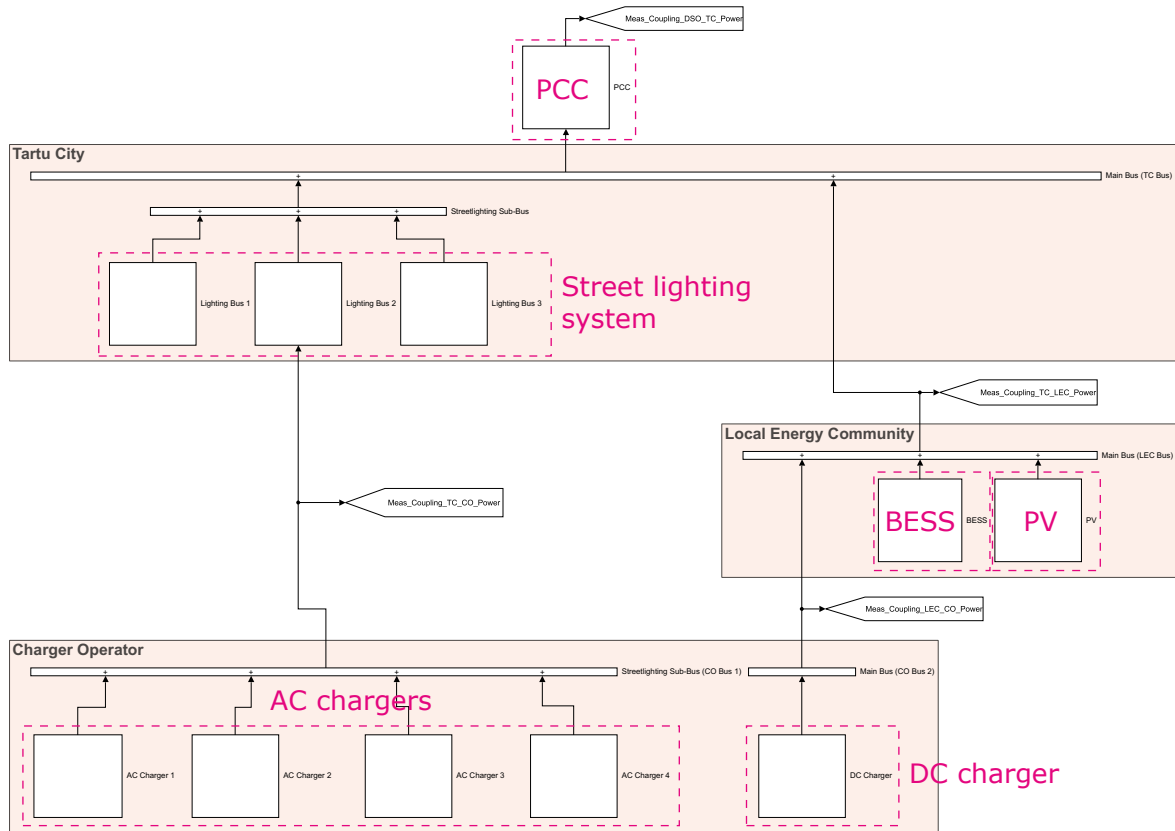
Figure 2.2: Simulink model of pilot site

three phases are combined into a single phase and transmission losses are neglected. The individual components are separated according to ownership (compare table 2.2). The interconnection between the owners is given by the physical layout. One exception is the connection of the DC charger. While the physical structure would suggest a direct connection to the main bus of TC, the project specifies that it is connected to the part of the main bus which is assigned to the LEC. The power flows at the coupling points between owners as well as the PCC power flow are metered.

Apart from the grid structure, another important parameter of the discrete-time simulation is the timestep ΔT that has to be specified in Simulink. In sub-section 1.3.3 a timestep between 1 min and 1 h is mentioned as a typical value for tertiary-level control. In this case, the smallest possible timestep is chosen. Due to computational effort, 5 min

or $\frac{5}{60}$ h is selected. Since management of active power is the most relevant quantity for economics (e.g. energy trading), the simulation is considering only active power P. Due to the finite and quasi-static timestep, the power values can be interpreted as 5 min averages or as energy values normalised by time. The direction of power flow is defined in equation (2.2).

$$P \begin{cases} > 0 & \text{if consumption,} \\ < 0 & \text{if generation.} \end{cases} \tag{2.2}$$

2.3 Simulation scenarios

Before modelling the individual components of the MG, simulation scenarios have to be declared. A scenario is defined here as a specific period of time on which other model parameters like market price and solar radiation are based. Following simulation scenarios were defined.

- Summer
  - 08.08.2022 to 14.08.2022 (UTC+3)
  - High PV production

- Winter
  - 17.01.2022 to 23.01.2022 (UTC+2)
  - Low PV production

PV produces cheap energy due to relatively small running costs and thus has a significant impact on the economic feasibility of the MG. To include seasonal effects and also varying market prices, one summer and one winter scenario are defined. The periods for both scenarios are chosen to represent relatively high or low PV production, but not the maximum or minimum. Furthermore, a one-week simulation also reflects the difference in consumption and market price patterns between business days and weekends. Thus, each simulation scenario covers one whole week (168 h) starting from Monday. In the following, when speaking of summer or winter, it refers to scenarios.

2.4 Component models

Based on the two simulation scenarios, the individual components can be modelled with Matlab system blocks. The modelling approaches for the BESS, the PV system, street lighting, and the EV chargers are described in the following sub-sections.

2.4.1 Battery energy storage system

A BESS with a gross energy capacity of 100 kWh and a maximum power output of 40 kW is foreseen in the MG. The project intends to install the PowerShaper 2 system from manufacturer Pixii (datasheet: [32]). This battery is using lithium nickel manganese cobalt oxide (NMC) technology, which is a sub-type of Lithium (Li)-ion technology. The BESS model is kept simple to avoid the specifics of the deployed battery technology. This is

sufficient for a high-level energy management simulation. Therefore, it is modelled with the state of charge (SoC) difference equation. Table 2.3 lists all BESS model parameters.

Table 2.3: BESS parameters

Parameter	Value
E_{BESS}	100 kWh
$SoC_{BESS,min}$	20 %
$SoC_{BESS,max}$	90 %
$P_{BESS,ch,max}$	40 kW
$P_{BESS,dis,max}$	−40 kW
$\eta_{BESS,ch}$	90 %
$\eta_{BESS,dis}$	90 %
$SoC_{BESS,init}$	20 %

The SoC describes to what level the battery is charged. The maximum energy capacity E_{BESS} corresponds to 100 % SoC. Depth of discharge (DoD), on the other hand, indicates how much of the battery is currently discharged. It is defined in equation (2.3), where $SoC_{BESS,max}$ defines the maximum permitted charging level (100 % or lower).

$$DoD_{BESS} = SoC_{BESS,max} - SoC_{BESS} \tag{2.3}$$

Cyclic battery degradation correlates with the maximum DoD. Battery degradation reduces capacity, and efficiency, and threatens safe operation [33]. Especially operating the battery in the low SoC range (deep discharge) causes harm. A straightforward way to reduce the degradation is to set lower and upper SoC limits. In [33, 34] values of 20 % and 90 % are used. This new SoC range defines the net battery capacity. In addition, for both simulation scenarios, an initial SoC equal to the minimum allowed SoC is defined to ensure that the performance of the energy management strategies is not distorted by having free energy available. Each charging or discharging procedure goes along with losses. Since the battery's datasheet does not provide any information, both the charging and discharging efficiencies are set to 90 %. This results in a round-trip efficiency of 81 %, which is a typical value in other MG simulation tools like HOMER [35].

Self-discharge effects are neglected since they are in the low percentage range per month and thus negligible for a simulation duration of one week [36]. But, if necessary, a constant self-discharge rate could be easily incorporated into the model. Also, temperature effects are not included.

The battery system model has one setpoint input $P_{BESS,set}$ which ranges from −100 % ($P_{BESS,dis,max}$) to 100 % ($P_{BESS,ch,max}$). Inside the system, the set power is then separated into mutually exclusive charging and discharging power according to equations (2.4a)

and (2.4b).

$$P_{BESS,ch} = \begin{cases} P_{BESS,set} & \text{if } P_{BESS,set} > 0, \\ 0 & \text{otherwise.} \end{cases} \tag{2.4a}$$

$$P_{BESS,dis} = \begin{cases} P_{BESS,set} & \text{if } P_{BESS,set} < 0, \\ 0 & \text{otherwise.} \end{cases} \tag{2.4b}$$

These variables are then used for the BESS state equation (2.5), where SoC_{BESS} at time t describes the current state of the battery. It allows the calculation of the SoC for the consecutive timestep.

$$SoC_{BESS}[t+1] = SoC_{BESS}[t] + \left(\left(P_{BESS,ch} \cdot \eta_{BESS,ch} \right) + \left(\frac{P_{BESS,dis}}{\eta_{BESS,dis}} \right) \right) \cdot \left(\frac{\Delta T}{E_{BESS}} \right) \tag{2.5}$$

In case the set power results in a new SoC that violates the defined limits, a feasible power setpoint is calculated by setting the next SoC value to the corresponding limit and solving equation (2.5) for the corresponding power.

The BESS system model has two outputs. The first one is the output power that could be measured at the connection point of the storage, denoted as $P_{BESS,meas}$. It is either equal to the power setpoint or the adjusted setpoint as mentioned. The second output is the calculated SoC_{BESS}.

2.4.2 Photovoltaic system

The PV system is designed for 30 kWp. Standard test conditions (STC) do not reflect solar radiation in Estonia. Thus, an actual power output below the peak power can be expected. In this case, a 21 kW PV inverter is sufficient. Table 2.4 summarises the parameters given by the project (compare appendix A.1).

Table 2.4: PV system parameters

Parameter	Value
$P_{PV,peak}$	30 kW
$P_{PV-inv,r}$	21 kW

This system can be easily modelled with profile data. Photovoltaic geographical information system (PVGIS) provides open-source information about solar radiation data. The integrated conversion to PV output power simplifies modelling. The PV generation data can be retrieved via the web API (documentation: [37]). Table 2.5 lists the used parameters. The location is specified by latitude and longitude coordinates in the area of the pilot site. The default horizon is used to approximate shadowing effects. The latest radiation data available is from the year 2020. PV will be installed on a carport (see figure 2.1) with a fixed slope of 15° and a fixed azimuth angle of −4°. For the mounting place parameter, the option "building" matches the carport at the pilot site the best. Electrical PV system losses, which include all losses except the solar energy conversion efficiency of panels, are set to the default value of 14 % since no other information is available.

Table 2.5: PVGIS API parameters

Parameter	Value
Latitude	58.3782044°
Longitude	26.7505643°
Use horizon	1 (true)
Radiation database	PVGIS-SARAH2
Start year	2020 (latest)
End year	2020 (latest)
PV calculation	1 (true)
Peak power	30 kWp
Mounting place	Building
PV technology	crystSi (default)
System loss	14 % (default)
Tracking type	0 (false)
Angle (slope)	15°
Aspect (azimuth)	−4°

The obtained power values have a timestep of 1 h. The simulation timestep of 5 min is much smaller. Linear interpolation is applied to get the desired timescale. For interpolation, the values of the hourly data are assumed to be valid in the middle of each hour. Matlab provides a convenient function for the interpolation of one-dimensional data (see [38]). Figure 2.3 shows the interpolated PV generation profiles for both simulation scenarios. For simulation, negative power values are used to indicate generation. It can be seen that the power does not exceed the inverter rating which does not necessitate further data processing.
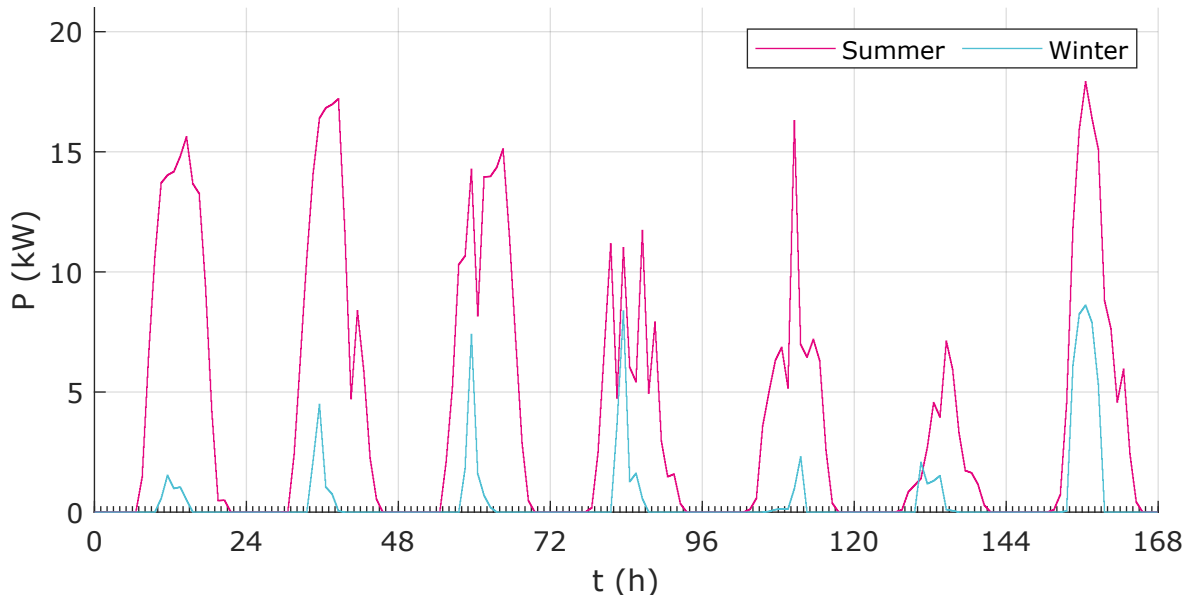
Figure 2.3: Interpolated PV generation profiles

The PV system model has no input that can be used for curtailment or other control actions. It only outputs the profile value $P_{PV,gen}$ at the current simulation timestep.

For one of the developed energy management strategies, PV forecasting is used (see

section 4.4). Forecasting is done for each day with a 1 h resolution. To include forecasting errors in the simulation, a forecasting model is required. A model similar to the one introduced in [39] is applied. In this model, a random (uniform probability distribution) relative error is added to the hourly PV generation data. The error limit is assumed to increase from zero up to ±50 % over 24 h in a linear way. Figure 2.4 shows an example of relative errors.
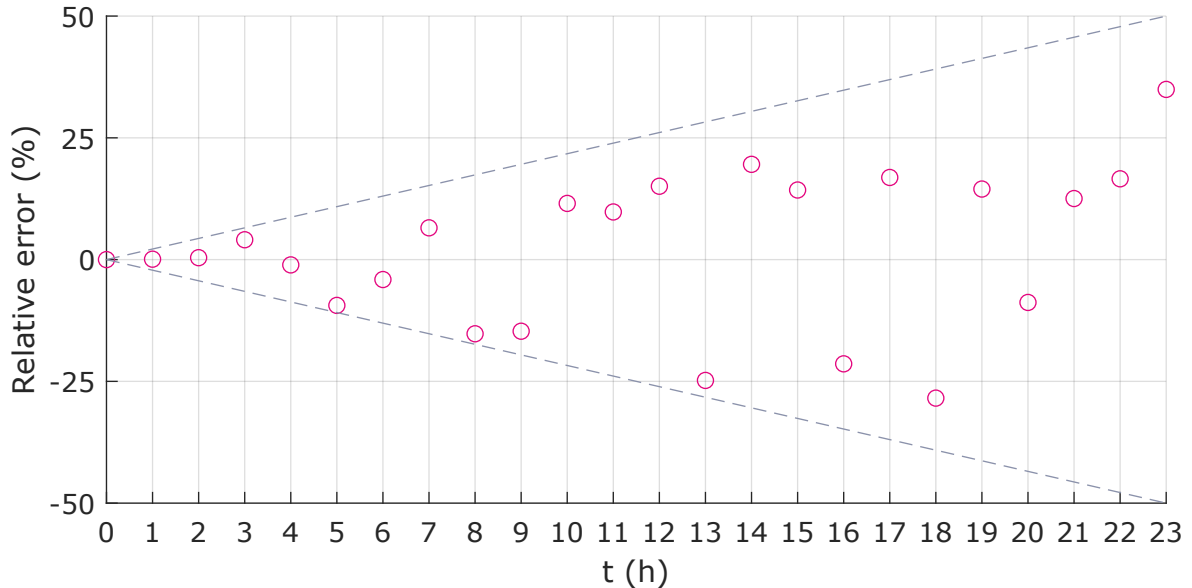
Figure 2.4: Example of relative prediction errors for PV forecasting model

2.4.3 Street lighting system

The street lighting system consists of uncontrollable loads. Thus, modelling with load profiles is suitable. Table 2.6 lists how the lights are distributed among the three feeders. Only the total number of lights per feeder is important since the simulation does not distinguish between the three phases.

Table 2.6: Street lighting feeder parameters

Feeder		No. lights			
Name	No.	L1	L2	L3	Total
Sõpruse jõe	1	3	4	4	11
Sõpruse jaam	2	3	3	4	10
Anne tn	3	9	6	5	20

No exact data for the power consumption of individual lights and their turn-on/turn-off times and dimming periods are known. But on-site measurements have been carried out from 01.05.2021 to 25.05.2022 on an hourly basis. The power was metered at the PCC which also includes the load demand of the small loads connected to the main bus (compare appendix A.1). This metering data can be still used for modelling. The summer scenario has to use the measurements from the year 2021 then. Figure 2.5 shows the measured load demand for both scenarios. Two things can be observed. First, the small

fluctuations that are caused by the small loads on the main bus. These fluctuations do not affect the simulation on a relevant scale and are therefore not filtered out. Second, consumption drops are visible during night-time. These are caused by dimming the lights at feeder 3 to 60 % and 40 %.
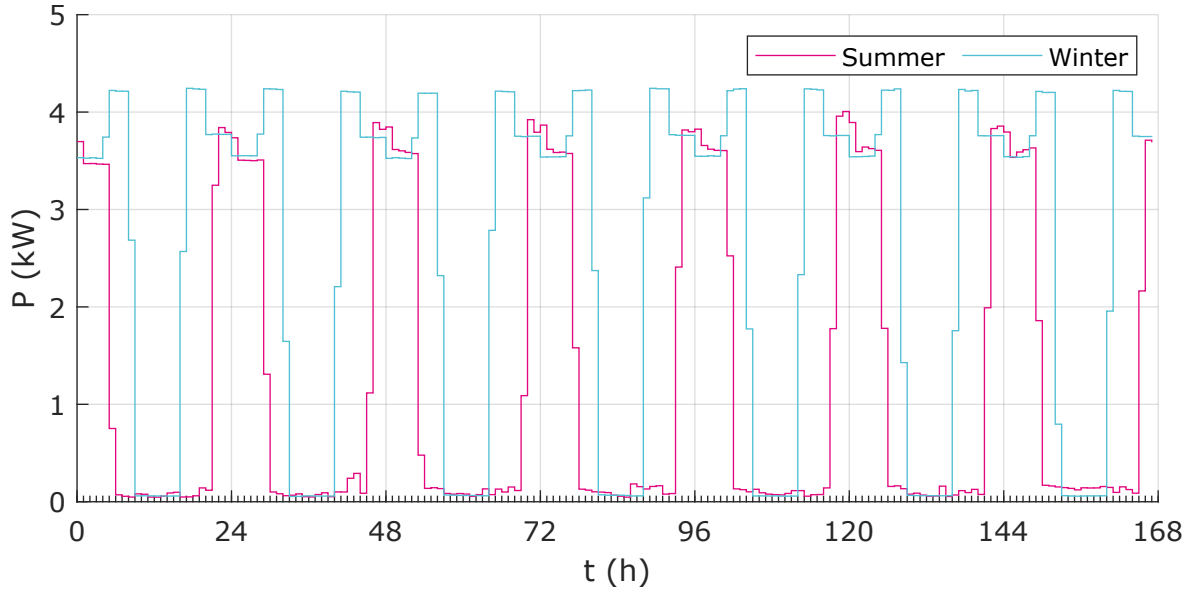
Figure 2.5: Street lighting measurements

To generate profiles for each street lighting feeder the measured power is distributed based on the number of installed lights (see equation (2.6)).

$$Scaling\ factor(Feeder) = \frac{Total\ lights(Feeder)}{\sum_{Feeder} Total\ lights(Feeder)} \qquad (2.6)$$

The dimming routine of the third feeder's lights is inevitably distributed to all three street lighting profiles. The consumption drops are only around 1 kW and are relatively small compared to the PCC power. Furthermore, for the economic analysis, only the total consumption is relevant. Therefore, the modelling error is negligible and does not influence simulation results. To get the desired timestep of 5 min, the same linear interpolation approach as in sub-section 2.4.2 is chosen. Appendix A.2 shows the street lighting load demand profiles for each scenario and each feeder.

Each of the three street lighting system models puts out the power demand of the current timestep. The sum of demand is denoted as $P_{SL,dem}$. Street lighting load demand is assumed to be deterministic and therefore known at any timestep.

2.4.4 Electric vehicle chargers

EV chargers are controllable loads that provide flexibility by DLC. V2G is considered to be not available here. The controller can set the maximum power limit for each charger, where 100 % means no limitation and 0 % means that the charger is not available for charging.

For EV charger modelling, power consumption metering data on an hourly basis is available as well. A 50 kW DC fast charger at a supermarket parking space (address: Marja 1a, Tallinn) was metered in 2021. Figure 2.6 shows the recorded profiles for both scenarios.
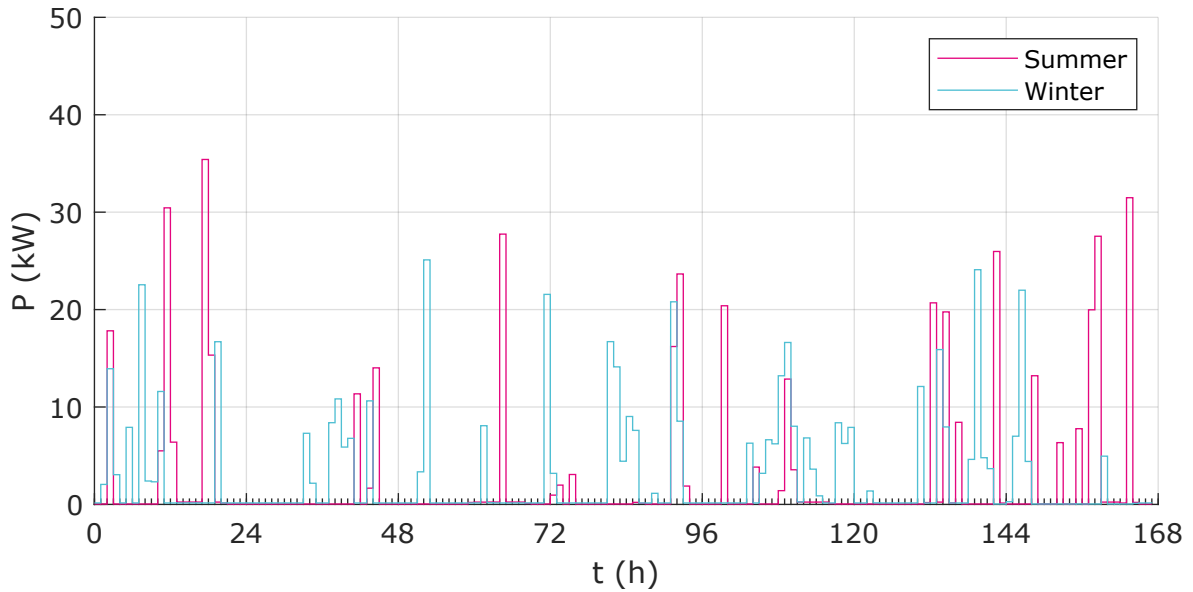
Figure 2.6: DC charger measurements

Since only one DC charger was measured, the four AC chargers use a scaling factor based on the rated charger power (see table 2.7, equation (2.7)).

Table 2.7: EV charger power ratings

Charger type	Symbol	Rated power (kW)
AC	$P_{AC,r}$	22
DC	$P_{DC,r}$	50

$$Scaling\ factor = \frac{P_{AC,r}}{P_{DC,r}} \qquad (2.7)$$

It is unlikely that five chargers have the same usage pattern. To add some variety, measurement data from different weeks are used. The DC charger model uses the week defined by the scenario, AC charger 1 uses the data from two weeks before, AC charger 2 the week before and the other two AC chargers the two weeks after. The scaled measurements for the AC chargers in addition to the DC charger are given in appendix A.3 to show the overall utilisation.

It can be seen that the hourly average power consumption is below the charger power ratings of 50 kW and 22 kW. EVs charge with high to maximum power for typically less than one hour. Linear interpolation would not produce accurate models in this case. Thus, a measurement-based approach is developed which, to the best of the author's knowledge, is novel. The main idea is to synthesise load demand profiles for EV chargers. Therefore in the first step, EV charging curves are generated as they occur in real-world situations. In the second step, the curves of individual cars are then arranged together for one week to give a load demand profile for each EV charger with the goal to match

the hourly measured energy consumption. The synthesised load profiles represent EV charger consumption in case of no limitation control. To account for limitation, profiles are further adjusted in the actual EV charger system models during simulation. This modelling approach is described in the following.

Generation of charging curves is based on the following two user mode definitions. It is assumed that cars arriving at a charger behave as one of these two user modes.

Definition (Time-based). *Either, cars charge for a specific time ΔT_{ch}, independent of the final SoC when leaving the charger.*

Definition (Target-based). *Or, cars charge until a target battery level $SoC_{EV,tgt}$ is reached, independent of the total charging time necessary.*

To generate practical charging curves $P_{EV,ch}(t)$ that can be used to synthesise demand profiles for chargers, information on EVs' charging characteristics is required. Many databases can be found on the internet that list data of tested EVs. Here, data from [40] is used. Maximum charging power related to the EV battery's SoC $P_{EV,ch}(SoC_{EV})$ is given from 10 % to 80 %. The database also gives the total charged energy within the tested SoC range. To add some degree of variety, the charging behaviour of a small car (Renault ZOE) and a big car (Tesla Model 3) is used. Table 2.8 lists the charged energy and figure 2.7 shows the charging characteristics of the two car models. Charging losses are neglected in the following.

Table 2.8: Total charged EV energy between 10 % and 80 % SoC, according to dataset [40]

Car model	$E_{EV,ch}$ (kWh)
Renault ZOE 52 kWh	36.9283
Tesla Model 3 LR (2021)	60.1438

To get accurate charging curves, the dataset points are linearly interpolated with index i ranging from 1 to a sufficiently large value of 1000. The EVs were tested at ultra-fast chargers where the EV itself is limiting the charging power. In the case of the MG with 22 kW and 50 kW chargers, the chargers themselves are limiting factors for the power (see sub-figure 2.7b). Therefore, thresholds based on the charger ratings are applied. Figure 2.7 illustrates the DC charger case.

The desired charging curves $P_{EV,ch}(t)$ are power related to time. Thus, a time axis needs to be computed. With the help of the total charged energy from table 2.8, each interpolated SoC value can be mapped to a specific energy in a linear way, starting with zero energy at 10 % SoC and the maximum charged energy at 80 % SoC. Further, each interpolated SoC value is already mapped to a maximum charging power by the dataset. With the energy and charging power sets, a set of time values can be calculated that represents the time axis (see equation (2.8)). It is assumed that for reaching the next energy value, the average charging power between these points is valid.

$$t[i] = \begin{cases} 0 & \text{if } i = 1, \\ t[i-1] + \frac{E[i]-E[i-1]}{(P_{EV,ch}[i]+P_{EV,ch}[i-1])\cdot 0.5} & \text{otherwise.} \end{cases} \tag{2.8}$$

where t – set of time values representing the time axis,
E – set of charged EV energy,
$P_{EV,ch}$ – set of EV charging power,
i – index for sets.

Figure 2.8 shows the derived charging characteristics $P_{EV,ch}(t)$ and $SoC_{EV}(t)$ for the small EV at the DC charger. When choosing a SoC value at arrival $SoC_{EV,arr}$ and a desired charging time ΔT_{ch} or a desired target SoC value $SoC_{EV,tgt}$, the corresponding part of the charging curve can be picked from the plot. Figure 2.8 shows examples for both user modes.

With the battery SoC at car arrival, the start of the charging curve can be found (dashed and dotted arrows). The start of the charging curve is common for both examples. In
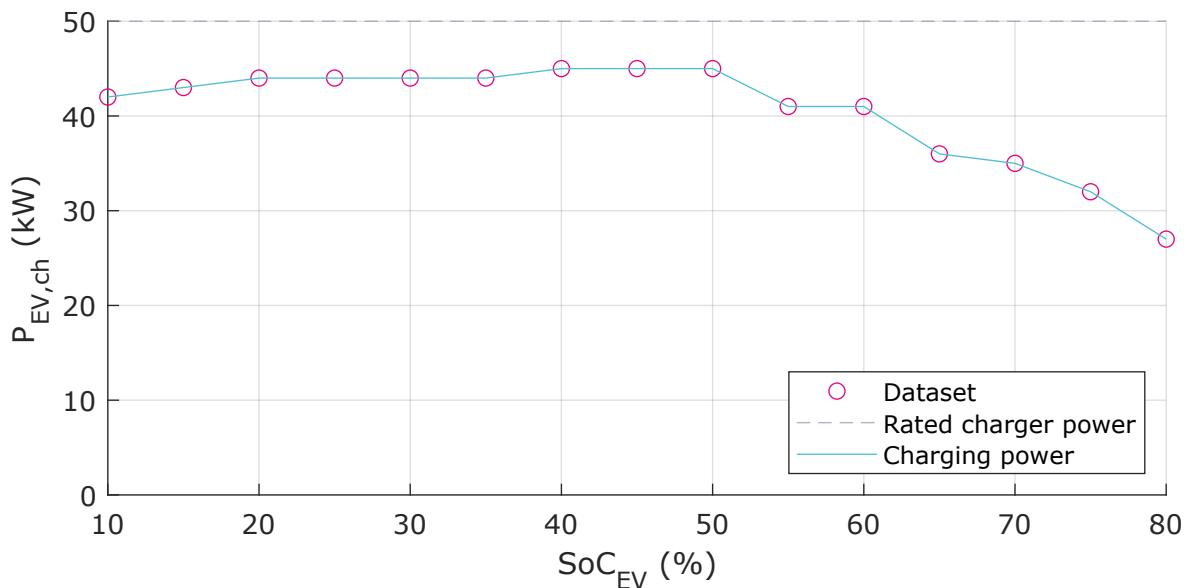
(a) Renault ZOE
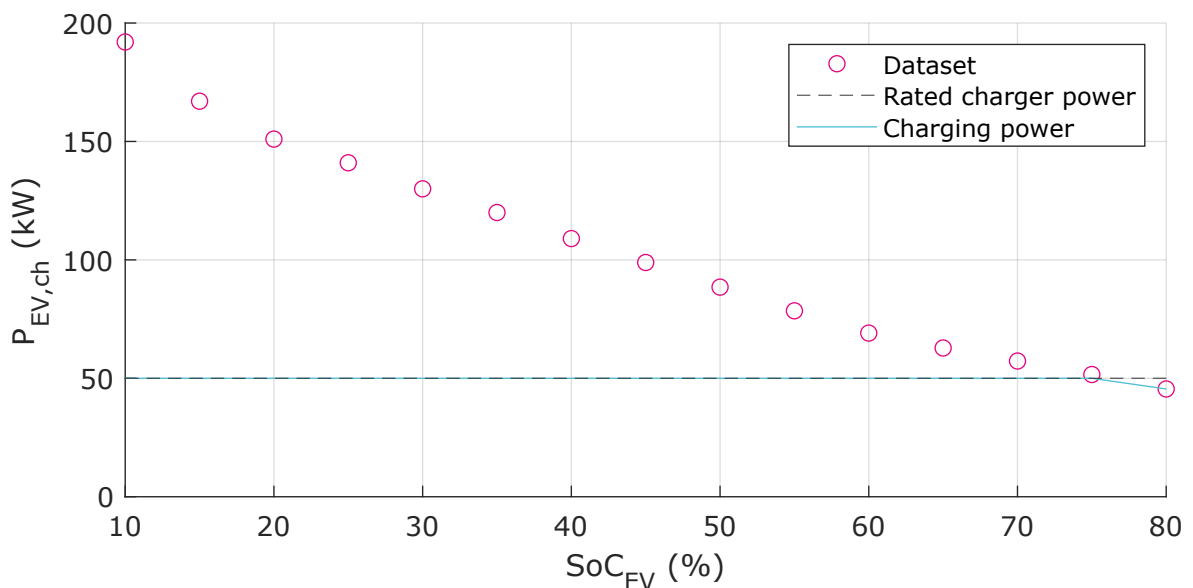
(b) Tesla Model 3

Figure 2.7: EV charging characteristics, maximum charging power related to SoC

47
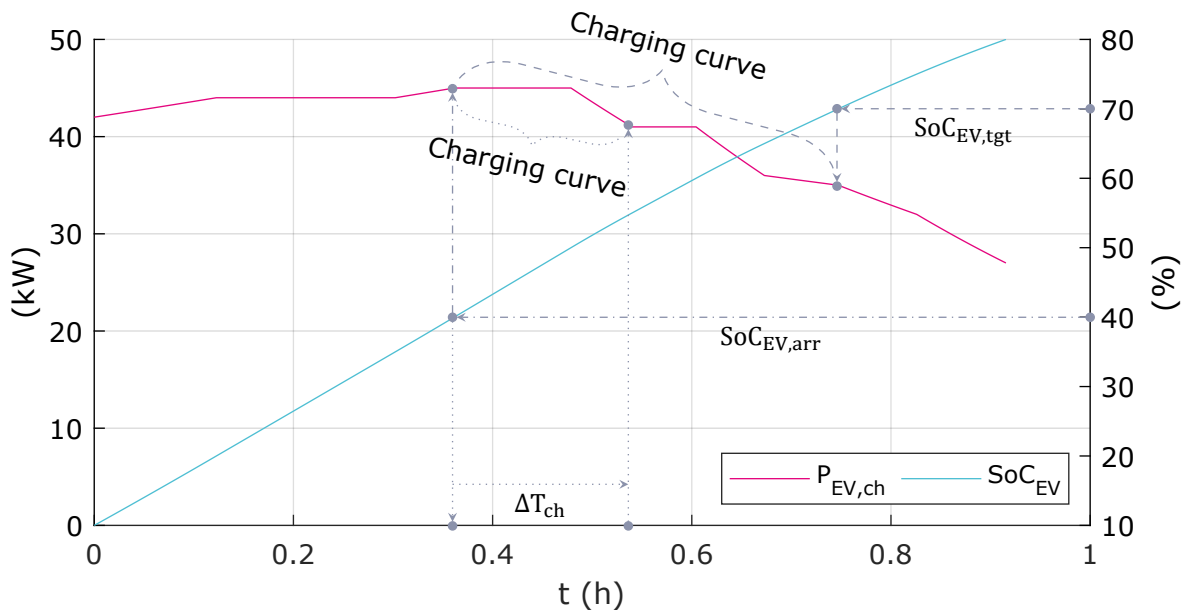
Figure 2.8: Derived charging characteristics for Renault ZOE, dotted: example time-based car, dashed: example target-based car, dash-dotted: common for both examples

the case of time-based cars (dotted arrows), the stop time is determined by adding the desired charging time to the start time. Based on the stop time, the stop point of the charging curve is selected. For target-based cars (dashed arrows), the target SoC determines the stop point of the charging curve. The charging curve between the start and stop points is then converted to the simulation timestep by averaging. The result is an approximation of the charging curve with respect to given EV parameters.

The generation of these parameters is subject to the constraints in table 2.9. All EVs have a general SoC limit based on the range given by the dataset. Target-based cars want to increase their battery charging level at least by 20 %. The minimum charging time for time-based cars is two timesteps or 10 min. The maximum time a car will stay at a charger is equal to the time when Estonian CO Enefit applies additional time tariffs (see [41]). This implies the assumption that every customer wants to avoid these surcharges. The time after this additional tariff is applied depends on the charger type. It is longer for AC chargers. The functionality of generating charging curves is encapsulated into a class object to simplify usage in the next modelling step.

Table 2.9: EV charging curve constraints

Parameter	Value
$SoC_{EV,min}$	10 %
$SoC_{EV,max}$	80 %
$\Delta SoC_{EV,min}$	20 %
$\Delta T_{ch,min}$	$\frac{10}{60}$ h $(2 \cdot \Delta T)$
$\Delta T_{ch,max,AC}$	3 h
$\Delta T_{ch,max,DC}$	1 h

Synthesising of load demand profiles requires preprocessing of the measurement data to ease the problem of fitting the generated charging curves to the measured profile. The measured power consumption data is interpreted as reference energy for each hour. First of all, the threshold $\Delta E_{min,idle}$ is applied in order to filter out low energy values due to idle consumption of the charger. Because of the 5 min timestep, a minimum chargeable energy per timestep exists. The idle threshold is chosen according to equation (2.9a) to filter also the infeasible energy reference values. Here, $P_{charger,r}$ denotes the power rating of the considered charger, either $P_{AC,r}$ or $P_{DC,r}$. The maximum charger power gives a good approximation of the minimum chargeable energy. The energy reference profile can be then split into periods of consumption. A period is limited by hours of zero energy. Each period consists of one or multiple hours. If a period is only a single hour, the minimum charging time of two timesteps requires an additional threshold $\Delta E_{min,sh}$ which is twice the idle threshold (see equation (2.9b)).

$$\Delta E_{min,idle} = P_{charger,r} \cdot \Delta T \tag{2.9a}$$

$$\Delta E_{min,sh} = P_{charger,r} \cdot \frac{\Delta T_{ch,min}}{\Delta T} \tag{2.9b}$$

Figure 2.9 shows the preprocessed energy reference profile and the resulting consumption periods for the DC charger in summer.
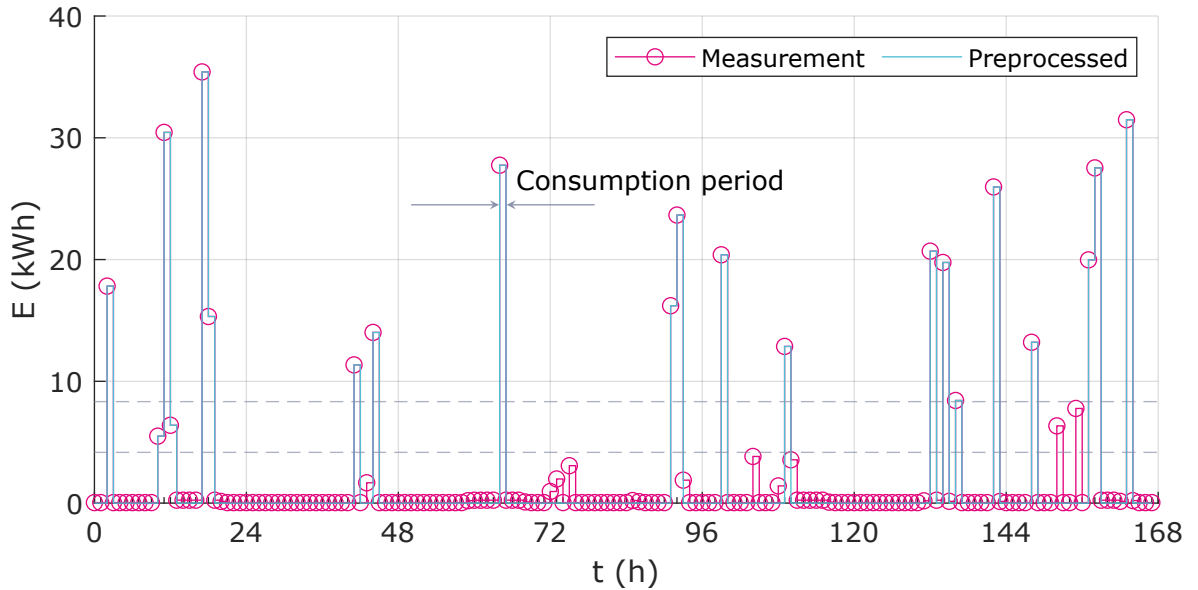
Figure 2.9: Preprocessed measurements for DC charger in summer, lower dashed line: idle / minimum consumption threshold, upper dashed line: single hour minimum consumption threshold

In the next step, the preprocessed reference profile is used in the synthesising algorithm. The synthesising algorithm breaks down the fitting of the charging curves by synthesising one consumption period after the other. The high-level program flow is depicted in figure 2.10 for one period. In general, for each period, charging (power) curves and related metadata are generated and saved as time series data. Metadata consists of the user type, the car model, and a counter for the total number of cars that arrive. After every period is processed, the time series data is compiled to get a full week.

In detail, the time series data for one period is initialised at first. It is referred to as
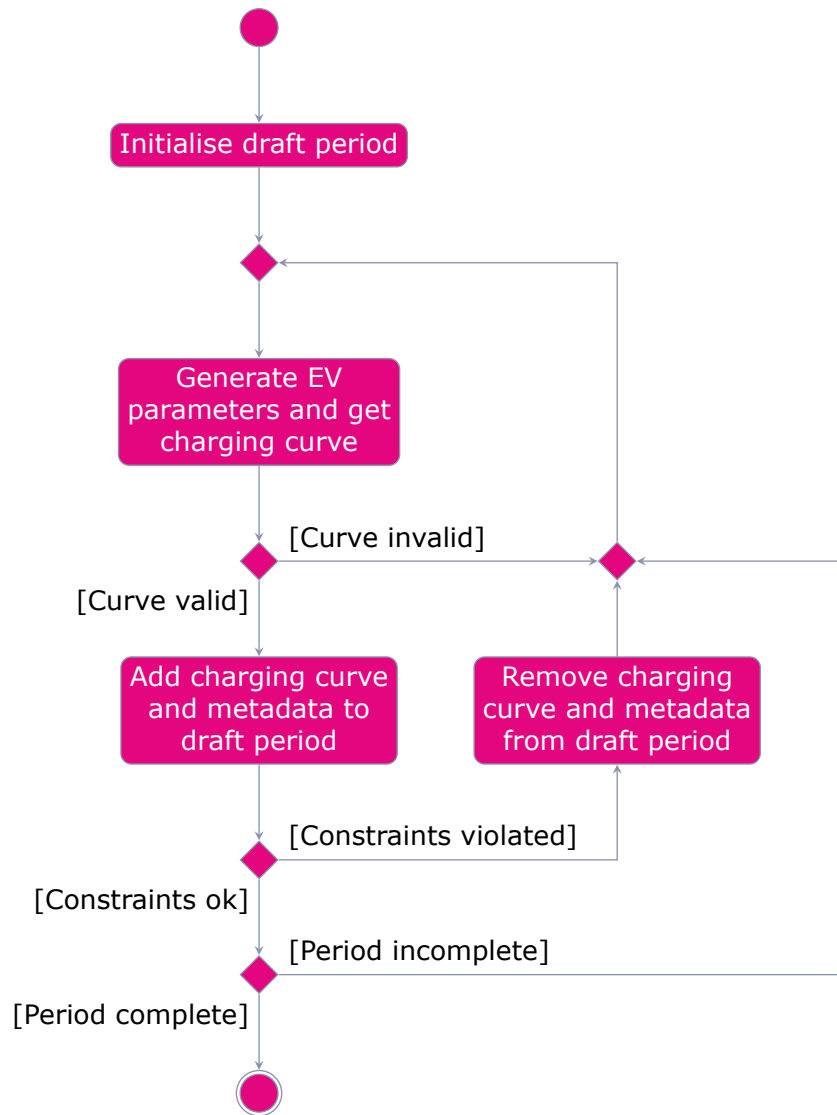
Figure 2.10: Flow chart for synthesising one consumption period

the draft period. Then EV parameters are randomly (uniform probability distribution) generated within the specified limits. The parameters are the car model (Renault or Tesla), the SoC at arrival $\text{SoC}_{\text{EV,arr}}$, the user type (time or target-based), and depending on that, either a charging time ΔT_{ch} or a SoC target $\text{SoC}_{\text{EV,tgt}}$. These parameters are used to generate a charging curve. In addition, a random duration of at maximum 1 hour is generated that represents the pause time between the departure of the previous car and the arrival of the new one. The charging curve is checked for validity. The curve is valid if EV parameters are valid and a curve is returned from the car object, and when the length of the curve does not violate the end of the consumption period. If the curve is invalid, the previous step is repeated.

The valid charging curve and related metadata are added to the draft period at the stop time of the previous car plus the pause time. Then constraints are set up and checked. The main constraint is that the hourly energy consumption of the so far synthesised hours must match the reference within a tolerance of $\pm\Delta E_{\text{min,idle}}$. This tolerance eases the synthesising procedure while ensuring sufficient fitting accuracy. In addition, it must be ensured that the added curve does not hinder fitting further curves.

If the draft period complies with the constraints, the period is checked again for completeness. For a complete period, every hourly energy consumption must match the reference within the tolerance range. Unless the draft period is complete and can be saved to the synthesised week profile, new parameters are generated and charging curves are added. In case the draft period violates constraints, the latest curve and metadata are removed from the draft before trying a new attempt.

Figure 2.11 shows the synthesised load demand for the DC charger in the summer scenario. For clarity, only Monday is depicted. It can be seen that the load demand profile has now narrow peaks that are close to the charger rating. This reflects the load demand patterns of an EV charger more realistically compared to the hourly measurements. Appendix A.4 figure A.4 shows the whole profile with metadata. By calculating the hourly
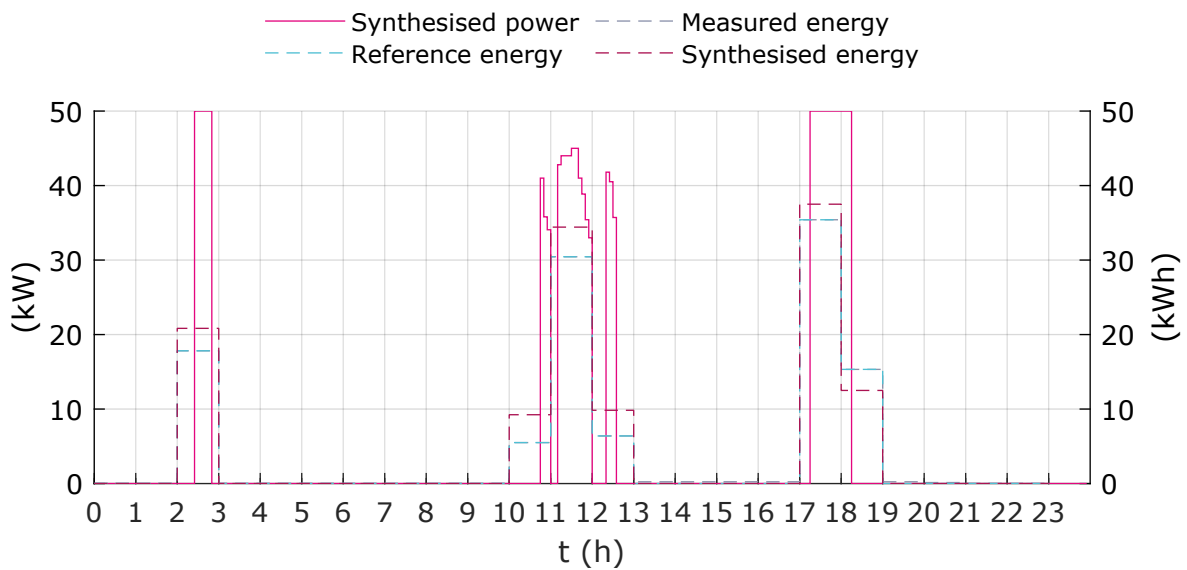
Figure 2.11: Comparison of synthesised load demand and energy reference profile of DC charger in summer scenario on Monday

energy consumption of the synthesised load demand profile, it can be compared to the measured data and the preprocessed energy reference profile. Figure 2.11 shows that the consumption is sufficiently matched. The validation for the whole week is given in appendix A.4 figure A.5 as well.

The synthesising algorithm is used for the five chargers present in the MG and both scenarios. Appendix A.5 shows the load demand profiles that are used for the next step of EV charger modelling. The profiles set the maximum energy that can be supplied to EVs. Without charger limitation, the energy of all AC chargers is 1.0688 MWh (summer) and 1.3090 MWh (winter). For the DC charger, it is 0.4186 MWh (summer) and 0.4538 MWh (winter).

Electric vehicle charger system model has one setpoint input that sets the allowed power limit. It ranges from 0 % to 100 % or from zero to maximum/rated power. The system outputs the power demand of the EV ($P_{AC,dem}$ or $P_{DC,dem}$), a binary/boolean signal that indicates the presence of a charging car (OCC_{AC} or OCC_{DC}), and the actual charging power that is used in the MG model.

The limitation of charging power affects the charging behaviour of cars. The following rules are defined. A time-based user will stay until the desired charging time is reached, independent of the amount of limitation. Though, target-based users are affected by the limitation and therefore will stay longer up to the maximum charging time defined in table 2.9. In the model, unsatisfied charging power is then added to the load demand of the next timestep. For simplicity, the maximum charging power of the EV is not considered in this step. If demand exceeds the charger rating, the difference is further pushed to future timesteps. Since both EV models are able to charge with powers close to the DC charger rating (compare figure 2.7), the error is negligible. When target-based cars prolong their charging time, other cars may want to arrive. In this case, the following car is cancelled and removed from the profile respectively. The user mode and the car count from the metadata time series are used for calculations.

3 DEVELOPMENT OF BUSINESS MODELS

For evaluating economic feasibility, business models need to be developed. This chapter describes the financial data that is used and how energy trading works based on market definitions.

Expenditures can be separated into capital expenditure (CapEx) and operational expenditure (OpEx). Since prices depend on the type of enterprise or type of legal person, only net prices excluding value-added tax (VAT) are used. Further, the high inflation rate of 24.1 % in Estonia (September 2022) affects the comparability of costs and prices from different sources [42]. Thus, the values presented in sections 3.1 and 3.2 have to be seen as guiding values. For sources that list values in US dollars, a conversion rate to euro of 1 is used (October 2022 [43]).

3.1 Investments

CapEx is the capital investments used for purchasing assets with a specific lifetime [44]. Investments are relevant for calculating the asset's payback period (PBP), which is one indicator of economic feasibility. Table 3.1 lists the capital investments and the typical lifetimes of the assets.

Table 3.1: Capital investments and lifetime of assets

Asset	Capital investment (€)	Lifetime (years)
Grid	0.00	–
Street lighting	0.00	–
PV	$30 \cdot 556.99 = 16{,}709.70$	25
BESS	$40 \cdot 1{,}876.00 = 75{,}040.00$	10
AC charger	$4 \cdot 1{,}458.38 = 5{,}833.52$	10
DC charger	27,000.00	10

Since the grid with street lighting already exists, it can be considered as paid-off. Investments necessary for reconstruction measures at the PCC are neglected due to a lack of more detailed information. Therefore, no investments are set for the owner TC. For the PV system, initial investments and the lifetime are given in [45] as 556.99 €/kWp and 25 years for the Baltic states. For absolute investments parameters defined in section 2.4 are used. For BESSs based on Li-ion technology, [46] states costs related to installed power and energy. Costs based on power result in higher absolute investment costs (1,876.00 €/kW vs. 469.00 €/kWh) and are used in this case. The lifetime of Li-ion batteries is ca. 10 years [46]. For estimating the CapEx of EV chargers, that are owned by the CO, products from manufacturer ABB are selected. The 22 kW chargers are Terra AC wall boxes (further information: [47]). Prices for one AC charger are taken from [48] (1,458.38 €). For the fast charger, an ABB Terra 54 UL DC charging station is chosen (further information: [49]). The price for that is 27,000.00 € [50]. Additional commissioning costs are neglected since COs are assumed to get lower prices due to quantity at purchase. A typical charger lifetime of 10 years is given in [51].

The total capital investments for the LEC are 91,749.70€ and the CO has to invest 32,833.52€. The assets' lifetime is averaged, weighted by the components' investments, to get one lifetime for each owner. The asset lifetime for the LEC is 12.73 years and for the CO 10 years. It is challenging to find investment costs that include the latest price developments. For analysis in this thesis, mentioned costs are used. But it is recommended to consider more accurate data, e.g. from manufacturer enquiries, in the future.

3.2 Costs and revenues

OpEx comprises expenditures for operation from day to day [44]. It can be generally separated into costs that depend on energy trading and fixed costs that have to be paid for a specific period of time. The same classification applies to revenues. These types of costs and revenues are referred to as variable and fixed. The following two sub-sections show how prices are generally selected. The markets, defined later, determine whether a price leads to revenue or cost from the viewpoint of each of the three owners.

3.2.1 Variable

Variable costs and revenues are made up of electricity market prices, the variable part of the grid tariff, and EV charger tariffs. The electricity market uses ToU tariffs here. Therefore, hourly day-ahead market price data for the year 2022 is retrieved from the Nord Pool Spot market (NPS) [52]. Day-ahead means that market prices are known a-priori for one day. In the following, the market price is referred to as Pr_{NPS}.

Electricity providers (EPs) add a profit margin on top of the market price. It is denoted as Pr_{EP}. Web portal [53] compares the margins of several providers. Eesti Gaas offers the smallest margin of 0.003 €/kWh without additional monthly fees [54]. This value is added to the NPS price when the MG imports energy from the main grid.

The grid tariff components are taken from the price list of the Estonian DSO Elektrilevi [55]. Prices are based on the PCC amperage capacity of the MG (40 A, see appendix A.1) and network package 4 (high consumption over 2900 kWh/year) valid from 01.06.2022. Table 3.2 lists the price components that make up the variable grid tariff. The pricing depends on day and night-time, and also on business days or weekends. This pricing scheme is illustrated in figure 3.1. The sum of the variable grid tariff components depending on time is denoted as $Pr_{grid,var}$.

Table 3.2: Price components of variable grid tariff

Component	Price (€/kWh)
Grid tariff day	0.0311
Grid tariff night	0.0178
Renewable energy fee	0.0113
Electricity exercise duty	0.0010

Figure 3.1: Daytime and night-time grid tariff pricing [55]

For EV charging, common prices in Estonia are taken from the CO Eleport, which are not subject to ToU but fixed tariffs (see table 3.3) [56].

Table 3.3: EV charger tariffs

Charger type	Symbol	Price (€/kWh)
AC	Pr_{AC}	0.33
DC	Pr_{DC}	0.39

Figure 3.2 shows the spot market prices for both simulation scenarios and the variable part of the grid tariff. It can be seen that the energy crisis has a big impact on the NPS price for the summer scenario.
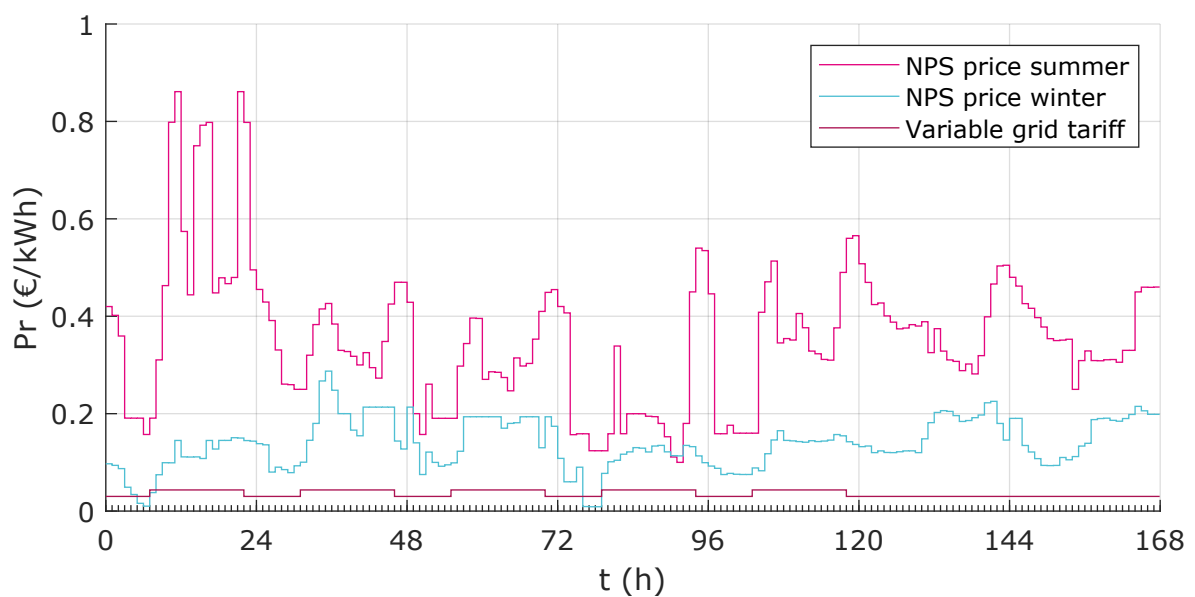
Figure 3.2: NPS prices and variable grid tariff

3.2.2 Fixed

Fixed costs and revenues are based on the fixed part of the grid tariff. It is a monthly fee of 25.29 €/month [55]. It is denoted as $Pr_{grid,fix}$.

Besides the fixed grid tariff, the maintenance costs of different assets are considered (see table 3.4). For TC assets, maintenance costs are neglected since maintenance is part of public services and does not affect the economic feasibility of the MG. The maintenance cost for PV systems in the Baltic states is 5.57 €/(kWp · year) [45]. In [46], 10.00 €/(kW · year) is stated for Li-ion BESSs. Here again, maintenance cost based on installed power is taken. Recommendations for budgeting the maintenance cost of EV chargers are given in [51]. Level 1 and Level 2 chargers (AC chargers) require around 100.00 €/year and level 3 chargers (DC chargers) 400.00 €/year.

Table 3.4: Maintenance cost of assets

Asset	Maintenance cost (€/year)
Grid	0.00
Street lighting	0.00
PV	$30 \cdot 5.57 = 167.10$
BESS	$40 \cdot 10.00 = 400.00$
AC chargers	$4 \cdot 100.00 = 400.00$
DC charger	400.00

The fixed grid tariff fee and maintenance costs are normalised to one timestep to have a common basis.

3.3 Peer-to-peer trading market

With the defined prices, a business model is developed for the MG. It specifies how the costs and revenues flow between the involved parties. Since the MG has multiple owners, a peer-to-peer (P2P) trading market is defined. The parties are the three owners of the MG which are involved in intra-MG trading. But also the EP and DSO, which represent the connection to the main grid, and the EV charger customers (abbreviated as AC and DC cars). This trading scheme is referred to as the P2P market. Figure 3.3 illustrates the power/energy flow (arrow direction) and the associated electricity pricing.

The EP and DSO define the prices for TC when importing energy from the main grid to the MG (see equation (3.1a)). TC can export energy to the main grid based on the market price. Grid tariff and margins of the EP do not apply in this case (see equation (3.1b)).

$$Pr_{imp}[t] = Pr_{NPS}[t] + Pr_{EP}[t] + Pr_{grid,var}[t] \tag{3.1a}$$

$$Pr_{exp}[t] = Pr_{NPS}[t] \tag{3.1b}$$

The CO sells energy to its customers with fixed charging tariffs specified in table 3.3. Trading energy with the main grid and selling energy to EV charger customers define revenue coming from outside the MG. Generally, this is also valid for cost.

The internal revenue is fixed and consequently, intra-MG trading represents a closed system in the sense that the available revenue can only be shared between the owners. In general, TC sells energy to both underlying owners CO (AC chargers) and LEC with an added margin but buys energy only at the export price to avoid losses when further exporting to the main grid. The LEC can also sell energy to the CO which is used to supply the DC charger. In this case, the LEC adds again its own margin.
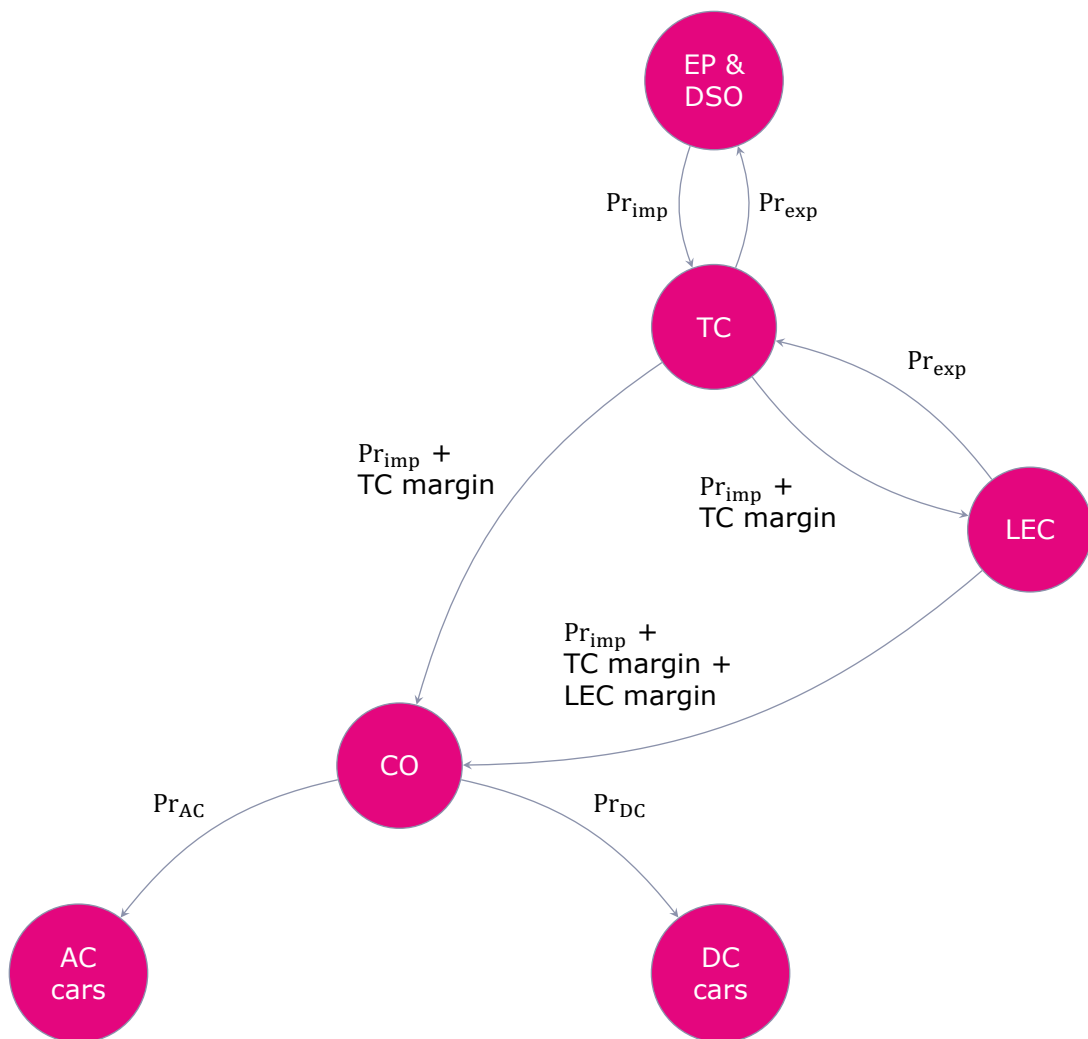
Figure 3.3: P2P energy trading scheme, arrow tip indicates direction of energy flow

Fixed OpEx is treated as follows. While maintenance costs are carried by each owner separately, the fixed part of the grid tariff, which has to be paid by TC, is shared as well. Sharing is defined similarly to the P2P energy trading scheme. The fixed grid tariff cost plus the margin of TC is split 50/50 and passed on to the CO and LEC. The LEC adds again a margin to its cost which has to be paid by the CO.

3.3.1 Business goals

The margins are important parameters of the business model that influence how cost and revenue are shared within the MG. Table 3.5 lists the relative margins. To reason the choice, the following assumptions for the owners' business goals are made.

Table 3.5: P2P trading margins

Owner	Symbol	Margin (%)
TC	m_{TC}	0
LEC	m_{LEC}	10

The TC municipality is interested in having more of these kinds of MGs to be able to provide the distribution grid for novel EV charging services and to avoid costly infrastructure enhancements. Consequently, the MG has to be attractive to other parties like LECs and COs. Thus, no extra margin is charged and TC only conveys energy between the main grid and the other participants. Though, it is not intended that the cost of TC for operating the street lighting system increases by P2P-trading energy compared to the case without MG.

The two other owners, the LEC and the CO, are interested in making profitable investments. An investment is profitable when the investment is paid off in as short as possible time or in other words when the break-even point is reached as soon as possible. For each of the two owners, more profit means better individual economic feasibility. Thus, the MG's economic feasibility is increased when exclusively both parties have profitable investments, and therefore, the profit margin of the LEC is set to a relatively low value of 10 %. This choice tries to trade off between the profitability of its own investments and communal profitability.

3.4 Collective revenue sharing market

It is relatively easy to define the economic feasibility of single-ownership MGs. The more profit, the better. In the multi-ownership scenario, each owner defines economic feasibility individually, which is not equal to the MG's economic feasibility. For instance, if the LEC increases its profit by a large amount, TC and/or the CO will lose profit and eventually become unviable. To be able to evaluate the fairness aspect of economic feasibility, a second model called collective revenue sharing (CRS) is developed that tries to represent optimal revenue sharing within the MG in a collaborative manner. It is used later to define fairness metrics when it comes to analysing the performance of energy management strategies (see section 5.1).

Figure 3.4 illustrated how this market model works. In this case, variable grid tariff cost is not passed to the LEC or the CO and intra-MG prices are set to zero. The individual maintenance costs are not shared and the fixed grid tariff fee is completely carried by TC. The revenue streams that come from outside the grid are gathered over the simulation time of one week. External revenues are generated by selling energy to the main grid and to the customers of the EV chargers. Based on the assumptions made for the

owners' business goals in sub-section 3.3.1, the total revenue is shared. First, the cost of TC, which exceeds the operational cost of the street lighting system, is covered. The remaining revenue is then split between the LEC and the CO based on the volume of investments (CapEx) made.

Collect revenue over whole week:

- Energy sold to main grid
- Energy delivered to EVs at AC chargers
- Energy delivered to EVs at DC charger

Total revenue

Cover cost of TC:

- Calculate street lighting cost without MG
- Refund additional cost
- Calculate remaining revenue

Remaining revenue

Split remaining revenue:

- Based on capital investments of LEC and CO
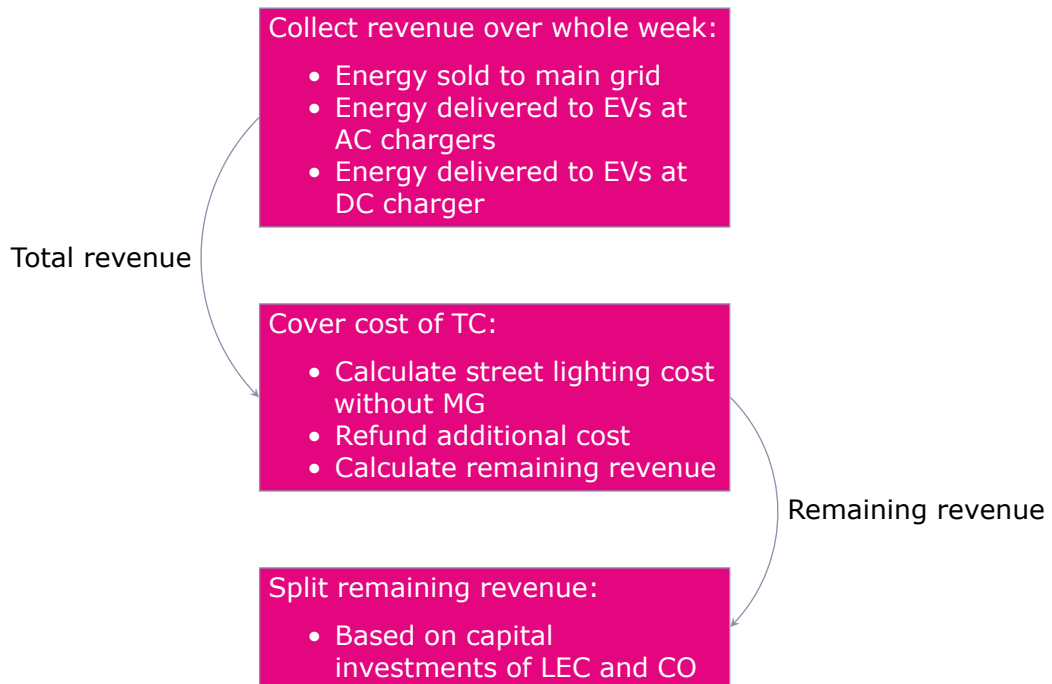
Figure 3.4: CRS scheme

4 DEVELOPMENT OF ENERGY MANAGEMENT STRATEGIES

The goal of this thesis is to develop simplified energy management strategies to increase the economic feasibility of the MG. Since the MG has multiple owners involved, classical approaches that try to minimise total cost cannot be applied.

The basic layout of the control system is defined in section 4.1. Based on this, three strategies have been developed. The baseline strategy, which represents a simple and robust rule-based approach, is covered in section 4.2. The price-sensitive strategy including economic decisions based on the market price is introduced in section 4.3, and section 4.4 presents the scheduling strategy.

4.1 Control system

The control loop is depicted in figure 4.1. It consists of a centralised tertiary-level controller that performs energy management. The controller outputs are the setpoints that have to be implemented by the controllable units inside the MG model. The setpoints are the power output of the BESS and the power limits for each of the four AC chargers and the DC charger. All setpoints use the value ranges defined in tables 2.3 and 2.7. It is assumed that the power at the PCC, the SoC, and the power output of the BESS can be measured. These metering devices are sited in a container at the PCC. Further, the EV chargers send boolean/binary (false/true or 0/1) status signals to the controller to indicate whether they are occupied or not together with the power demand for one timestep. The control outputs are a function of the measured quantities. Each iteration of the control loop equals one simulation timestep.

Tertiary-level controller (EMS)

Measurements:

- $P_{PCC,meas}$
- $P_{BESS,meas}$
- SoC_{BESS}
- OCC_{AC}^k, $P_{AC,dem}^k$, $k \in \{1, 4\}$
- OCC_{DC}, $P_{DC,dem}$

Setpoints:

- $P_{BESS,set}$
- $P_{AC,set}^k$, $k \in \{1, 4\}$
- $P_{DC,set}$

MG model

Figure 4.1: Basic layout of control system

Based on the measurement signals, the power flow values at each node can be estimated since the power demand for street lighting is quasi-deterministic. To simplify the simulation, the power flow at each node is assumed to be known for the current timestep. Control loop delays or the behaviour of underlying controllers are neglected.

The following intermediate variables are defined to set up the control strategies. They are calculated for each timestep. The PV excess power is considered the sum of all uncontrollable DG units (PV system) and the uncontrollable loads (street lighting system). If it is positive, excess power is available (see equation (4.1)). PV excess power determines also how much power reserve is available for the controllable loads.

$$P_{PV,excess} = -\left(P_{PV,gen} + P_{SL,dem}\right) \tag{4.1}$$

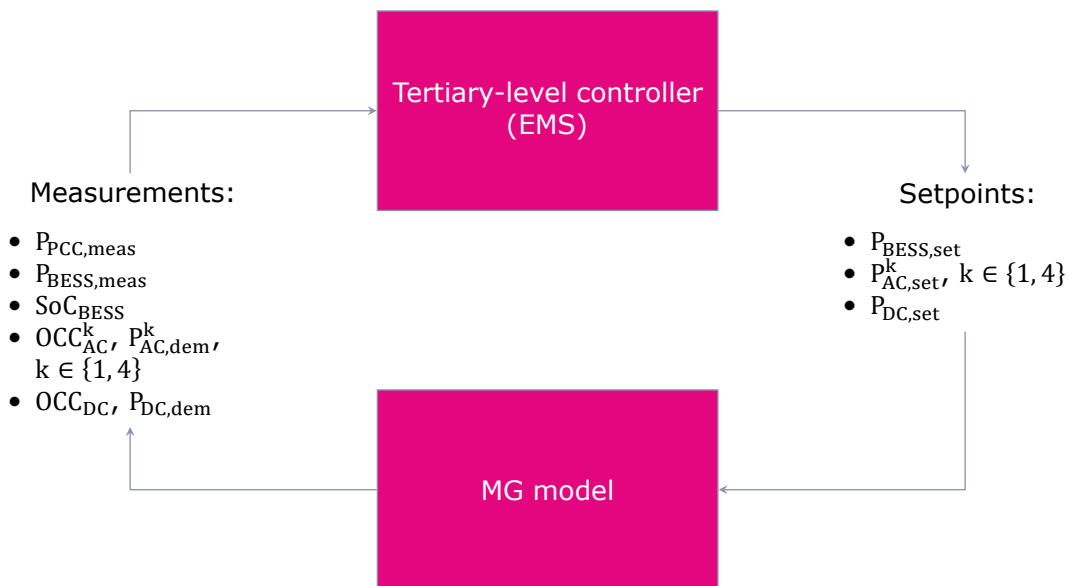The maximum charging and discharging power of the BESS are constrained by high or low SoC levels. In particular, the BESS power setpoint is infeasible if the resulting charged or discharged energy for one timestep would violate the SoC limits. These available charging and discharging powers are calculated to avoid setting infeasible setpoints (see equations (4.2a) and (4.2b)).

$$P_{BESS,ch,avail} = \frac{\left(SoC_{BESS,max} - SoC_{BESS}\right) \cdot E_{BESS} \cdot \frac{1}{\eta_{BESS,ch}}}{\Delta T} \tag{4.2a}$$

$$P_{BESS,dis,avail} = -\frac{\left(SoC_{BESS} - SoC_{BESS,min}\right) \cdot E_{BESS} \cdot \eta_{BESS,dis}}{\Delta T} \tag{4.2b}$$

Also, the limited PCC capacity constraints the feasible BESS setpoints in case of no EV chargers are active. The available power reserves for this case are formulated in equations (4.3a) and (4.3b).

$$P_{BESS,ch,res} = P_{PCC,max} + P_{PV,excess} \tag{4.3a}$$

$$P_{BESS,dis,res} = -P_{PCC,max} + P_{PV,excess} \tag{4.3b}$$

For convenience, the numbers of occupied AC and DC chargers are denoted as follows (see equations (4.4a) and (4.4b)). The occupied signals are interpreted as binary values (0: free, 1: occupied).

$$N_{occ,AC} = \sum_k OCC_{AC}^k, \quad k \in \{1, 4\} \tag{4.4a}$$

$$N_{occ,DC} = OCC_{DC} \tag{4.4b}$$

Further, the total load demand of all chargers is defined in equation (4.5) as the sum of AC and DC charger load demand.

$$P_{EV,dem} = \sum_k P_{AC,dem}^k + P_{DC,dem}, \quad k \in \{1, 4\} \tag{4.5}$$

EV chargers provide more flexibility since their feasible setpoints do not depend on the SoC compared to the battery. Thus, BESS control is executed at first. Based on the PV excess power and the power setpoint for the BESS, the maximum amount of power that

can be reserved for the EV chargers is determined with equation (4.6).

$$P_{EV,res} = P_{PCC,max} + P_{PV,excess} - P_{BESS,set} \tag{4.6}$$

These signals can be used for energy management strategies. Strategies are in principle divided into the control of the BESS first and then the limitation of the EV chargers. The approaches are described in the next sections.

4.2 Baseline

As concluded in section 1.4, it is preferable to keep the control approaches as simple and robust as possible. The first strategy is developed based on this paradigm. Therefore, it is called the baseline. The BESS control enacts peak shaving by trying to store unused and cheap PV energy to make it available when the MG is in deficiency. This basic idea is widespread and can be found for instance in [57]. EV charger limitation control is done based on a lookup table.

Pseudo code in algorithm 4.1 shows the implementation of the baseline energy management strategy in detail. The battery is charged with a fixed rate, set to the PCC power capacity when excess PV power is available and at maximum, only one AC charger is occupied. This additional AC charger rule avoids that the battery is unavailable in case chargers are occupied for a long period. Charging power is limited by the BESS availability and the reserve (equations (4.2a) and (4.3a)) through a minimum operation. If no PV excess power is available or if more than one AC charger is in use, then the BESS is discharged at the same fixed rate. The goal is to support the EV chargers and reduce the energy that needs to be imported from the main grid. The discharging power is limited to availability and reserve represented by a maximum operation (equations (4.2b) and (4.3b)). In this case, limitation based on the BESS charging reserve is included to avoid relying on the EV load demand signals for increased robustness. The BESS setpoint is also limited by the maximum charging or discharging power defined in table 2.3, which is not depicted in the pseudo code. In case none of the two aforementioned conditions is fulfilled, the battery output is set to zero.

Based on the BESS setpoint the total available power for the EV chargers can be calculated according to equation (4.6). For limitation control of the EV chargers, a fixed scheme is developed. The task of the charger control is to assign $P_{EV,res}$ to the five chargers. Since the DC charger has a higher tariff and therefore can generate more revenue (see table 3.3), there is less limiting. Table 4.1 shows how the power reserve is split based on the number of active chargers $N_{occ,AC}$ and $N_{occ,DC}$.

It can be interpreted as a lookup table (LUT) with $N_{occ,AC}$ and $N_{occ,DC}$ as inputs. The percentage values indicate how much of the reserve is assigned to which type of charger. For instance, if two AC chargers and one DC charger are occupied, each AC charger gets 20 % of the reserve while the DC charger gets 60 %. In total always 100 % of the reserve is assigned. The resulting powers are then set as power limits for the specific chargers. In the pseudo code, the multiplication with the binary occupied signals for EV charger limitation indicates that only occupied chargers are limited. Furthermore, the

Table 4.1: LUT for EV charger limitation, percentage values correspond to share of EV power reserve

AC chargers $N_{occ,AC}$ \ DC chargers $N_{occ,DC}$	0	1
0	− (upper), − (lower)	100 % (upper), − (lower)
1	− (upper), 100 % (lower)	80 % (upper), 20 % (lower)
2	− (upper), 50 % (lower)	60 % (upper), 20 % (lower)
3	− (upper), 33.3 % (lower)	40 % (upper), 20 % (lower)
4	− (upper), 25 % (lower)	20 % (upper), 20 % (lower)

percentage value (lookup table output depending on charger type), which describes the share of power reserve, is symbolically referred to as LUT value and is always used in the context of the relevant charger type. Checking and potentially saturating the EV setpoints to their allowed limits defined in table 2.7 is not shown in the pseudo code.

Algorithm 4.1: Baseline

Input: SoC_{BESS}, $P_{PV,gen}$, $P_{SL,dem}$, $N_{occ,AC}$, $N_{occ,DC}$
Output: $P_{BESS,set}$, $P_{AC,set}$, $P_{DC,set}$
// BESS control

1   *Calculate* $P_{PV,excess}$, $P_{BESS,ch,avail}$, $P_{BESS,dis,avail}$, $P_{BESS,ch,res}$, $P_{BESS,dis,res}$;
2   **if** $P_{PV,excess} > 0$ **and** $N_{occ,AC} \leq 1$ **and** $N_{occ,DC} = 0$ **then**
3 | $P_{BESS,set} = \min\{P_{PCC,max}, P_{BESS,ch,avail}, P_{BESS,ch,res}\}$;
4   **else if** $P_{PV,excess} < 0$ **or** $N_{occ,AC} > 1$ **or** $N_{occ,DC} = 1$ **then**
5 | $P_{BESS,set} = \max\{-P_{PCC,max}, P_{BESS,dis,avail}, P_{BESS,dis,res}\}$;
6   **else**
7 | $P_{BESS,set} = 0$;
8   **end**
   // EV charger limitation
9   *Calculate* $P_{EV,res}$;
10   **for** $k = 1$ **to** 4 **do**
11 | $P^k_{AC,set} = OCC^k_{AC} \cdot LUT\ value \cdot P_{EV,res}$;
12   **end**
13   $P_{DC,set} = OCC_{DC} \cdot LUT\ value \cdot P_{EV,res}$;

The baseline strategy is a reasonable benchmark to compare the two other strategies. It can show if a more sophisticated approach is worth to be implemented.

4.3 Price-sensitive

The baseline strategy indirectly assumes that the market price tends to be low when cheap PV energy is available, or vice versa, high when PV is not available. Since the

NPS day-ahead prices are used, the current price can be set in relation to the price development over one day. The second strategy adds rules that are sensitive to price to foster economic decisions. Therefore, three price thresholds are defined. The average NPS day-ahead price $Pr_{NPS,avg}$ and the two EV charger tariffs Pr_{AC} and Pr_{DC}. The thresholds in relation to the market price are illustrated in figure 4.2.
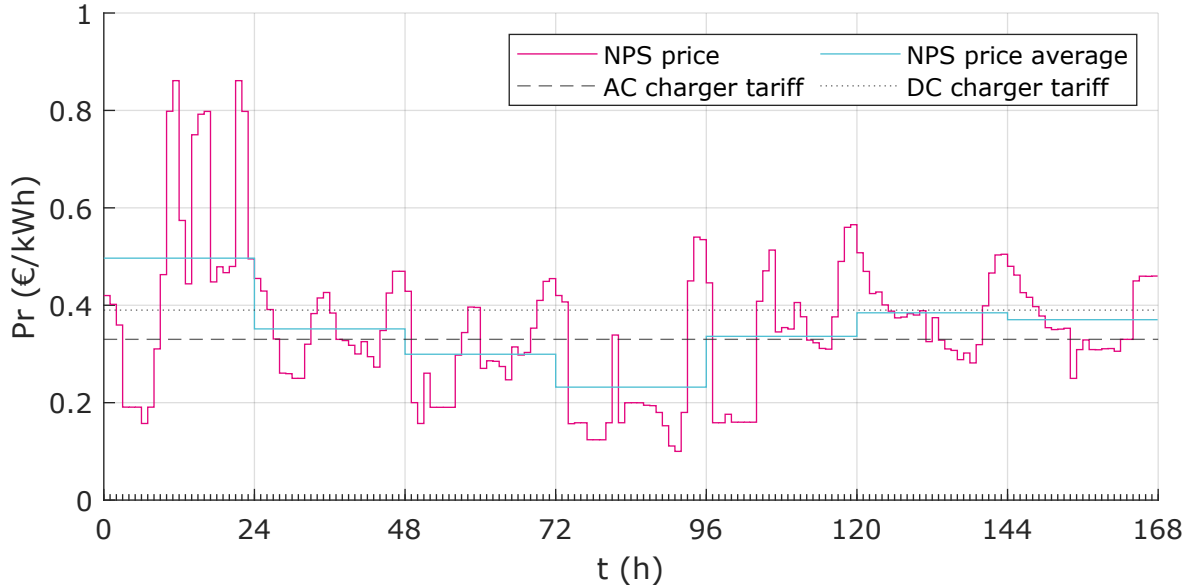
(a) Summer
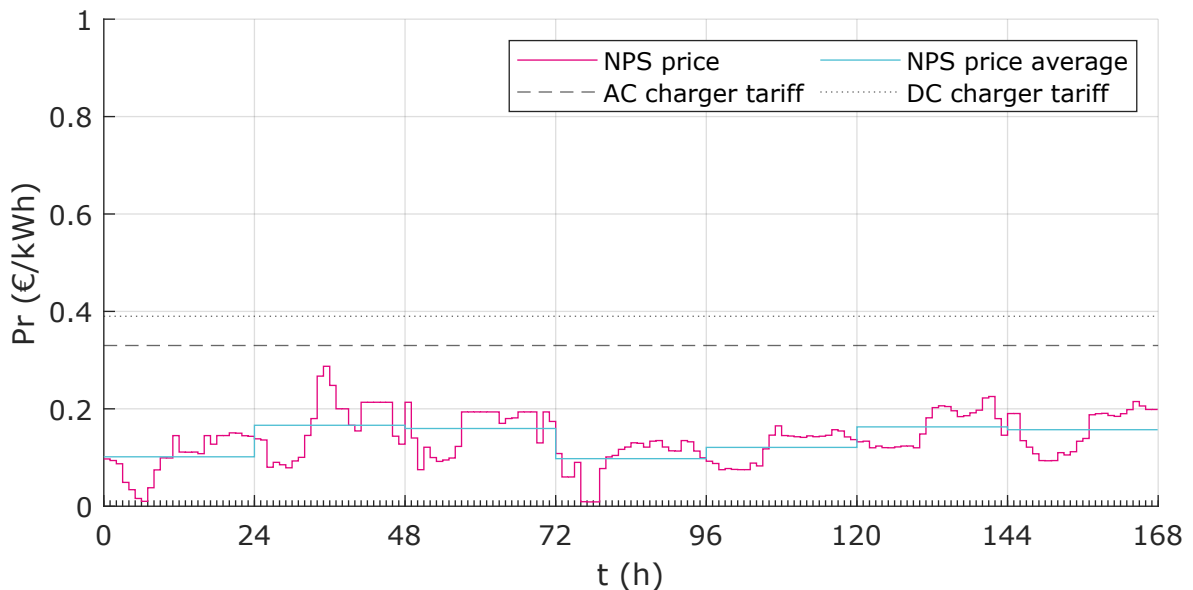
(b) Winter

Figure 4.2: NPS price and price thresholds

Which threshold to choose depends on the EVs that are charging. Consequently, the strategy is divided into four cases. Case 1 stands for no EV charging, case 2 means only cars at AC chargers, case 3 corresponds to only the DC charger in use and case 4 represents mixed charger types active. The general idea of this strategy is to increase external revenue by increasing the BESS energy available for supporting EVs when the market price is low. Therefore, the battery's SoC range is divided into a lower reserve range (20 % to 40 %) to keep energy available and an upper trading range (40 % to

90 %) that can be used for selling energy to the main grid. The threshold is defined in equation (4.7).

$$SoC_{BESS,th} = SoC_{BESS,min} + 20\,\%$$ (4.7)

The battery reserve is filled when no EV chargers are in use. If EVs start charging, the battery supports by discharging in case of low prices. In case of high prices, the battery stops support and the EV chargers are further curtailed based on the market price to avoid significant economic loss of the CO. The maximum, to which the EV power reserve is reduced, is set to 50 %.

The setpoints depend also on scaling factors, which are described later. Here, the scaling factors are calculated by mapping an input value within a certain input range to a desired output range (see equation (4.8)).

$$y = \frac{y_2 - y_1}{x_1 - x_2} \cdot (x - x_1) + y_1$$ (4.8)

where x − input value to be mapped to new interval,
        y − output value in the new interval,
        x_1 − left boundary of input interval,
        x_2 − right boundary of input interval,
        y_1 − left boundary of output interval,
        y_2 − right boundary of output interval.

The calculation of scaling factors y is symbolically denoted as $x\colon \{x_1, x_2\} \mapsto \{y_1, y_2\}$ in the pseudo code. Scaling factors outside the output range are implicitly saturated to the corresponding boundary of the output interval.

In the following, each case and its features are discussed in detail. The first case applies when no chargers are in use and is described in algorithm 4.2. If the current SoC is below the set reserve threshold (40 %), the BESS is charged with the maximum possible power. This power is reduced the closer the SoC gets to the threshold. This avoids oscillations between the two SoC ranges. Therefore a scaling factor is calculated by mapping the current SoC from the lower half of the usable SoC range (55 % to 20 %) to the value range zero to one (equation (4.8)). The maximum possible charging power is set when the battery is fully discharged. The reserve filling is done independently of the current market price to increase availability. When the SoC is reaching the trading range, the price is checked. If it is below the average market price, the battery is charged to store cheap energy. The charging power is at maximum when the battery's SoC is equal to the reserve threshold and at minimum when the battery is fully charged. In case of an above-average market price, the battery is discharged to sell energy to the main grid. This happens again with a scaling factor which is based on the inverse mapping. The saturation of the BESS setpoint to the maximum charging or discharging powers is done implicitly. EV charger limitation is not necessary in this case.

The second case is valid when only AC chargers are occupied. It is shown in algorithm 4.3. An additional rule similar to the baseline strategy for SoC reserve filling is added to ensure that the battery is available when chargers are occupied for a long time. Here, PV excess power is used to fill the reserve. If the reserve is available and the market price is below the AC charger tariff, the battery supports the chargers by discharging

---

Algorithm 4.2: Price-sensitive case 1

    Input: SoC_{BESS}, $P_{PV,gen}$, $P_{SL,dem}$, $P_{EV,dem}$, $N_{occ,AC}$, $N_{occ,DC}$, Pr_{NPS}
    Output: $P_{BESS,set}$, $P_{AC,set}$, $P_{DC,set}$

1 *Calculate* $P_{PV,excess}$, $P_{BESS,ch,avail}$, $P_{BESS,dis,avail}$, $P_{BESS,ch,res}$, $P_{BESS,dis,res}$;
     // Case 1: No chargers occupied

2 **case** $N_{occ,AC} = 0$ **and** $N_{occ,DC} = 0$ **do**
       // BESS control

3   **if** $SoC_{BESS} < SoC_{BESS,th}$ **then**

4   *Calculate scaling factor* SoC_{BESS}: $\{SoC\ centre, SoC_{BESS,min}\} \mapsto \{0, 1\}$;

5 $P_{BESS,set} = \min\{scaling\ factor \cdot P_{BESS,ch,res}, P_{BESS,ch,avail}\}$;

6   **else**

7   **if** $Pr_{NPS} < Pr_{NPS,avg}$ **then**

8   *Calculate scaling factor* SoC_{BESS}: $\{SoC_{BESS,th}, SoC_{BESS,max}\} \mapsto \{1, 0\}$;

9 $P_{BESS,set} = \min\{scaling\ factor \cdot P_{BESS,ch,res}, P_{BESS,ch,avail}\}$;

10   **else if** $Pr_{NPS} > Pr_{NPS,avg}$ **then**

11   *Calculate scaling factor* SoC_{BESS}: $\{SoC_{BESS,th}, SoC_{BESS,max}\} \mapsto \{0, 1\}$;

12 $P_{BESS,set} = \max\{scaling\ factor \cdot P_{BESS,dis,res}, P_{BESS,dis,avail}\}$;

13   **else**

14 $P_{BESS,set} = 0$;

15   **end**

16   **end**

17 **end**

---

to increase the revenue of the CO. The discharging power is set to the load demand of the EVs. BESS support is limited to the BESS reserve (equation (4.3b)) not because resulting setpoints would be infeasible but to avoid significant economic loss of the LEC. The resulting power reserve for EV charging is then calculated (equation (4.6)). It is further reduced if the BESS does not support and the market price is above the AC charger tariff to reduce economic loss of the CO. The minimum scaling factor is set to 50 % and is applied when the market price is greater or equal to twice the charger tariff. In between this price range, the scaling factor is calculated based on linear mapping of the market price (equation (4.8)). Finally, the reserve is split the same way as in the baseline strategy (see table 4.1).

Descriptive pseudo code for the third and fourth cases are given in appendix A.6. In case 3 (algorithm A.1) only the DC charger is in use. The control is similar to case 2, but the extra reserve filling rule does not apply and the EV charging reserve limitation is done based on the DC charger tariff.

Case 4 means both charger types are occupied. Algorithm A.2 shows the implementation. The only difference compared to case 3 is the price threshold for EV reserve limitation. Here, the average of both charger tariffs is used.

The second control strategy is a rule-based approach that adds economic decisions. The day-ahead price allows the classification of the current market price as low or high in relation to the day-ahead price development, and thus introduces kinds of predictive decisions. Further, fair revenue sharing is fostered by defining the SoC trading range for the LEC and the supportive reserve range for improving the revenue streams of the CO.

Algorithm 4.3: Price-sensitive case 2

```
   // Case 2: Only AC chargers occupied
```
1 **case** $N_{occ,AC} > 0$ **and** $N_{occ,DC} = 0$ **do**
```
      // BESS control
```
2   **if** $SoC_{BESS} < SoC_{BESS,th}$ **and** $P_{PV,excess} > 0$ **and** $N_{occ,AC} = 1$ **then**

3 $P_{BESS,set} = \min\{P_{PV,excess}, P_{BESS,ch,avail}, P_{BESS,ch,res}\}$;

4   **else if** $Pr_{NPS} < Pr_{AC}$ **then**

5 $P_{BESS,set} = \max\{-P_{EV,dem}, P_{BESS,dis,avail}, P_{BESS,dis,res}\}$;

6   **else**

7 $P_{BESS,set} = 0$;

8   **end**
```
      // EV charger limitation
```
9   *Calculate* $P_{EV,res}$;

10   **if** $P_{BESS,set} = 0$ **then**

11   *Calculate scaling factor* $Pr_{NPS} \colon \{Pr_{AC}, 2 \cdot Pr_{AC}\} \mapsto \{1, 0.5\}$;

12 $P_{EV,res} = $ *scaling factor* $\cdot P_{EV,res}$;

13   **end**

14   **for** $k = 1$ **to** 4 **do**

15 $P_{AC,set}^{k} = OCC_{AC}^{k} \cdot LUT\ value \cdot P_{EV,res}$;

16   **end**

17 **end**

4.4 Scheduling

The third strategy, which is called scheduling, fosters predictive decisions further by applying an optimisation technique and 24 h forecasting. While forecasting is sufficiently accurate for PV production, the EV charging behaviour is highly stochastic and reliable forecasting is not possible. Therefore, this scheduling strategy tries to find near-optimal BESS setpoints and the power that should be reserved for both EV charger types on an hourly basis. The optimisation problem tries to maximise the total profit of the MG based on the P2P trading market (see section 3.3). The resulting power schedule is then used in the RT control loop for dispatch. The hourly BESS setpoints are treated as a reference that the battery tries to track. The EV charger schedules are interpreted as hourly power/energy budgets to compensate for the absence of an EV charging forecast.

An approach to mitigate the uncertainties due to no precise EV forecasting is to use the information on peak charging hours. Here, the peak hours are assumed to be the yearly average of charger power consumption for every hour of one week. The measurement data of the DC charger used for EV charger modelling in sub-section 2.4.4 is the basis for calculating the peak hours. When computing the normalised cross-correlation of the peak hours and the measurement data of the scenario weeks, it can be observed that the consumption patterns correlate with the peak hour (see figure 4.3, Matlab function [58]). This finding suggests that each week has basically similar consumption patterns and thus, peak-hour information is used for scheduling.

The fairness aspect according to the individual business goals is introduced by constraints and weight factors (compare sub-section 3.3.1). For TC, just cost is optimised. The revenue of TC is therefore weighted by zero. Since the objective is to maximise the total profit of the MG, constraints are needed to avoid the scheduling algorithm exploiting the LEC's or the CO's profit in case of high or low market prices. Equivalent full cycles (EFCs)
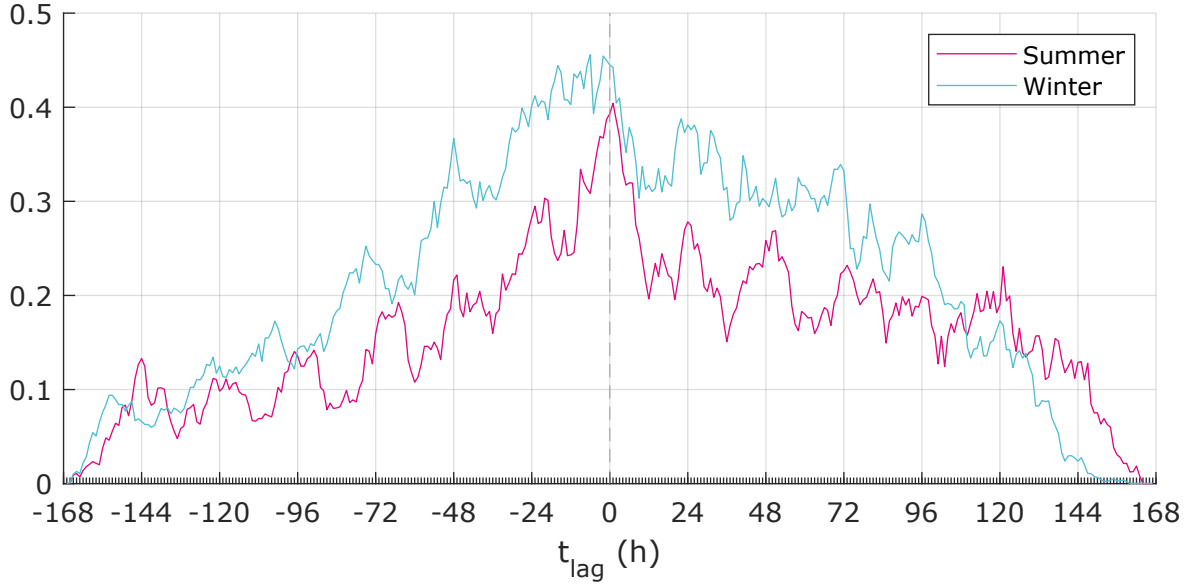
Figure 4.3: EV peak hours cross-correlation, t_{lag}: time shift between scenario and peak-hour data

describe how often the BESS is fully charged and then fully discharged and therefore describe the main aspect of BESS utilisation. First, the daily EFCs of the battery need to be at least equal to half a full cycle. Second, the minimum reserved EV charger energy for each hour is set to the peak-hour values. This ensures a minimum amount of EV charging. The details are explained in sub-section 4.4.1.

4.4.1 Formulation of optimisation problem

An optimisation problem consists of three parts. The optimisation or decision variables whose optimal values are to be found within certain boundaries. The objective function that is meant to be optimised and the equality and inequality constraints that the objective function is subject to [59].

The scheduling problem is formulated as mixed-integer linear programming (MILP) problem. Programming is the mathematical term for optimisation. Linear solvers are preferred because they require less computational effort and can find the global optimum. Matlab provides a problem-based approach to optimisation problems that simplifies the implementation of large problems with many variables (more information: [60]). The formulation is described in the following.

Input parameters of the problem are described first. The number of timesteps of the optimisation horizon $T_{horizon}$ is 24 (h) and it has a timestep $\Delta T_{horizon}$ of 1 h. For each day, the initial SoC is denoted as $SoC_{BESS,start}$. Further, the forecast of the PV generation $P_{PV,pred}$ and the demand of the street lighting system $P_{SL,dem}$ is required. The DC charger peak-hour profile is denoted as $P_{DC,avg}$. To also have peak hours for the AC chargers $P_{AC,avg}$, scaling according to the charger ratings is applied (see equation (4.9)).

$$P_{AC,avg} = P_{DC,avg} \cdot \left(\frac{4 \cdot P_{AC,r}}{P_{DC,r}} \right) \tag{4.9}$$

Optimisation variables that make up the desired power schedule are defined in equations (4.10a) to (4.10c). The length of the variables is equal to the timesteps of the optimisation horizon and t is the corresponding time index. For the battery, a setpoint schedule is determined. For both charger types, the available power reserve is scheduled. The AC chargers are treated as one load. The lower and upper boundaries of the optimisation variables are set to the limits defined in section 2.4.

$$P_{BESS,sched} = \mathbb{R}^{1 \times T_{horizon}} : P_{BESS,dis,max} \leq P_{BESS,sched}[t] \leq P_{BESS,ch,max} \tag{4.10a}$$

$$P_{AC,sched} = \mathbb{R}^{1 \times T_{horizon}} : 0 \leq P_{AC,sched}[t] \leq 4 \cdot P_{AC,r} \tag{4.10b}$$

$$P_{DC,sched} = \mathbb{R}^{1 \times T_{horizon}} : 0 \leq P_{DC,sched}[t] \leq P_{DC,r} \tag{4.10c}$$

Auxiliary parameters are required because the P2P trading model defined in section 3.3 is non-linear. The non-linearities are introduced by different prices for different power flow directions. When calculating costs and revenues for each owner, the power flows have to be separated according to the direction. This involves mathematical minimum and maximum operators. In the case of the P2P market, two power flows can be bidirectional. The power flow between TC and the main grid and the power that flows between the LEC and TC (see figure 3.3). A way to transform those operations to get a linear problem is described in [61]. It is called the big-M method. This method basically constrains the feasible solution space to the linear areas. Therefore, scalar and positive big-M parameters are introduced for every direction. Import indicates the direction from top to bottom, and export the reverse direction (related to figure 3.3). These parameters have to be set to a sufficiently large value. Here, the big-M parameters are set to the maximum possible values as described in equations (4.11a) to (4.12b). The usage of these parameters is explained later.

$$M_{LEC,imp} = P_{BESS,ch,max} + P_{DC,r} \tag{4.11a}$$

$$M_{LEC,exp} = P_{PV\text{-}inv,r} + |P_{BESS,dis,max}| \tag{4.11b}$$

$$M_{TC,imp} = P_{PCC,max} \tag{4.12a}$$

$$M_{TC,exp} = P_{PCC,max} \tag{4.12b}$$

Auxiliary optimisation variables are introduced to separate each power flow, which can be bidirectional, into two directions. The variables for the import and export direction can take on any positive values (see equations (4.13a), (4.13b) and (4.14a), (4.14b)). In addition, binary variables are defined for each bidirectional power flow (see equations (4.13c) and (4.14c)). The binary variables together with the big-M parameters are used for constraints to ensure that each power flow is mutually exclusive.

$$P_{LEC,imp} = \mathbb{R}^{1 \times T_{horizon}} : 0 \leq P_{LEC,imp}[t] \leq \infty \tag{4.13a}$$

$$P_{LEC,exp} = \mathbb{R}^{1 \times T_{horizon}} : 0 \leq P_{LEC,exp}[t] \leq \infty \tag{4.13b}$$

$$Y_{LEC} = \mathbb{Z}^{1 \times T_{horizon}} : 0 \leq Y_{LEC}[t] \leq 1, \quad 0 \cong \text{export}, 1 \cong \text{import} \tag{4.13c}$$

$$P_{TC,imp} = \mathbb{R}^{1 \times T_{horizon}} : 0 \leq P_{LEC,imp}[t] \leq \infty \tag{4.14a}$$

$$P_{TC,exp} = \mathbb{R}^{1 \times T_{horizon}} : 0 \leq P_{TC,exp}[t] \leq \infty \tag{4.14b}$$

$$Y_{TC} = \mathbb{Z}^{1 \times T_{horizon}} : 0 \leq Y_{TC}[t] \leq 1, \quad 0 \mathrel{\widehat{=}} \text{export, } 1 \mathrel{\widehat{=}} \text{import} \tag{4.14c}$$

A similar problem occurs when including separated charging and discharging efficiencies for the BESS. The BESS power schedule is therefore separated into charging and discharging variables (see equations (4.15a) and (4.15b)). Both of these auxiliary variables can take on positive values only. Here, no big-M parameters and the binary variable are necessary since both variables are bounded.

$$P_{BESS,ch,sched} = \mathbb{R}^{1 \times T_{horizon}} : 0 \leq P_{BESS,ch,sched}[t] \leq P_{BESS,ch,max} \tag{4.15a}$$

$$P_{BESS,dis,sched} = \mathbb{R}^{1 \times T_{horizon}} : 0 \leq P_{BESS,dis,sched}[t] \leq |P_{BESS,dis,max}| \tag{4.15b}$$

Constraints are formulated to limit the solution space to technically feasible and otherwise desirable areas. The PCC has a limited capacity, which requires constraints for the lower and the upper power flow limit (see equations (4.16a) and (4.16b)).

$$P_{BESS,sched}[t] + P_{AC,sched}[t] \, P_{DC,sched}[t] \geq -P_{PCC,max} - P_{SL,dem}[t] - P_{PV,pred}[t] \tag{4.16a}$$

$$P_{BESS,sched}[t] + P_{AC,sched}[t] \, P_{DC,sched}[t] \leq P_{PCC,max} - P_{SL,dem}[t] - P_{PV,pred}[t] \tag{4.16b}$$

The first constraint for the BESS defined in equation (4.17) makes sure that the battery schedule is the composition of the separate and mutually exclusive charging and discharging schedules.

$$P_{BESS,sched}[t] = P_{BESS,ch,sched}[t] - P_{BESS,dis,sched}[t] \tag{4.17}$$

Further, the BESS setpoints are constrained by the SoC limits defined in table 2.3. The lower and upper SoC limits are formulated in equations (4.18a) and (4.18b).

$$
\begin{aligned}
\left(SoC_{BESS,start} \cdot E_{BESS} \right) + \left(\sum_{1}^{t} P_{BESS,ch,sched} \cdot \eta_{BESS,ch} \cdot \Delta T_{horizon} \right) & \\
- \left(\sum_{1}^{t} P_{BESS,dis,sched} \cdot \frac{\Delta T_{horizon}}{\eta_{BESS,dis}} \right) \geq \left(SoC_{BESS,min} \cdot E_{BESS} \right) &
\end{aligned}
\tag{4.18a}
$$

$$
\begin{aligned}
\left(SoC_{BESS,start} \cdot E_{BESS} \right) + \left(\sum_{1}^{t} P_{BESS,ch,sched} \cdot \eta_{BESS,ch} \cdot \Delta T_{horizon} \right) & \\
- \left(\sum_{1}^{t} P_{BESS,dis,sched} \cdot \frac{\Delta T_{horizon}}{\eta_{BESS,dis}} \right) \leq \left(SoC_{BESS,max} \cdot E_{BESS} \right) &
\end{aligned}
\tag{4.18b}
$$

EFCs are calculated by adding up the total charged and total discharged energy, and dividing it by twice the usable battery capacity. The minimum EFC constraint in equation

(4.19) is set to half a full cycle per day. This ensures minimum battery usage.

$$\frac{\sum_1^{T_{horizon}} P_{BESS,ch,sched}[t] \cdot \eta_{BESS,ch} \cdot \Delta T_{horizon} + \sum_1^{T_{horizon}} P_{BESS,dis,sched}[t] \cdot \frac{\Delta T_{horizon}}{\eta_{BESS,dis}}}{2 \cdot (SoC_{BESS,max} - SoC_{BESS,min}) \cdot E_{BESS}} \geq 0.5 \quad (4.19)$$

For EV chargers, two constraints are defined that are responsible for ensuring that a minimum amount of power is reserved for both types of chargers. The minimum for each charger type is equal to the peak-hour averages (see equations (4.20a) and (4.20b)). A minimum is necessary because in some periods it would be economically more beneficial to completely shut down the chargers.

$$P_{AC,sched}[t] \geq P_{AC,avg}[t] \qquad (4.20a)$$

$$P_{DC,sched}[t] \geq P_{DC,avg}[t] \qquad (4.20b)$$

At last, auxiliary constraints for separating the bidirectional power flows are defined. The equality constraint in equation (4.21) specifies the separation of the bidirectional power flow between LEC and TC by setting it equal to the difference of the unidirectional power flows.

$$P_{DC,sched}[t] + P_{BESS,sched}[t] + P_{PV,pred}[t] = P_{LEC,imp}[t] - P_{LEC,exp}[t] \qquad (4.21)$$

Inequality constraints in equations (4.22a) and (4.22b) make sure that the unidirectional power flows are mutually exclusive since the binary variable can only take on 0 (export) or 1 (import).

$$P_{LEC,imp}[t] \leq M_{LEC,imp} \cdot Y_{LEC}[t] \qquad (4.22a)$$

$$P_{LEC,exp}[t] \leq M_{LEC,exp} \cdot (1 - Y_{LEC}[t]) \qquad (4.22b)$$

The same constraints are formulated for the power flow between TC and the main grid (see equations (4.23) and (4.24a), (4.24b)).

$$P_{DC,sched}[t] + P_{BESS,sched}[t] + P_{PV,pred}[t] + $$
$$P_{AC,sched}[t] + P_{SL,dem}[t] = P_{TC,imp}[t] - P_{TC,exp}[t] \qquad (4.23)$$

$$P_{TC,imp}[t] \leq M_{TC,imp} \cdot Y_{TC}[t] \qquad (4.24a)$$

$$P_{TC,exp}[t] \leq M_{TC,exp} \cdot (1 - Y_{TC}[t]) \qquad (4.24b)$$

Objective function can be formulated with the variables defined and the constraints set. The idea is to maximise the total profit of the MG over the optimisation horizon. The total revenue of each owner is the sum of all the variable revenues that come from trading energy and the fixed revenues (fixed grid tariff passed from TC to other owners).

Equations (4.25a) to (4.25c) show the revenue expressions in detail.

$$R_{TC} = \sum_{1}^{T_{horizon}} \left(\left(P_{TC,exp}[t] \cdot \Delta T_{horizon} \right) \cdot Pr_{exp}[t] \right)$$

$$+ \sum_{1}^{T_{horizon}} \left(\left(P_{AC,sched}[t] \cdot \Delta T_{horizon} \right) \cdot \left(Pr_{imp}[t] \cdot (1 + m_{TC}) \right) \right) \qquad (4.25a)$$

$$+ \sum_{1}^{T_{horizon}} \left(\left(P_{LEC,imp}[t] \cdot \Delta T_{horizon} \right) \cdot \left(Pr_{imp}[t] \cdot (1 + m_{TC}) \right) \right)$$

$$+ \left(FR_{TC} \cdot T_{horizon} \right)$$

$$R_{LEC} = \sum_{1}^{T_{horizon}} \left(\left(P_{DC,sched}[t] \cdot \Delta T_{horizon} \right) \cdot \left(Pr_{imp}[t] \cdot (1 + m_{TC}) \cdot (1 + m_{LEC}) \right) \right)$$

$$+ \sum_{1}^{T_{horizon}} \left(\left(P_{LEC,exp}[t] \cdot \Delta T_{horizon} \right) \cdot Pr_{exp}[t] \right) \qquad (4.25b)$$

$$+ \left(FR_{LEC} \cdot T_{horizon} \right)$$

$$R_{CO} = \sum_{1}^{T_{horizon}} \left(\left(P_{AC,sched}[t] \cdot \Delta T_{horizon} \right) \cdot Pr_{AC}[t] \right)$$

$$+ \sum_{1}^{T_{horizon}} \left(\left(P_{DC,sched}[t] \cdot \Delta T_{horizon} \right) \cdot Pr_{DC}[t] \right) \qquad (4.25c)$$

$$+ \left(FR_{CO} \cdot T_{horizon} \right)$$

The counterpart costs are defined in equations (4.26a) to (4.26c). The total cost of each owner is the sum of the variable trading costs and fixed cost components (maintenance and fixed grid tariff).

$$C_{TC} = \sum_{1}^{T_{horizon}} \left(\left(P_{TC,imp}[t] \cdot \Delta T_{horizon} \right) \cdot Pr_{imp}[t] \right)$$

$$+ \sum_{1}^{T_{horizon}} \left(\left(P_{LEC,exp}[t] \cdot \Delta T_{horizon} \right) \cdot Pr_{exp}[t] \right) \qquad (4.26a)$$

$$+ \left(FC_{TC} \cdot T_{horizon} \right)$$

$$C_{LEC} = \sum_{1}^{T_{horizon}} \left(\left(P_{LEC,imp}[t] \cdot \Delta T_{horizon} \right) \cdot \left(Pr_{imp}[t] \cdot (1 + m_{TC}) \right) \right) \qquad (4.26b)$$

$$+ \left(FC_{LEC} \cdot T_{horizon} \right)$$

$$C_{CO} = \sum_{1}^{T_{horizon}} \left(\left(P_{AC,sched}[t] \cdot \Delta T_{horizon} \right) \cdot \left(Pr_{imp}[t] \cdot (1 + m_{TC}) \right) \right)$$

$$+ \sum_{1}^{T_{horizon}} \left(\left(P_{DC,sched}[t] \cdot \Delta T_{horizon} \right) \cdot \left(Pr_{imp}[t] \cdot (1 + m_{TC}) \cdot (1 + m_{LEC}) \right) \right) \qquad (4.26c)$$

$$+ \left(FC_{CO} \cdot T_{horizon} \right)$$

The actual objective function, depicted in equation (4.27), is then the sum of the owners' total profits, which again are the difference between each total revenue and total cost.

$$TP = \left(w_{TC,R} \cdot R_{TC} - w_{TC,C} \cdot C_{TC}\right) + (R_{LEC} - C_{LEC}) + (R_{CO} - C_{CO}) \tag{4.27}$$

The weights for TC profit, which are meant to introduce fairness, are listed in table 4.2. These weights complement the BESS EFC and the EV charger constraints.

Table 4.2: Revenue and cost weights for TC

Weight	Value
$w_{TC,R}$	0
$w_{TC,C}$	1

The final problem is summed up in equation (4.28). The total profit of the MG is maximised, subject to the afore-defined equality and inequality constraints.

$$\max_{P_{BESS,sched},\, P_{AC,sched},\, P_{DC,sched}} TP$$

$$\text{subject to} \quad \textit{set of equality constraints,} \tag{4.28}$$

$$\textit{set of inequality constraints.}$$

where   *equality constraints* − equations (4.17), (4.21), (4.23),
        inequality constraints − equations (4.16a), (4.16b), (4.18a) to (4.20b),
                                    (4.22b), (4.24b).

This problem is solved in Matlab with default settings for each day (more information on solver: [62, 63]). The daily schedules are then put together to get a schedule for the whole week. This simplifies simulation since no optimisation problem has to be solved during simulation. Figure 4.4 shows the obtained schedules for both simulation scenarios. As mentioned, only the P2P market is used for scheduling even though both markets are simulated.
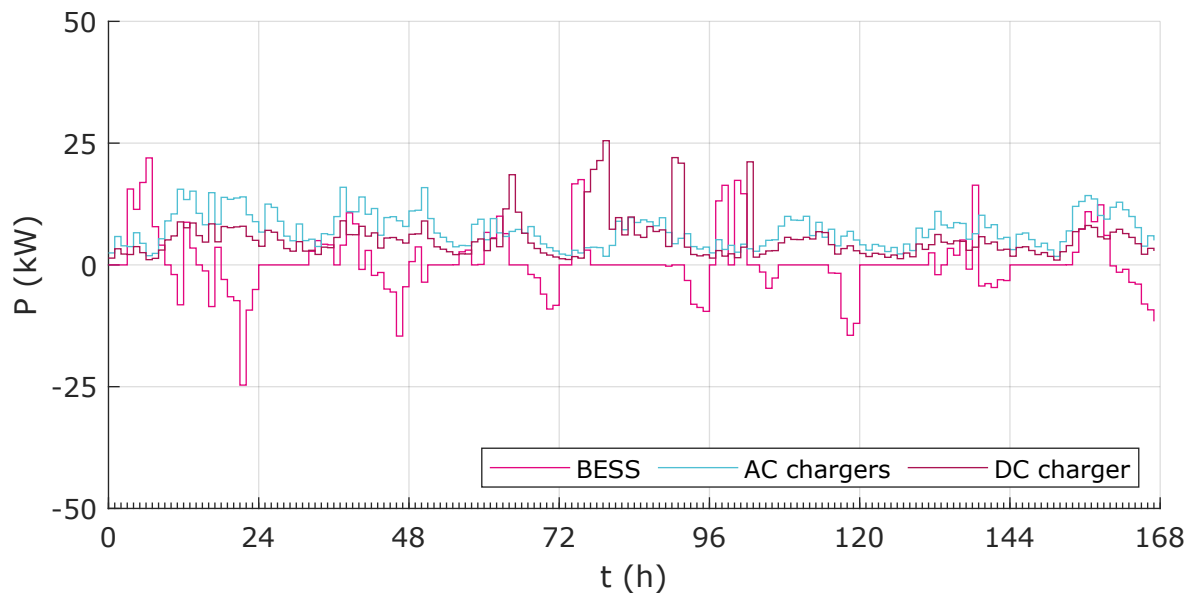
(a) Summer
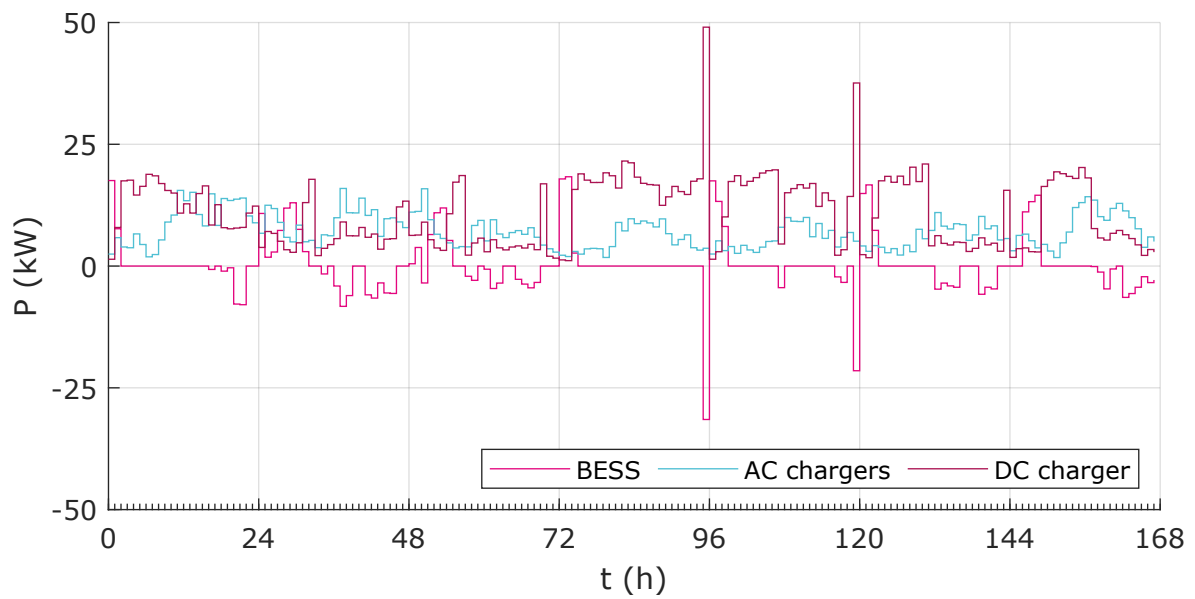
(b) Winter

Figure 4.4: Power schedules

4.4.2 Real-time dispatch

The power schedule is then used in the RT dispatch control. RT means that the control is executed once for every simulation timestep. The power schedule represents economically beneficial setpoints. RT control tries to implement these setpoints within the limits of the MG. For EV chargers, schedules represent the total power budgets that have been reserved. The hourly schedule values are the average powers for each hour. Therefore, the EV charger schedules are multiplied by the number of simulation timesteps per hour (here: 12) to get the hourly budgets. Generally, it consists of three steps. First, feasible BESS setpoints are selected assuming that no EVs are charging. Second, EV charger limits are set to the maximum possible power and if necessary and feasible, further increased by additional BESS discharging. In the last step, the BESS setpoint for the next timestep is adjusted to track the scheduled reference. The RT control approach is described in detail in algorithm 4.4 and the following paragraphs.

The BESS schedule proposes to support EV charging. However, if no chargers are occupied, the BESS power setpoint has to be limited according to the PCC capacity and the available battery energy. This is done in the first step referred to as BESS pre-control.

Step two of the control is about charger limitation. If EV chargers are occupied, the maximum charger powers are calculated. These powers are limited either by the demand or the remaining budget per hour. With the battery setpoint from pre-control, the actual available power reserve for the chargers (equation (4.6)) and the difference to the desired EV charger powers are calculated. If the reserve is not sufficiently large, the BESS setpoint is adjusted to increase the charger reserve. BESS support is the difference between the pre-control setpoint and the maximum available discharging power. Support is eventually limited to the additionally required charger reserve. The BESS support power is added to the former setpoint and the updated EV charger reserve is split according to the desired AC and DC charger powers. Then, the actual charger powers are assigned to the individual charger setpoints. In the case of AC chargers, the power reserve is distributed equally to the occupied chargers. Thereafter, the EV power budgets are updated.

Deviations from the scheduled BESS setpoints would lead to different SoC levels at future timesteps, which affects the economic dispatch of the schedule. To keep track of the scheduled BESS energy, the inverted power deviation from the scheduled setpoint (control error) is added to the scheduled setpoint of the next timestep.

Algorithm 4.4: RT dispatch of power schedule

Input: SoC_{BESS}, $P_{PV,gen}$, $P_{SL,dem}$, $P_{AC,dem}$, $P_{DC,dem}$, $N_{occ,AC}$, $N_{occ,DC}$
Output: $P_{BESS,set}$, $P_{AC,set}$, $P_{DC,set}$

1 begin
 // BESS pre-control
2 *Calculate* $P_{PV,excess}$, $P_{BESS,ch,avail}$, $P_{BESS,dis,avail}$, $P_{BESS,ch,res}$, $P_{BESS,dis,res}$;
3 **if** $P_{BESS,sched} \geq 0$ **then**
4 $P_{BESS,set} = \min\{P_{BESS,sched}, P_{BESS,ch,avail}, P_{BESS,ch,res}\}$;
5 **else**
6 $P_{BESS,set} = \max\{P_{BESS,sched}, P_{BESS,dis,avail}, P_{BESS,dis,res}\}$;
7 **end**
 // EV charger limitation
8 **if** $N_{occ,AC} > 0$ **or** $N_{occ,DC} > 0$ **then**
9 $P_{AC,max} = \min\{P_{AC,dem}, P_{AC,sched}\}$;
10 $P_{DC,max} = \min\{P_{DC,dem}, P_{DC,sched}\}$;
11   *Calculate* $P_{EV,res}$;
12 $\Delta P_{EV,res} = (P_{AC,max} + P_{DC,max}) - P_{EV,res}$;
13   **if** $\Delta P_{EV,res} > 0$ **then**
   // Increase BESS support
14 $\Delta P_{BESS,support} = \max\{-\Delta P_{EV,res}, P_{BESS,dis,avail} - P_{BESS,set}\}$;
15 $P_{BESS,set} = P_{BESS,set} + \Delta P_{BESS,support}$;
16   *Update* $P_{EV,res}$;
17 $P_{AC} = P_{EV,res} \cdot \frac{P_{AC,max}}{P_{AC,max} + P_{DC,max}}$;
18 $P_{DC} = P_{EV,res} \cdot \frac{P_{DC,max}}{P_{AC,max} + P_{DC,max}}$;
19   **end**
20   **for** $k = 1$ **to** 4 **do**
21 $P_{AC,set}^k = \frac{OCC_{AC}^k}{N_{occ,AC}} \cdot P_{AC}$;
22   **end**
23 $P_{AC,sched} = P_{AC,sched} - P_{AC}$;
24 $P_{DC,set} = OCC_{DC} \cdot P_{DC} \cdot P_{EV,res}$;
25 $P_{DC,sched} = P_{DC,sched} - P_{DC}$;
26 **end**
 // BESS reference tracking
27 $P_{BESS,sched}[t+1] = P_{BESS,sched}[t+1] + (P_{BESS,sched}[t] - P_{BESS,set})$;
28 end

5 DISCUSSION ON SIMULATION RESULTS

The three energy management strategies are simulated for both the summer and the winter scenario. This chapter defines at first the metrics for evaluating the simulation results. Then the simulation results are presented for each energy management strategy. Finally, the metrics are applied and compared to find out which strategy increases the economic feasibility of the MG the most.

5.1 Evaluation metrics

The simulations are only carried out for one week. The summer and winter scenarios contain seasonal effects, so it is beneficial to combine the results of both scenarios. This procedure averages out the seasonal differences to obtain more general results. Hence, evaluation metrics are based on results from 14 days.

Economic feasibility can be generally defined as the number of economic advantages exceeding economic costs [64]. Advantages or revenue as well as cost do not only come from cash flow. For instance, battery degradation affects the lifetime and consequently costs in the long run. Therefore, the economic feasibility of the MG is evaluated from different perspectives to get an overall or more generalised picture. These perspectives are introduced in the following.

Profit mainly represented economic feasibility. It is the remaining revenue when subtracting cost. The more profit, the higher the economic feasibility. This perspective views economic feasibility in a linear way since no initial investments as negative offsets are considered. When looking at the CRS market, which is considered inherently fair due to revenue sharing based on the owners' business goals (see sub-section 3.3.1 and section 3.4), the total profit of the MG is an adequate metric to compare the performance of energy management strategies. For the P2P market, where each owner trades on its own, evaluating only total profit is insufficient. Therefore, two additional metrics are defined that give insights into how fair revenue is shared. Fairness is important since the individual economic feasibilities of owners need to be balanced to increase also the MG's economic feasibility.

The fairness metric is defined in equation (5.1) as the mean absolute deviation of the P2P profits from the ideal CRS profits. It is normalised by the total profit of the MG to ensure that fairness is evaluated in relation to the profit. A fairness value of 100 % indicates ideal revenue sharing while 0 % means that the average deviation is the same as the total MG profit.

$$Fairness = 100\,\% - \frac{1}{3 \cdot Total\ profit_{MG}} \cdot \sum_{Owner} |Profit_{CRS}(Owner) - Profit_{P2P}(Owner)| \quad (5.1)$$

For the P2P market, the effective total profit (ETP) metric is defined to combine the total profit and fairness aspects. It is expected that 100 % fairly shared profit is fully contributing to economic feasibility. Though, worse fairness reduces the effectiveness of

profit. ETP is therefore defined as the product of the MG's total profit and fairness (see equation (5.2)).

$$ETP = Total\ profit_{MG} \cdot Fairness \qquad (5.2)$$

But when looking at the business goals in more detail, total profit and fairness do not show all perspectives of economic feasibility. The LEC and the CO are interested in making attractive investments. The PBP of capital investments is an adequate and simple metric that describes at which point in time (break-even point) the investments are paid-off. The PBP should be at least shorter than the lifetime of the components to avoid upcoming replacement costs before the investments are amortised. This perspective means that the individual, as well as the overall economic feasibility, are non-linear. The MG will be highly non-feasible if any of the owners' PBPs is longer than the lifetime of the components and no long-term profit can be expected. If PBPs are below the lifetime, economic feasibility increases more and more. The PBP is defined in equation (5.3) as the capital investments of an owner divided by the yearly profit.

$$PBP(Owner) = \frac{Capital\ investment(Owner)}{Profit(Owner) \cdot \frac{365}{14}} \qquad (5.3)$$

Even though 14-day profits result in more precise estimations of the PBPs than one-week data, other financial effects like inflation are neglected. Hence, this metric is less precise than the profit and fairness metrics.

TC is interested in reducing the cost that exceeds the current cost for operating the distribution system including street lighting without the MG. Therefore, the savings of TC are calculated to complement the PBP metric. Ideally, the savings are zero. Negative savings equivalent to additional costs are not desired and reduce the individual economic feasibility of TC. Positive savings on the other hand affect the economic feasibility of the whole MG negatively since investments of the other owners become less attractive. The cost of operating the street lighting system is calculated as equation (5.4) states.

$$C_{SL} = Pr_{grid,fix} + \sum_{t} P_{SL,dem} \cdot Pr_{imp} \qquad (5.4)$$

The savings are the difference between the street lighting cost and the actual profit of TC. The profit of TC for the CRS market is ideally negative and equal to $-C_{SL}$.

Apart from economic metrics, technical aspects are evaluated that also have an impact on the economic feasibility. Technical aspects do not depend on the used market structure. Here, only qualitative statements are possible, as the modelling effort of economic impact is beyond the scope of this work.

The limitation of the EV charging service can have negative effects on the economic feasibility. When EV charging happens too slowly or is even disrupted, customers might tend to prefer other locations or other COs. To estimate the impact of energy management strategies on the charging service, the amount of energy, that is actually charged, compared to the unlimited / no control case is calculated. It is assumed that lower limitation has less of a negative impact on the economic feasibility.

BESSs are commonly the most expensive component of MGs (see table 3.1). The usage

pattern has effects on the battery lifetime. The most basic metric is counting EFCs. It is defined in equation (5.5) similarly to the previously defined EFC constraint in section 4.4 equation (4.19). To get the gross amount of charged and discharged energy (numerator), the charging and discharging efficiencies have to be considered because simulation gives out the net power of the BESS.

$$EFC = \frac{\sum_t P_{BESS,ch} \cdot \eta_{BESS,ch} \cdot \Delta T + \sum_t |P_{BESS,dis}| \cdot \frac{\Delta T}{\eta_{BESS,dis}}}{2 \cdot (SoC_{BESS,max} - SoC_{BESS,min}) \cdot E_{BESS}} \tag{5.5}$$

Battery full cycles do not consider DoD. Yet, DoD is an important parameter for estimating the impact of battery usage on lifetime, and in turn, the impact on economic feasibility. Other factors like battery technology and temperature play a role as well. Thus, EFCs do not allow to give precise estimations of the economic feasibility. Fewer EFCs do not necessarily mean less degradation. However, they are calculated to check if battery usage is in an acceptable range, which is roughly defined here as 0.5 to 2 EFCs per day. This metric can be used to model the impact in the future.

5.2 Simulation results

This section shows the simulation results for the three energy management strategies. For all strategies and scenarios, the power flows at the coupling points are depicted. The main coupling point is the PCC which connects the MG with the main grid. The other coupling points are the connections between the owners within the MG. On the one hand, the connection between TC and the LEC, and on the other hand, the connections to the CO. Coupling between TC and the CO shows the power supplied to the four AC chargers, while the point LEC-CO represents the power supplied to the DC charger. In addition, the BESS usage is depicted in form of the output power and the SoC. Further, all the numerical data are listed, which is necessary to compute metrics defined in section 5.1.

5.2.1 Baseline

Only the graphical results for the baseline strategy and the summer scenario are shown here. Results for the winter scenario can be found in appendix A.7.

Figure 5.1 shows the power flow at coupling points. It can be seen that the MG imports and exports energy without violating the PCC limits (sub-plot 1). Furthermore, the street lighting system has only a small impact on the power flow. The second sub-plot shows the behaviour of PV and the BESS respectively the DC charger. PV excess power is mostly exported to the main grid since often only one AC charger is occupied. The maximum load power of the AC chargers (sub-plot 3) stays below 50 kW since the battery supports only with fixed power. But the DC charger is able to charge cars with mostly over 40 kW (sub-plot 4).

Figure 5.2 shows the battery usage. The power of the BESS is mostly equal to the PCC power capacity, as it was intended. In some time instances, charging or discharging
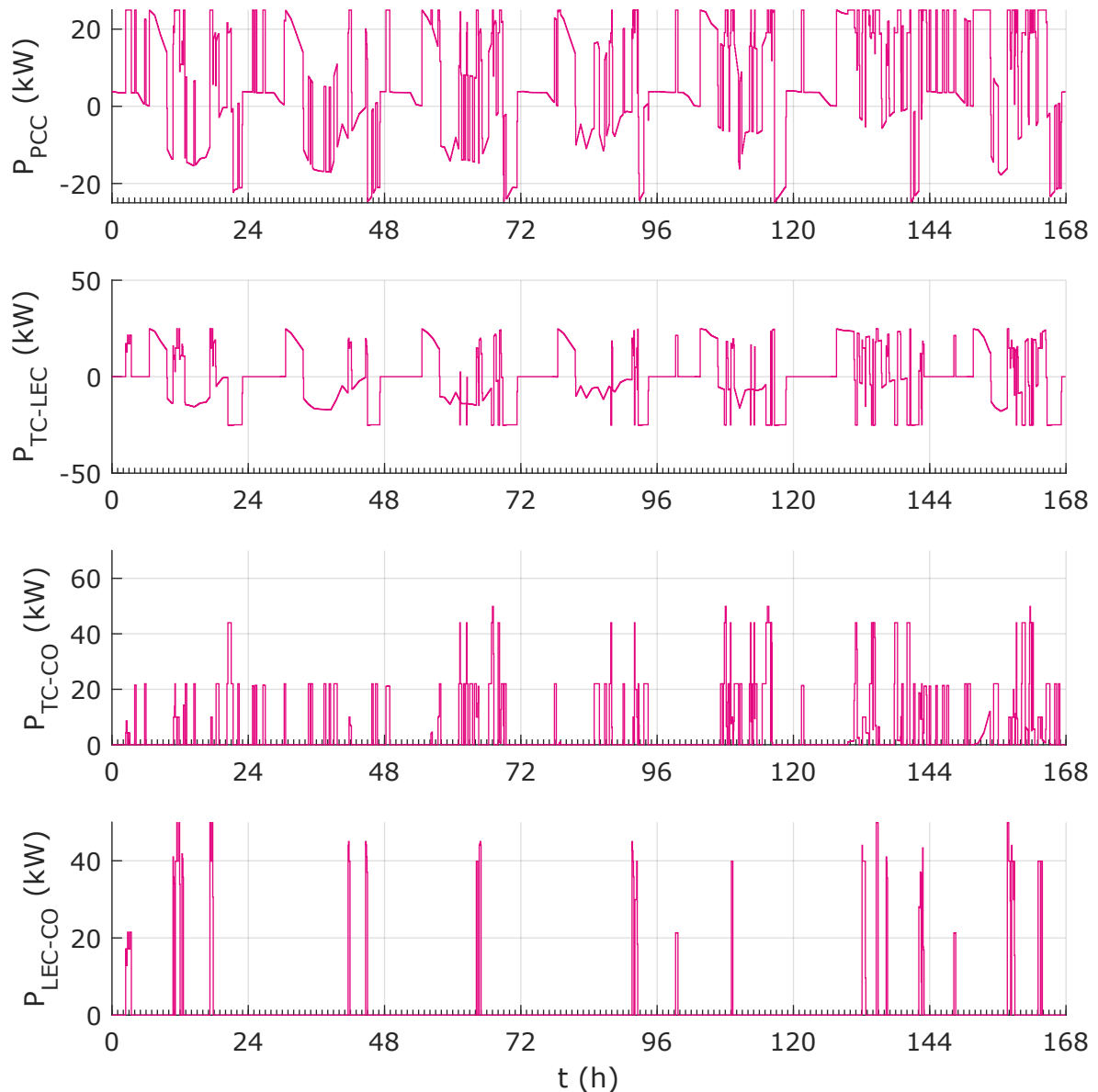
Figure 5.1: Power flow at coupling points for baseline strategy in summer

power is reduced to avoid violation of the PCC limits. The SoC varies between the defined limits of 20 % and 90 %. During the daytime when PV is available, the battery is charged. Then, EV charging can be supported. During late night-time and morning, when the battery is fully discharged, EV charging has to be significantly limited.

Table 5.1 shows the retrieved numerical simulation results rounded to two decimal places. Sub-table 5.1a lists the economic results, which are the profits for each owner and each market. It can be seen that the profits of TC are varying in a small range, while the profits of the LEC and the CO strongly depend on the scenario. In summer where market prices are higher and PV generation is higher (compare figures 4.2 and 2.3), the LEC can make significantly more profit. In the winter, where conditions are reversed, the CO is more profitable. Sub-table 5.1b lists technical parameters that are evaluated later. First, the total energy that has been delivered to the two types of chargers. And second, the total charged and the total discharged energy of the battery which are necessary for calculating the EFCs. This strategy uses the BESS more in summer.
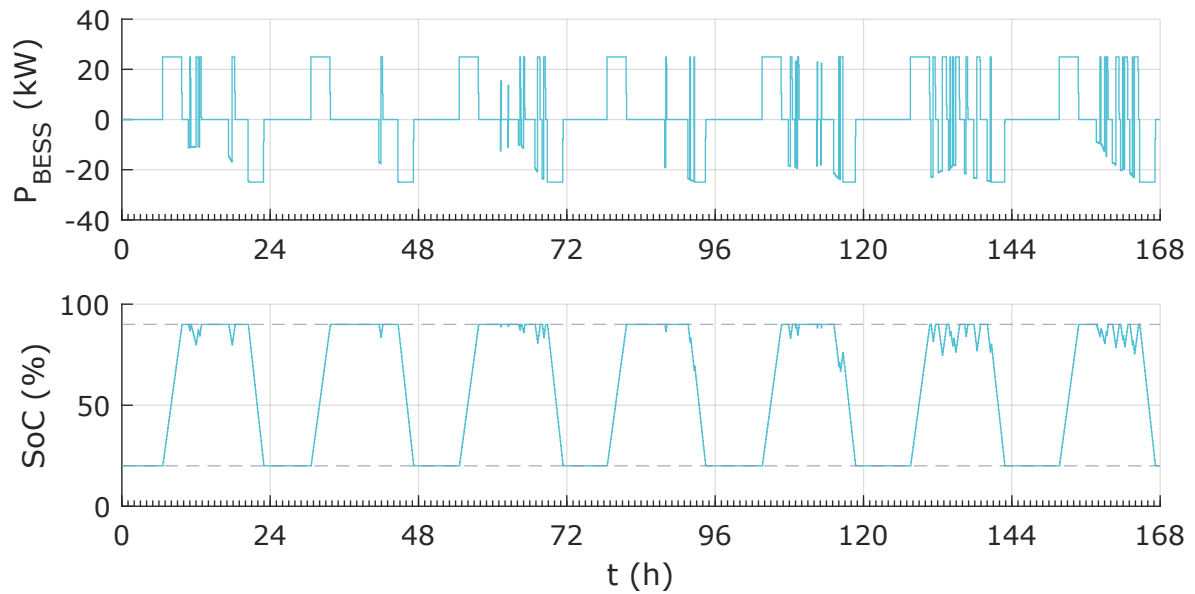
Figure 5.2: BESS usage for baseline strategy in summer

Table 5.1: Simulation results for baseline strategy

(a) Economic

Metric	Summer		Winter	
	P2P	CRS	P2P	CRS
Profit TC (€)	−73.45	−95.84	−63.49	−79.15
Profit LEC (€)	276.03	143.05	−29.55	130.10
Profit CO (€)	−115.63	39.74	179.11	35.11

(b) Technical

Metric	Summer	Winter
Energy AC chargers (kWh)	886.68	984.70
Energy DC charger (kWh)	349.59	328.63
Charged energy BESS (kWh)	704.69	561.96
Discharged energy BESS (kWh)	−704.69	−561.96

5.2.2 Price-sensitive

For the price-sensitive strategy, graphical results for power flows and battery usage can be found in appendices A.8 (summer) and A.9 (winter).

Table 5.2 shows the economic and technical outcomes. Again, the LEC is more profitable in summer, while the CO is more profitable in winter. TC makes significantly more profit in winter compared to the baseline strategy. In general, the total profit of the MG is higher. Further, the BESS is used more in winter for this strategy.

Table 5.2: Simulation results for price-sensitive strategy

(a) Economic

Metric	Summer		Winter	
	P2P	CRS	P2P	CRS
Profit TC (€)	−70.38	−95.84	−43.94	−79.15
Profit LEC (€)	244.06	138.06	−40.90	167.56
Profit CO (€)	−93.50	37.96	221.76	48.51

(b) Technical

Metric	Summer	Winter
Energy AC chargers (kWh)	911.26	1199.50
Energy DC charger (kWh)	327.32	381.18
Charged energy BESS (kWh)	727.32	1141.56
Discharged energy BESS (kWh)	−707.20	−1133.04

5.2.3 Scheduling

The graphical results for the scheduling strategy can be found in appendices A.10 (summer) and A.11 (winter).

Table 5.3 shows the numerical outcomes. The scheduling strategy achieves positive profits for the LEC in both scenarios when looking at the P2P trading market. The BESS is used significantly less and also the energy supplied to the chargers is less than for the other strategies.

Additional simulation results for the three strategies and for each scenario, which are not used for evaluation, can be found in appendix A.12. These metrics are the total energy that the MG imports from and exports to the main grid. The total charging time of all EVs, the charging time that was cancelled due to the extended stay time of target-based cars, and the overall extended charging time of these cars. Further, the exact number of cancelled EVs is given. The additional EV charging metrics deliver similar results compared to the main limitation metric (compare table 5.8).

Table 5.3: Simulation results for scheduling strategy

(a) Economic

Metric	Summer		Winter	
	P2P	CRS	P2P	CRS
Profit TC (€)	−80.91	−95.84	−70.00	−79.15
Profit LEC (€)	300.31	173.04	9.89	117.54
Profit CO (€)	−91.72	50.47	129.12	30.61

(b) Technical

Metric	Summer	Winter
Energy AC chargers (kWh)	649.92	717.18
Energy DC charger (kWh)	144.43	251.10
Charged energy BESS (kWh)	310.93	241.85
Discharged energy BESS (kWh)	−310.93	−241.85

5.3 Comparison

For comparison of the three strategies, the summer and the winter scenario are combined for each strategy to average seasonal effects. This makes the estimated profits more accurate. Table 5.4 shows the combined profits for each owner. It can be seen that the LEC as well as the CO have positive 14-day profits for every case.

Table 5.4: Profits of combined scenarios, separated according to P2P and CRS markets

Owner	Baseline		Price-sensitive		Scheduling	
	P2P	CRS	P2P	CRS	P2P	CRS
TC (€)	−136.94	−174.99	−114.32	−174.99	−150.91	−174.99
LEC (€)	246.48	273.15	203.16	305.62	310.20	290.58
CO (€)	63.48	74.85	128.26	86.47	37.40	81.08

Total profits for the MG and the fairness respectively ETP metrics are calculated based on table 5.4. Table 5.5 compares the three strategies according to these metrics.

Table 5.5: Comparison of profits

Profit metric	Baseline	Price-sensitive	Scheduling
Total MG profit (€)	173.02	217.10	196.69
Fairness (%)	85.34	68.54	85.19
ETP (€)	147.66	148.80	167.56

For the CRS market, only total profit is compared due to inherent fairness. The price-sensitive strategy performs the best relative to the baseline strategy since it makes 25.48 % more profit. Also, the scheduling strategy is 13.68 % more profitable. This shows that it is worth implementing more sophisticated energy management strategies. Though, scheduling does not perform as well as the price-sensitive strategy. For the P2P

trading market, also the fairness of revenue sharing is important, which is expressed by ETP. In this case, the baseline and the scheduling strategies share revenue almost equally well with a fairness value of around 85 %. Scheduling performs here 13.48 % better in terms of ETP compared to the baseline strategy. The price-sensitive strategy achieves only a 0.77 % improvement due to less fairness (69 %), even though its total profit is the highest. From the perspective of ETP and the P2P market, the scheduling strategy provides the most balanced performance.

Depending on the market structure, the price-sensitive or the scheduling performs the best. Total profit and ETP view economic feasibility in a linear-like way, where initial investments are neglected. PBPs in table 5.6 set the P2P trading profits of the LEC and the CO in relation to their investments. This is a more non-linear interpretation of economic feasibility. The average lifetimes of assets (see section 3.1) are used for calculations. The relative deviation of the PBP from the asset lifetime describes how much longer or shorter the PBP is compared to the lifetime. Results show that the estimated PBPs are only for the price-sensitive strategy and the CO 1.80 %, and for the scheduling strategy and the LEC 10.92 % lower than the lifetime. This indicates that none of the investments is attractive. For the CO and scheduling, the deviation from the lifetime is even 236.70 % higher. From this perspective, the price-sensitive strategy provides the most balanced performance because chargers make the most revenue.

Table 5.6: Comparison of PBPs for P2P market

PBP metric	Baseline		Price-sensitive		Scheduling	
	LEC	CO	LEC	CO	LEC	CO
Lifetime (years)	12.73	10.00	12.73	10.00	12.73	10.00
PBP (years)	14.28	19.84	17.32	9.82	11.34	33.67
Relative ΔPBP (%)	+12.18	+98.40	+36.06	−1.80	−10.92	+236.70

Even though investments and yearly profits are only rough estimations, it can be said that none of the investments is significantly profitable and therefore, the economic feasibility of the MG is poor. The main issue of all strategies is the low overall profit not able to compensate for the offset introduced by investment cost. Thus, PBPs for the CRS market do not need to be further investigated. The second takeaway is that total profit metrics in table 5.5 only indicate economic feasibility if profits are high enough to provide PBPs significantly below the assets' lifetimes.

TC though saves money in all strategies when comparing the P2P market with the CRS market. Relative to street lighting operational cost, savings vary between 13.76 % (scheduling strategy) and 34.67 % (price-sensitive strategy). From the viewpoint of TC, the economic feasibility is not affected negatively.

Table 5.7: Comparison of TC savings

Saving metric	Baseline	Price-sensitive	Scheduling
Savings (€)	38.05	60.67	24.08
Relative savings (%)	21.74	34.67	13.76

Technical metrics, which are described in the following, give intuition about the quality of EV charging service and the usage of BESS. They allow to derive the qualitative impact on the economic feasibility and complement the perspectives of total profit and PBP.

Table 5.8 compares strategies according to the amount of charger curtailment. The maximum energy of AC chargers or the DC charger is the energy that would have been supplied with no limitation control (see sub-section 2.4.4). The actual supplied energy is compared to the maximum. The price-sensitive strategy achieves the best result with only 13.26 % limitation, even though EV charging support through BESS discharging is limited due to economic reasons (compare section 4.3). The baseline strategy limits chargers by 21.56 %, which is still a decent performance for a simple control approach. The scheduling strategy stands out with a total limitation of 45.77 %, where particular the DC charger is limited over 50 %. This indicates that EV forecasting cannot be fully compensated by using peak hours and power dispatch of hourly power budgets.

Table 5.8: Comparison of EV charger limitation

EV metric	Baseline		Price-sensitive		Scheduling	
	AC	DC	AC	DC	AC	DC
Max energy (kWh)	2377.80	872.40	2377.80	872.40	2377.80	872.40
Supplied energy (kWh)	1871.38	678.22	2110.76	708.50	1367.10	395.53
Limitation (%)	21.30	22.26	11.23	18.79	42.51	54.66
	21.56		13.26		45.77	

Based on limitation figures, the scheduling strategy tends to affect economic feasibility strongly due to inconsistent EV charging quality. In the case of the baseline and price-sensitive strategies, economic feasibility is likely to be compromised significantly less.

Battery usage is described at a high level by EFCs per day. Table 5.9 lists EFCs for the 14-day period and normalised to one day. The baseline strategy does 1.29 cycles per day which is a result of charging based on PV availability and additional EV charger support. The price-sensitive strategy performs the most cycles per day (1.89) which correlates with less charger limitation and BESS energy trading. The scheduling strategy does only 0.56 full cycles per day which is mainly determined by the schedule. Since the LEC makes the most profit with this strategy, it can be said that scheduling of the BESS performs well compared to EV charger scheduling. Overall, EFCs stay within 0.5 and 2 full cycles per day, which is considered to be within the acceptable range.

Table 5.9: Comparison of BESS usage

BESS metric	Baseline	Price-sensitive	Scheduling
Charged energy (kWh)	1266.65	1868.88	552.78
Discharged energy (kWh)	−1266.65	−1840.24	−552.78
Total EFCs	18.10	26.49	7.90
Daily EFCs	1.29	1.89	0.56

By combining economic and technical perspectives on economic feasibility, the following conclusions can be made. Considering the CRS market, the price-sensitive strategy

increases the economic feasibility the most due to the highest total profit of the MG. For the P2P market, the price-sensitive strategy shares revenue less fair but still provides the most balanced PBPs. Further, the quality of EV charging service is the best for this strategy. Although the scheduling strategy shares revenue fair while achieving medium total profit, the deviations of owners' PBPs and the strongly limited EV charging service affects economic feasibility negatively. The baseline strategy provides solid performance with respect to total profit, fairness, and EV charger limitation. For these reasons, the price-sensitive strategy increases economic feasibility the most.

SUMMARY

Conclusion

This thesis aimed to develop energy management strategies for urban microgrids (MGs) that increase their economic feasibility. Improving the economic feasibility is the main goal because urban distribution grids are not prepared for the integration of electric vehicle (EV) charging services and renewable distributed generation (DG). To mitigate the problem of costly infrastructure enhancements, MGs with energy management can be used. However, investments in urban MGs will only be made when they can operate the grid in an economically beneficial way.

Chapter 1 gave a state-of-the-art overview of the main MG topologies, their main components and operation modes. Multi-level control is a prerequisite for the successful operation of MGs. Thus, the hierarchical control approach was described. Energy management with a focus on economics is part of tertiary-level control. Commonly, it is implemented with a centralised controller. Stochastic access of EVs does not allow the application of classical optimisation techniques. Also, multi-ownership is an important aspect of designing energy management systems (EMSs).

Chapter 2 introduced the pilot site that is considered in this thesis. The main components were identified and suitable modelling approaches were described. For the battery energy storage system (BESS), a simplified mathematical model is used. The street lighting system and the photovoltaic (PV) system are modelled with load and generation profiles. Modelling EV chargers requires a more sophisticated approach since hourly power consumption data does not represent typical charging procedures of EVs. Therefore, a modelling approach based on existing measurements was developed. It assumes that EV owners act either time or state of charge (SoC)-target-based.

Chapter 3 gave an overview of the financial data that is used. For energy trading, a peer-to-peer (P2P) trading market was developed. It defines how cost and revenue are shared inside the MG. The economic feasibility of the whole MG depends on the profits of each owner. Thus, a second collective revenue sharing (CRS) market was introduced that represents optimal revenue sharing. It helps to evaluate the fairness aspect of revenue sharing for the P2P market.

Three energy management strategies were developed in chapter 4. The first strategy represents the baseline. It was developed with the aim to provide simple and robust control based on rules. EV charger limitation is done with a fixed lookup table (LUT) that is also used in the second strategy. The second price-sensitive strategy includes the market price signal to define price-sensitive rules. Further, the BESS SoC range is divided into a lower range for supporting EV charging and an upper range for trading energy. The third scheduling strategy schedules power setpoints on an hourly basis without EV charger forecasting. Constraints based on peak-hour data of chargers are used to account for the lack of precise predictions. A simple forecasting model for PV is used to include forecasting errors in the simulation. The schedules are obtained by

mixed-integer linear programming (MILP) and the hourly setpoints are then used for real-time (RT) dispatch control.

Finally, chapter 5 defines economic metrics to compare the strategies. Since economic feasibility cannot be completely defined by one metric, further economic and technical metrics are introduced to make additional qualitative statements about the performance of the different strategies.

For the CRS market, the total profit of the MG mainly indicates economic feasibility. The price-sensitive strategy performs 25.48 % better than the baseline. The scheduling strategy can still generate 13.68 % more profit. This shows that it is beneficial to implement more sophisticated strategies. For the P2P trading market also the fairness of revenue sharing is evaluated. Both the baseline and the scheduling strategies reach around 85 % fairness. The price-sensitive strategy achieves only 69 % fairness, which results in 0.77 % better effective total profit (ETP) compared to the baseline. When looking at the ETP of the scheduling strategy, an improvement of 13.48 % can be observed. It has the most balanced performance for P2P trading. Further, individual economic feasibility is evaluated by the payback periods (PBPs) of the local energy community (LEC) and the charger operator (CO), and savings of Tartu city (TC). While TC can save money within a range of 13.76 % to 34.67 % in any case, PBPs of the other owners are not significantly below the lifetimes of the assets, which translates into poor economic feasibility. Economic feasibility is indirectly affected by EV charger limitation. The price-sensitive strategy limits chargers only by 13.26 %. The scheduling strategy has a major impact on the quality of charging service by limitation of 45.77 %. Significant charger limitation is likely to affect the economic feasibility of the MG negatively. BESS usage in terms of equivalent full cycles (EFCs) varies between 0.56 and 1.89 cycles per day which is estimated to be acceptable. Overall, the price-sensitive strategy increases the economic feasibility of the considered MG the most.

Future work

This thesis looked at economic feasibility mainly from the perspective of total profit and fairness of revenue sharing. Future work could include modelling the impact of BESS utilisation and the limitation of EV chargers on economic feasibility. PBPs include investments to quantify economic feasibility from another perspective. Simulation for longer periods, e.g. one year, and better estimations of required capital investments, e.g inquiry of companies, could deliver more accurate estimations. The main issue identified is the low overall profit of the MG. Applying also time of use (ToU) pricing to EV chargers based on the day-ahead market instead of using fixed tariffs could increase external revenue coming from outside the MG and therefore, increase the economic feasibility further.

KOKKUVÕTE (SUMMARY IN ESTONIAN)

Järeldused

Käesoleva lõputöö eesmärk oli arendada energiahaldusstrateegiad linnade mikrovõrkude jaoks, mis suurendaksid nende majanduslikku tasuvust. Majandusliku tasuvuse parandamine on tähtis eesmärk, sest linnade jaotusvõrgud ei ole ette valmistatud elektrisõidukite (EV) laadimisteenuste ja taastuvenergia hajutatud tootmise integreerimiseks. Kulukate elektrivõrgu tugevdamiste asemel võib kasutada energiahaldusega mikrovõrkusid. Linnade mikrovõrkudesse investeerimise oluliseks eelduseks on selle majanduslik tasuvus.

Peatükis 1 anti ülevaade peamistest mikrovõrkude topoloogiatest, nende peamistest komponentidest ja talitlusviisidest. Mitmekihiline juhtimine on mikrovõrkude eduka toimimise eelduseks. Seega kirjeldati hierarhilist juhtimismudelit. Energiahaldus, mis keskendub ökonoomsusele, on osa kolmanda tasandi juhtimisest. Tavaliselt rakendatakse seda tsentraliseeritud kontrolleri abil. EVde stohhastiline laadimine ei võimalda rakendada klassikalisi optimeerimismeetodeid. Energiahaldussüsteemide kavandamisel on oluline arvestada mitme omaniku huvidega.

Peatükis 2 tutvustati käesolevas töös käsitletavat pilootprojekti. Määrati kindlaks peamised komponendid ja kirjeldati sobivaid modelleerimisviise. Aku energiasalvestussüsteemi puhul kasutatakse lihtsustatud matemaatilist mudelit. Tänavavalgustussüsteemi ja päikesepaneelide süsteemi (PV) modelleeritakse koos koormus- ja tootmisprofiilidega. EV laadijate modelleerimiseks on vaja keerukamat lähenemisviisi, kuna tunnipõhised tarbimismõõtmise andmed ei kajasta EVde laadimise tüüpilisi protseduure. Seetõttu töötati välja olemasolevatel mõõtmistel põhinev modelleerimismeetod, mis eeldab, et EV omanikud tegutsevad kas laadimisaja või laadimistsükli sihi alusel.

Peatükis 3 anti ülevaade kasutatud finantsandmetest. Energiakaubanduse jaoks töötati välja vastastikune (*peer-to-peer*, P2P) kauplemismudel, mis määratleb, kuidas kulud ja tulud jagunevad mikrovõrgu siseselt. Kogu mikrovõrgu majanduslik tasuvus sõltub iga osalise kasumist. Seega võeti kasutusele teine ärimudel, mis kujutab endast optimaalset tulude jagamist (*collective revenue sharing*, CRS), mis aitab hinnata tulude jagamise õigsust kõigi osapoolte suhtes.

Peatükis 4 töötati välja kolm energiamajandusstrateegiat. Esimene strateegia kujutab endast baasstrateegiat. See töötati välja eesmärgiga pakkuda lihtsat ja töökindlat, reeglitel põhinevat juhtimist teiste strateegiatega võrdlemiseks. EV-laadijate piiramine toimub fikseeritud otsingutabeli (*lookup table*, LUT) abil, mida kasutatakse ka teises strateegias. Teine strateegia seisneb hinnapõhises juhtimises, mis hõlmab turuhinnasignaali, et määratleda hinnatundlikud reeglid. Lisaks on akusüsteemi tööpiirkond jagatud EV laadimise toetamiseks mõeldud alumiseks piirkonnaks ja energiaga kauplemise ülemiseks piirkonnaks. Kolmas strateegia kavandab seadmetele tunnupõhise juhtimisgraafiku ilma EV-laadijate prognoosideta. Täpse prognoosi puudumisest tingitud vigade vähendamiseks kasutatakse optimeerimispiiranguid, mis on tuletatud laadijate tipptunni andmete analüüsis. Simulatsioonis kasutatakse lihtsat PV prognoosimudelit, et võtta prognoosivigu

arvesse. Sõiduplaanid saadakse segatud täisarvulise lineaarse programmeerimise abil ja seejärel kasutatakse tunnipõhiseid seadistuspunkte reaalajas toimuvaks juhtimiseks.

Lõpuks määratletakse 5 peatükis majandusnäitajad strateegiate võrdlemiseks. Kuna majanduslikku tasuvust ei saa täielikult määratleda ühe mõõdiku abil, võetakse kasutusele täiendavad majanduslikud ja tehnilised mõõdikud, et tõhusamalt analüüsida strateegiate tulemusi.

Mikrovõrgu kogukasumi tulemuste alusel on võimalik öelda, et CRS turg on majanduslikult tasuv. Strateegia 2 saavutab 25,48 % parema tulemuse kui alusstrateegiaga (strateegia 1). ning strateegia 3 suudab 13,68 % rohkem tulu teenida võrreldes alusstrateegiaga. See näitab, et keerukamate strateegiate rakendamine on kasulik. P2P-kaubandusturu puhul hinnatakse ka tulude jagamise õiglust. Nii strateegia 1 kui ka strateegia 3 saavutavad umbes 85 % õigluse. Strateegia 2 saavutab ainult 69 % õigluse, mis annab 0,77 % kõrgema tegeliku kogukasumi võrreldes alusstrateegiaga. Kui vaadata strateegia 3 kogukasumit, siis on täheldatav 13,48 %-ne kogukasumi kasv. See on kõige tasakaalustatum tulemuslikkus P2P-kauplemisel. Lisaks hinnatakse individuaalset majanduslikku tasuvust kohaliku energiaühistu (LEC) ja laadimisseadme operaatori (CO) tasuvusperioodi ning Tartu linna munitsipaali (TC) kokkuhoiu alusel. Kui Tartu linn võib igal juhul säästa 13,76 % kuni 34,67 %, siis teiste omanike tasuvusperioodid ei ole oluliselt madalamad varade eluteast, mis tähendab kehva majanduslikku tasuvust. Majanduslikku tasuvust mõjutab kaudselt EV-laadijate võimsuspiirangud. Strateegia 2 piirab laadijaid ainult 13,26 % võrra. Strateegia 3 mõjutab oluliselt laadimisteenuse kvaliteeti, kuna see piirab laadimisvõimsust lausa 45,77 %. Laadijate märkimisväärne piiramine mõjutab negatiivselt mikrovõrgu majanduslikku tasuvust. Akusüsteemi kasutus ekvivalentsete laadimistsüklite näol varieerub vahemikus 0,56 kuni 1,89 laadimistsüklit ööpäevas. See vahemik on vastuvõetav, kuid laadimistsüklite mõju majanduslikule tasuvusele ei ole antud lõputöös täiendavalt uuritud. Üldiselt suurendab strateegia 2 kõige rohkem vaatlusaluse mikrovõrgu majanduslikku tasuvust.

Tulevane töö

Käesolevas lõputöös vaadeldi majanduslikku tasuvust peamiselt kogukasumi ja tulude jagamise õigluse seisukohast. Tulevases töös võiks uurida akusüsteemi kasutamise ja EV-laadijate piirangute mõju majanduslikule tasuvusele. Samuti on tasuvusaeg sobiv mõõdik majandusliku tasuvuse kvantifitseerimiseks. Täpsemaid hinnanguid võiks anda pikema perioodi (nt ühe aasta) simulatsioon ja vajalike kapitaalinvesteeringute kohta ettevõtete küsitlemine. Peamine tuvastatud probleem on mikrovõrgu madal kogukasum. Päev ette turul põhineva tariifi rakendamine EV laadijatele simulatsioonides kasutatud fikseeritud tariifi asemel võiks suurendada mikrovõrgust väljastpoolt tulevat tulu ja seega suurendada majanduslikku tasuvust.

REFERENCES

[1] IEA, *Key World Energy Statistics 2021*, International Energy Agency. Available at *https://www.iea.org/reports/key-world-energy-statistics-2021* (accessed on 16.11.2022).

[2] C. Issawi, "The 1973 Oil Crisis and After", *Journal of Post Keynesian Economics*, vol. 1, no. 2, pp. 3–26, 1978. Available at *https://www.jstor.org/stable/4537467*.

[3] ERR News, "Estonia to stop importing Russian gas by end of 2022", *Eesti Rahvusringhääling*, 7th Apr. 2022. Available at *https://news.err.ee/1608557521/estonia-to-stop-importing-russian-gas-by-end-of-2022* (accessed on 30.09.2022).

[4] Guardian, "'We were all wrong': how Germany got hooked on Russian energy", *Guardian*, Available at *https://www.theguardian.com/world/2022/jun/02/germany-dependence-russian-energy-gas-oil-nord-stream* (accessed on 30.09.2022).

[5] IPCC, *Climate Change 2022: Impacts, Adaptation and Vulnerability*, Summary for Policymakers, Intergovernmental Panel on Climate Change, 2022. Available at *https://www.ipcc.ch/report/ar6/wg2/* (accessed on 16.11.2022).

[6] DW, "From Deepwater to Chernobyl: Counting the casualties", *Deutsche Welle*, 20th Apr. 2015. Available at *https://www.dw.com/en/from-deepwater-to-chernobyl-counting-the-casualties/a-18393176* (accessed on 01.10.2022).

[7] UN, *Paris Agreement*, United Nations, 2015.

[8] EC, *European Green Deal*, European Commission, 2019.

[9] M. Pavičević *et al.*, "The potential of sector coupling in future European energy systems: Soft linking between the Dispa-SET and JRC-EU-TIMES models", *Applied Energy*, vol. 267, p. 115 100, 2020, ISSN: 03062619. DOI: *10.1016/j.apenergy.2020.115100*.

[10] V. Quaschning and C. Quaschning, *Energierevolution jetzt!: Mobilität, Wohnen, grüner Strom und Wasserstoff: Was führt uns aus der Klimakrise – und was nicht?* München: Hanser, 2022, 1282 pp., ISBN: 9783446274860.

[11] BBC News, "Major breakthrough on nuclear fusion energy", *British Broadcasting Corporation*, 9th Feb. 2022. Available at *https://www.bbc.com/news/science-environment-60312633* (accessed on 08.10.2022).

[12] IRENA, *Renewable Power Generation Costs in 2021*, International Renewable Energy Agency, Ed., Abu Dhabi, 2021. Available at *https://www.irena.org/publications/2022/Jul/Renewable-Power-Generation-Costs-in-2021#:~:text=The%20global%20weighted%20average%20levelised,%25%20to%20USD%200.075%2FkWh.* (accessed on 16.11.2022).

[13] M. A. Hossain, H. R. Pota, M. J. Hossain and F. Blaabjerg, "Evolution of microgrids with converter-interfaced generations: Challenges and opportunities", *International Journal of Electrical Power & Energy Systems*, vol. 109, pp. 160–186, 2019, ISSN: 01420615. DOI: *10.1016/j.ijepes.2019.01.038*.

[14] UCTE. "Final Report: System Disturbance on 4 November 2006". (2006), Available at *https://www.entsoe.eu/fileadmin/user_upload/_library/publications/ce/otherreports/Final-Report-20070130.pdf* (accessed on 08.10.2022).

[15] L. Mehigan, J. P. Deane, B. Gallachóir and V. Bertsch, "A review of the role of distributed generation (DG) in future electricity systems", *Energy*, vol. 163, pp. 822–836, 2018, PII: S0360544218315366, ISSN: 03605442. DOI: *10.1016/j.energy.2018.08.022*.

[16] DW, "German wind power cable sparks protests", *Deutsche Welle*, 22nd Apr. 2019. Available at *https://www.dw.com/en/germany-protesters-oppose-suedlink-wind-energy-cable/a-48437451* (accessed on 30.09.2022).

[17] T. L. Vandoorn, J. C. Vasquez, J. de Kooning, J. M. Guerrero and L. Vandevelde, "Microgrids: Hierarchical Control and an Overview of the Control and Reserve Management Strategies", *IEEE Industrial Electronics Magazine*, vol. 7, no. 4, pp. 42–55, 2013, ISSN: 1932-4529. DOI: *10.1109/MIE.2013.2279306*.

[18] EC. "Establishment of Smart City Center of Excellence", European Commission. (2019), Available at *https://cordis.europa.eu/project/id/856602* (accessed on 12.10.2022).

[19] FinEst Centre. "Reducing Energy Supply Requirements Using Microgrids and Energy Storages". (2022), Available at *https://www.finestcentre.eu/microgrids* (accessed on 26.04.2022).

[20] X. Lu, K. Zhou, X. Zhang and S. Yang, "A systematic review of supply and demand side optimal load scheduling in a smart grid environment", *Journal of Cleaner Production*, vol. 203, pp. 757–768, 2018, PII: S0959652618326623, ISSN: 09596526. DOI: *10.1016/j.jclepro.2018.08.301*.

[21] S. Ishaq, I. Khan, S. Rahman, T. Hussain, A. Iqbal and R. M. Elavarasan, "A review on recent developments in control and optimization of micro grids", *Energy Reports*, vol. 8, pp. 4085–4103, 2022, PII: S2352484722000804, ISSN: 23524847. DOI: *10.1016/j.egyr.2022.01.080*.

[22] A. Ahmad Khan, M. Naeem, M. Iqbal, S. Qaisar and A. Anpalagan, "A compendium of optimization objectives, constraints, tools and algorithms for energy management in microgrids", *Renewable and Sustainable Energy Reviews*, vol. 58, pp. 1664–1683, 2016, PII: S1364032115016421, ISSN: 13640321. DOI: *10.1016/j.rser.2015.12.259*.

[23] E. Mohagheghi, M. Alramlawi, A. Gabash and P. Li, "A Survey of Real-Time Optimal Power Flow", *Energies*, vol. 11, no. 11, p. 3142, 2018, PII: en11113142. DOI: *10.3390/en11113142*.

[24] R. H. Lasseter, "MicroGrids", in *2002 IEEE Power Engineering Society Winter Meeting. Conference Proceedings (Cat. No.02CH37309)*, (New York, NY, USA), IEEE, 2002, pp. 305–308, ISBN: 0-7803-7322-7. DOI: *10.1109/PESW.2002.985003*.

[25] D. Y. Yamashita, I. Vechiu and J.-P. Gaubert, "A review of hierarchical control for building microgrids", *Renewable and Sustainable Energy Reviews*, vol. 118, p. 109 523, 2020, PII: S1364032119307312, ISSN: 13640321. DOI: *10.1016/j.rser.2019.109523*.

[26] E. O. Arwa and K. A. Folly, "Reinforcement Learning Techniques for Optimal Power Control in Grid-Connected Microgrids: A Comprehensive Review", *IEEE Access*, vol. 8, pp. 208 992–209 007, 2020. DOI: *10.1109/ACCESS.2020.3038735*.

[27] T. Ackermann, G. Andersson and L. Söder, "Distributed generation: a definition", *Fuel and Energy Abstracts*, vol. 43, no. 3, p. 191, 2002, PII: S01406701028576 29, ISSN: 01406701. DOI: *10.1016/S0140-6701(02)85762-9*.

[28] D. W. Gao, *Energy Storage for Sustainable Microgrid*. Burlington: Elsevier, 2015, 153 pp., ISBN: 9780128033746. DOI: *10.1016/C2014-0-04144-5*.

[29] Y. Zhou and C. Ngai-Man Ho, "A review on Microgrid architectures and control methods", in *2016 IEEE 8th International Power Electronics and Motion Control Conference (IPEMC-ECCE Asia)*, (Hefei, China), IEEE, 2016, pp. 3149–3156, ISBN: 978-1-5090-1210-7. DOI: *10.1109/IPEMC.2016.7512799*.

[30] Enefit Volt. "Are we ready for the breakthrough of electric cars?" (2022), Available at *https://enefitvolt.com/en/blogi/Kas-me-oleme-elektriautode-labimurdeks-valmis* (accessed on 11.10.2022).

[31] MathWorks. "MATLAB System Block", Available at *https://ch.mathworks.com/help/simulink/ug/what-is-matlab-system-block.html* (accessed on 15.10.2022).

[32] Pixii. "PowerShaper 2: Flexible grid tied energy storage system". (2022), Available at *https://www.pixii.com/wp-content/uploads/2022/08/2022-05-04-PowerShaper2-50kW-v2.pdf* (accessed on 15.10.2022).

[33] Y. WANG, Z. ZHOU, A. BOTTERUD, K. ZHANG and Q. DING, "Stochastic coordinated operation of wind and battery energy storage system considering battery degradation", *Journal of Modern Power Systems and Clean Energy*, vol. 4, no. 4, pp. 581–592, 2016, PII: 238, ISSN: 2196-5625. DOI: *10.1007/s40565-016-0238-z*.

[34] M. A. Hossain, H. R. Pota, S. Squartini, F. Zaman and K. M. Muttaqi, "Energy management of community microgrids considering degradation cost of battery", *Journal of Energy Storage*, vol. 22, pp. 257–269, 2019, PII: S2352152X18305620, ISSN: 2352152X. DOI: *10.1016/j.est.2018.12.021*.

[35] UL Solutions. "HOMER Pro 3.15: Battery Roundtrip Efficiency", Available at *https://www.homerenergy.com/products/pro/docs/latest/battery_roundtrip_efficiency.html* (accessed on 18.11.2022).

[36] B. Su, X. Ke and C. Yuan, "Electrochemical Modeling of Calendar Capacity Loss of Nickel-Manganese-Cobalt (NMC)-Graphite Lithium Ion Batteries", *arXiv*, 2021. DOI: *10.48550/arXiv.2103.02166*.

[37] EU Science Hub. "API Non-Interactive Service", Eurpean Union, Available at *https://joint-research-centre.ec.europa.eu/pvgis-photovoltaic-geographical-information-system/getting-started-pvgis/api-non-interactive-service_en* (accessed on 16.10.2022).

[38] MathWorks. "1-D data interpolation (table lookup) - MATLAB interp1", Available at *https://ch.mathworks.com/help/matlab/ref/interp1.html* (accessed on 16.10.2022).

[39] A. Hooshmand, B. Asghari and R. Sharma, "A novel cost-aware multi-objective energy management method for microgrids", in *2013 IEEE PES Innovative Smart Grid Technologies Conference (ISGT)*, (Washington, DC), IEEE, 2013, pp. 1–6, ISBN: 978-1-4673-4896-6. DOI: *10.1109/ISGT.2013.6497882*.

[40] A. de Kwaasteniet. "EV spreadsheet". version 4, Available at *https://docs.google. com/spreadsheets/d/1k1DOw-NwvW8E8tQeXlacnt201fNc5qZyAPC0_vnoFBw/edi t#gid=735351678* (accessed on 16.10.2022).

[41] Enefit Volt. "Public charging", Available at *https://enefitvolt.com/en/elektriauto- avalik-laadimine* (accessed on 12.10.2022).

[42] eurostat. "Annual inflation up to 9.9% in the euro area", Available at *https://ec. europa.eu/eurostat/documents/2995521/15131946/2-19102022-AP-EN.pdf/ 92861d37-0275-8970-a0c1-89526c25f392* (accessed on 26.10.2022).

[43] ECB. "Euro foreign reference exchange rate: US dollar (USD)", European Central Bank. (2022), Available at *https://www.ecb.europa.eu/stats/policy_and_excha nge_rates/euro_reference_exchange_rates/html/eurofxref-graph-usd.en.html* (accessed on 26.10.2022).

[44] Integrify. "CapEx vs. OpEx: What's the Difference?", Available at *https://www. integrify.com/capex-vs-opex/* (accessed on 18.10.2022).

[45] D. Lugo-Laguna, A. Arcos-Vargas and F. Nuñez-Hernandez, "A European Assess- ment of the Solar Energy Cost: Key Factors and Optimal Technology", *Sustainabil- ity*, vol. 13, no. 6, p. 3238, 2021, PII: su13063238. DOI: *10.3390/su13063238*.

[46] K. Mongird *et al.*, *Energy Storage Technology and Cost Characterization Report*, 2019. DOI: *10.2172/1573487*. Available at *https://energystorage.pnnl.gov/pdf/ PNNL-28866.pdf* (accessed on 26.10.2022).

[47] ABB. "The home of charging: Terra AC wallbox". (2020), Available at *https://new. abb.com/docs/librariesprovider54/publikationer/9akk107680a2257_rev-d_terra_ ac_wallbox_brochure.pdf?sfvrsn=c4070c17_2* (accessed on 17.10.2022).

[48] Chargingshop.eu. "ABB Terra AC Display - 22 kW, Type 2 cable, RFID, MID, 4G, Wifi", Available at *https://chargingshop.eu/product/abb-terra-ac-display-22-kw- type-2-cable-rfid-mid-display-wifi/* (accessed on 17.10.2022).

[49] ABB. "Datasheet: Terra 54 UL 50 kW Data Sheet 50 kW DC fast charging station", Available at *https://search.abb.com/library/Download.aspx?DocumentID=4EVC 800801-LFUS&LanguageCode=en&DocumentPartId=&Action=Launch* (accessed on 17.10.2022).

[50] Chargingshop.eu. "ABB Terra 54 DC - 50kW fast charging station", Available at *https://chargingshop.eu/product/abb-terra-54-dc-50kw-fast-charging-station/* (accessed on 17.10.2022).

[51] Enphase Energy. "Electric Vehicle Charger Maintenance Basics". (2022), Available at *https://www.365pronto.com/blog/electric-vehicle-charger-maintenance* (ac- cessed on 25.10.2022).

[52] Elering. "Power market prices". (2022), Available at *https://dashboard.elering. ee/en/nps/price?interval=minute&period=days&start=2022-10-17T21:00: 00.000Z&end=2022-10-18T20:59:59.999Z* (accessed on 18.10.2022).

[53] ElektriHind. "Börsipaketid", Available at *https://elektrihind.ee/paketid* (accessed on 26.10.2022).

[54] Eesti Gaas. "Electricity". (2022), Available at *https://www.gaas.ee/en/estonian- gas/electricity/* (accessed on 26.10.2022).

[55] Elektrilevi. "Elektrilevi network service price list: Valid from June 1, 2022". (2022), Available at *https://www.elektrilevi.ee/-/doc/8644141/kliendile/Elektrilevi_ hinnakiri_vorguteenuse_hinnad_alates_1_juuni_2022_ENG.pdf* (accessed on 18.10.2022).

[56] Eleport. "Public charging", Available at *https://eleport.ee/en/charging-network/* (accessed on 12.10.2022).

[57] N. Shabbir, L. Kutt, V. Astapov, M. Jawad, A. Allik and O. Husev, "Battery Size Optimization With Customer PV Installations and Domestic Load Profile", *IEEE Access*, vol. 10, pp. 13 012–13 025, 2022. DOI: *10.1109/ACCESS.2022.3147977*.

[58] MathWorks. "Cross-correlation - MATLAB xcorr", Available at *https://ch.mathwor ks.com/help/matlab/ref/xcorr.html* (accessed on 05.11.2022).

[59] D. Bertsimas and J. N. Tsitsiklis, *Introduction to linear optimization* (Athena scientific books). Belmont, Massachusetts: Athena Scientific and Dynamic Ideas LLC, 1997, vol. 7, 587 pp., ISBN: 9781886529199.

[60] MathWorks. "Problem-Based Optimization Setup", Available at *https://ch.mathwor ks.com/help/optim/problem-based-approach.html?s_tid=CRUX_lftnav* (accessed on 23.10.2022).

[61] M. Asghari, A. M. Fathollahi-Fard, S. M. J. Mirzapour Al-e-hashem and M. A. Dulebenets, "Transformation and Linearization Techniques in Optimization: A State-of-the-Art Survey", *Mathematics*, vol. 10, no. 2, p. 283, 2022, PII: math10020283. DOI: *10.3390/math10020283*.

[62] MathWorks. "Solve optimization problem or equation problem - MATLAB solve", Available at *https://ch.mathworks.com/help/optim/ug/optim.problemdef.optimiz ationproblem.solve.html#d124e146870* (accessed on 07.12.2022).

[63] MathWorks. "Mixed-integer linear programming (MILP) - MATLAB intlinprog", Available at *https://ch.mathworks.com/help/optim/ug/intlinprog.html?s_tid=doc_ta# btv2x05* (accessed on 07.12.2022).

[64] Cambridge Dictionary. "Economic feasibility". (2022), Available at *https://dictionary.cambridge.org/dictionary/english/economic-feasibility* (accessed on 20.11.2022).

A APPENDICES

Figure A.1: Grid network diagram of MG at pilot site, pink: planned extensions
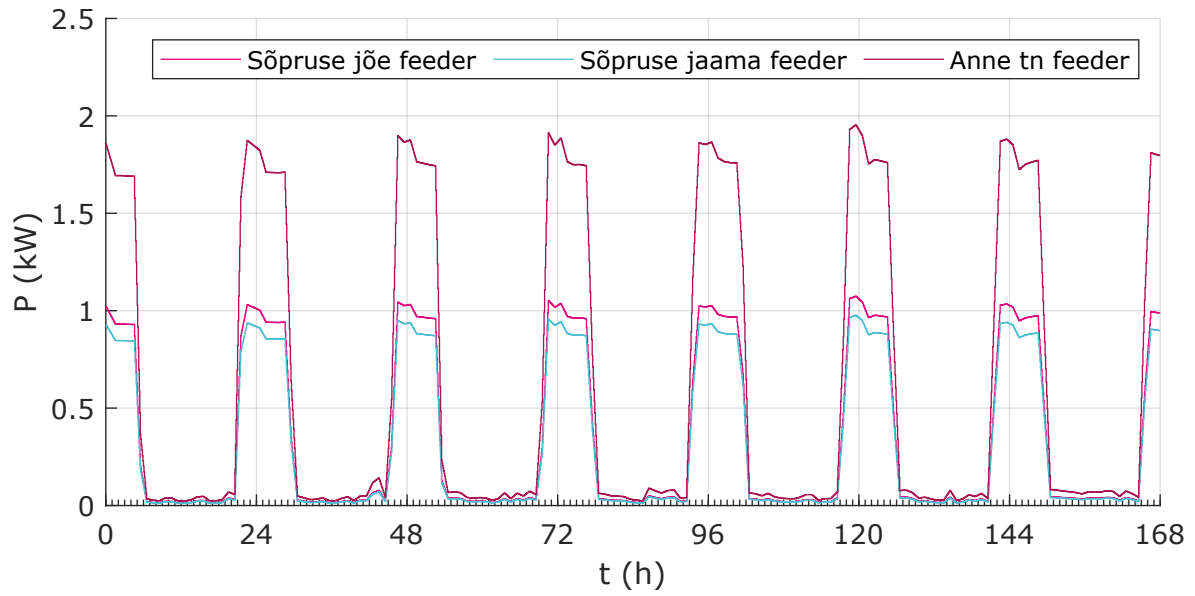
(a) Summer
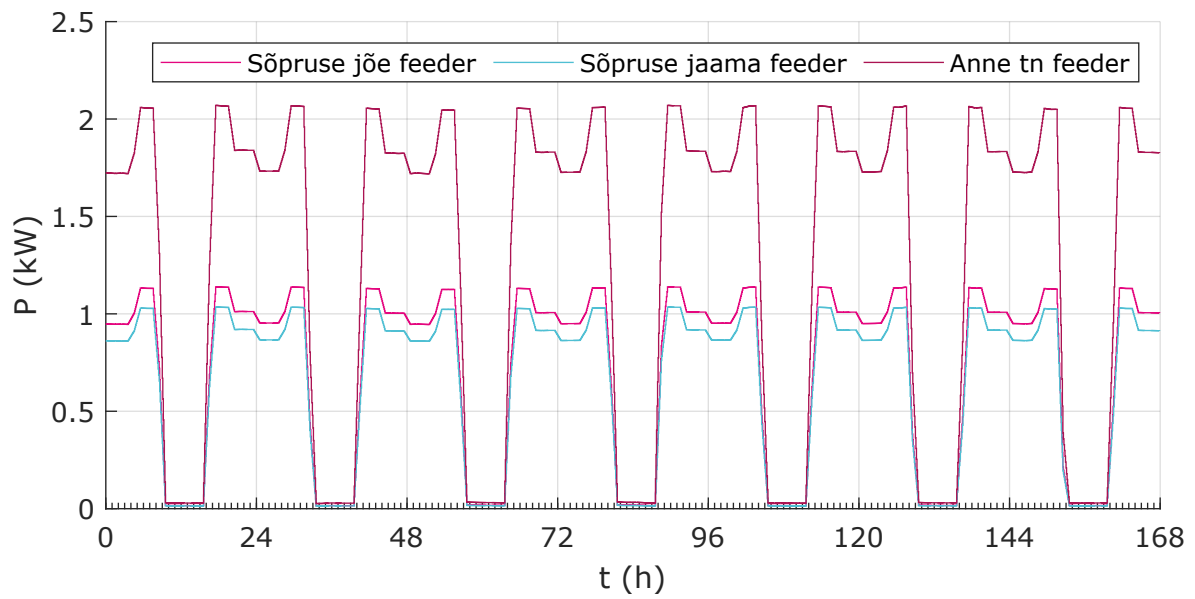
(b) Winter

Figure A.2: Scaled and interpolated street lighting load demand profiles
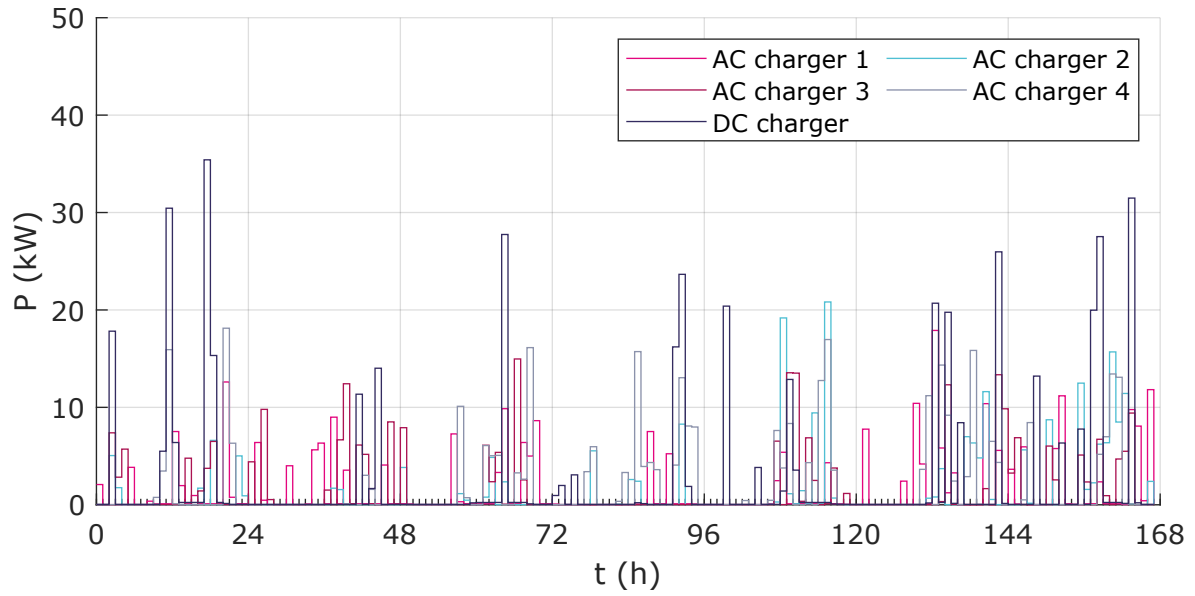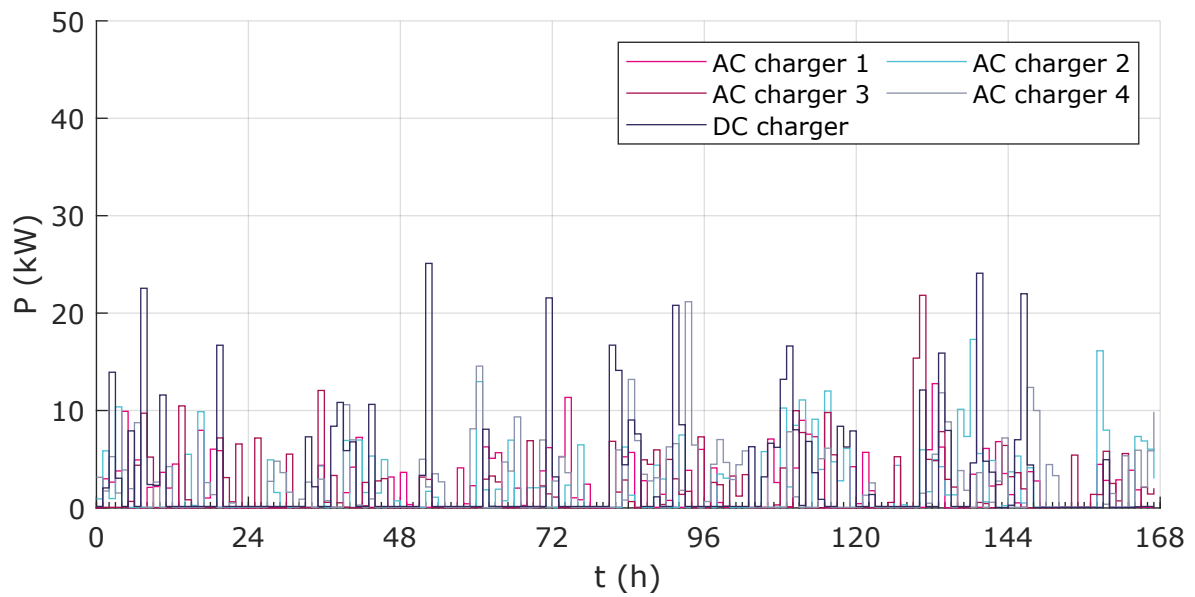
(a) Summer

(b) Winter

Figure A.3: EV charger measurements, measurements for AC chargers scaled based on charger rating

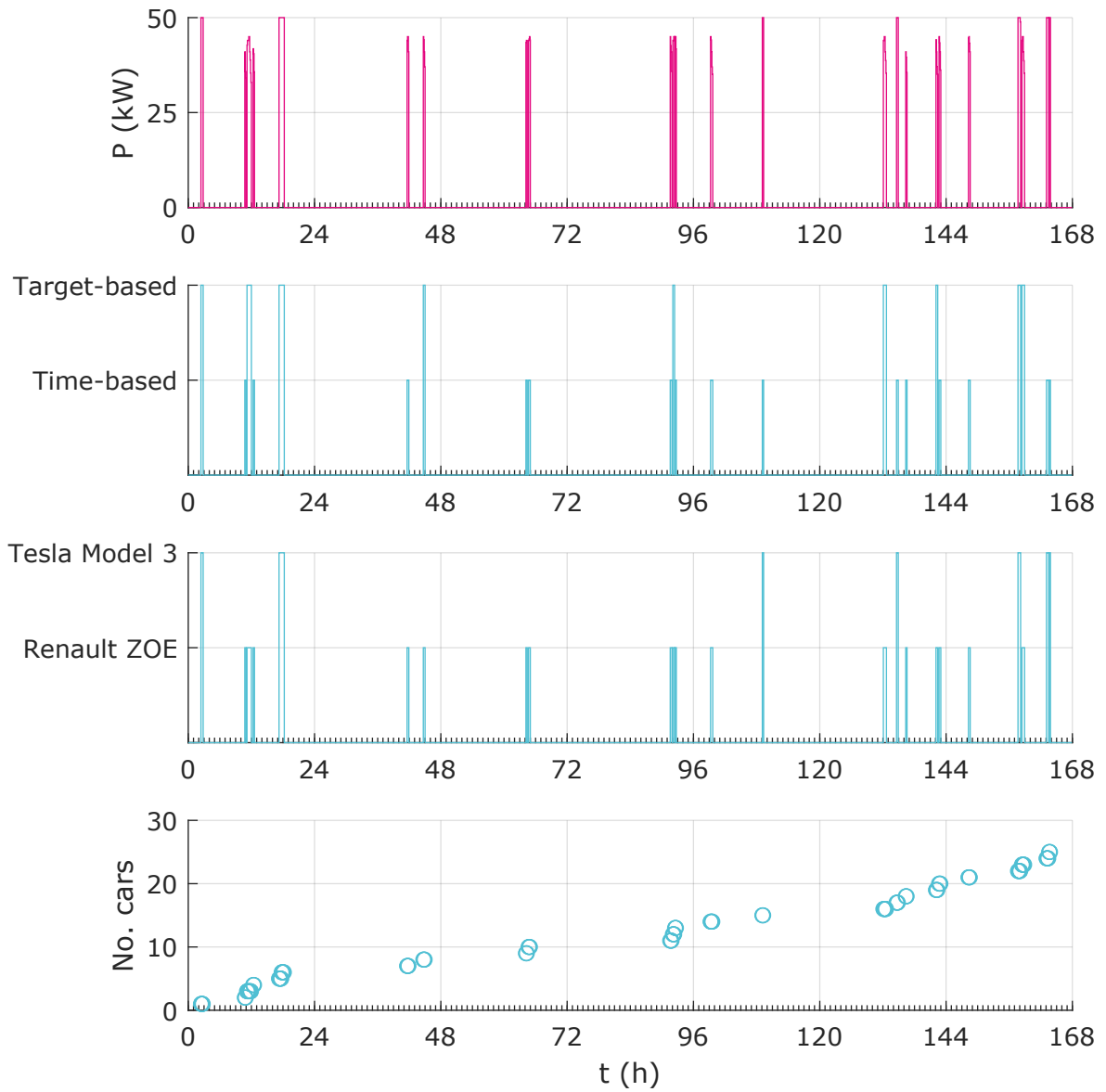**A.4 Synthesised load demand profile and metadata of DC charger in summer**

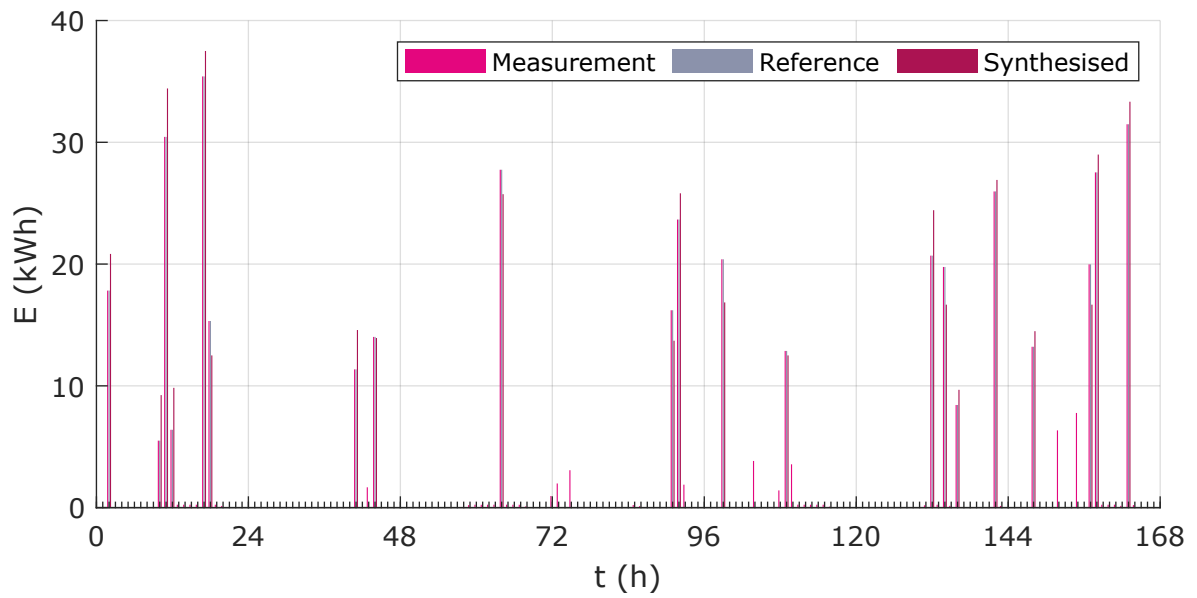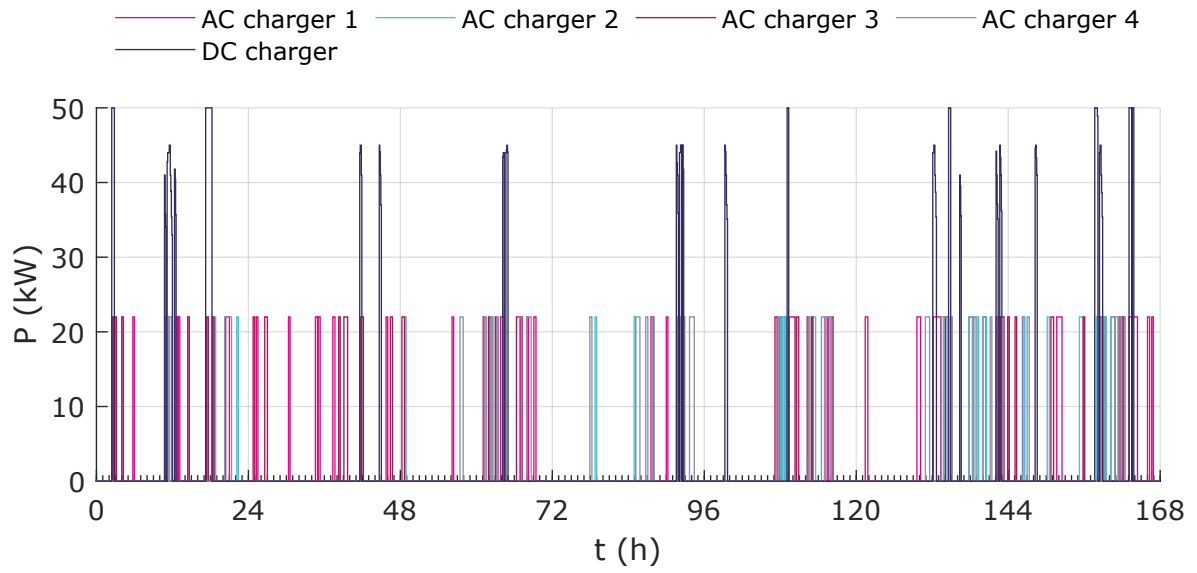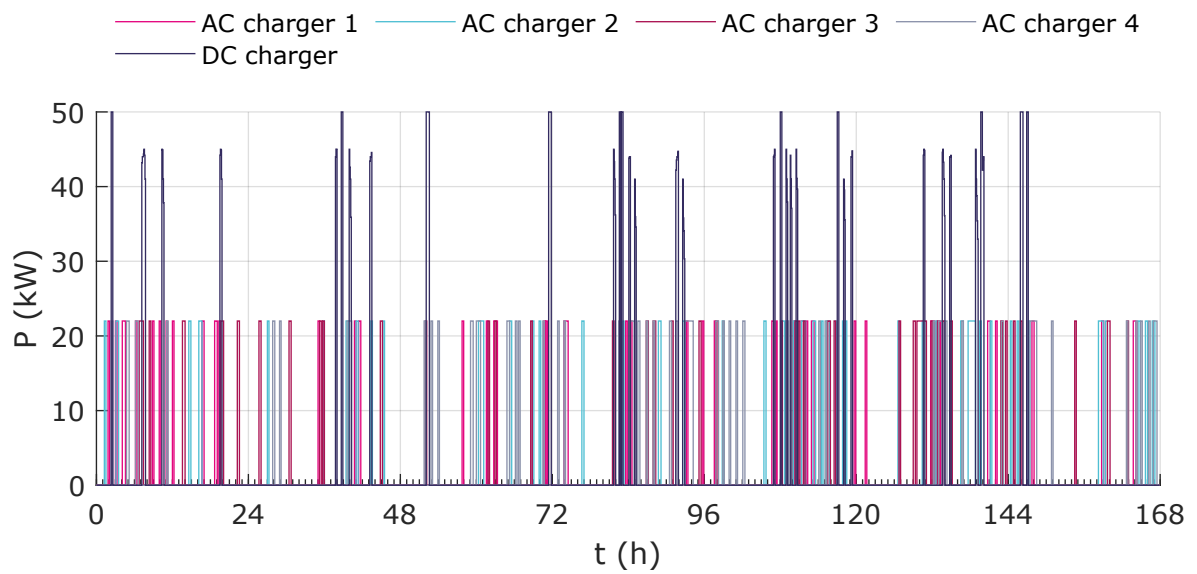Figure A.4: Synthesised load demand profile and metadata of DC charger in summer

Figure A.5: Validation of synthesised DC charger load demand in summer

(a) Summer

(b) Winter

Figure A.6: EV charger load demand profiles

Algorithm A.1: Price-sensitive case 3

```
// Case 3: Only DC charger occupied
```
1 **case** $N_{occ,AC} = 0$ **and** $N_{occ,DC} = 1$ **do**
```
   // BESS control
```
2   **if** $Pr_{NPS} < Pr_{DC}$ **then**
3       $P_{BESS,set} = \max\{-P_{EV,dem}, P_{BESS,dis,avail}, P_{BESS,dis,res}\}$;
4   **else**
5       $P_{BESS,set} = 0$;
6   **end**
```
   // EV charger limitation
```
7   *Calculate* $P_{EV,res}$;
8   **if** $P_{BESS,set} = 0$ **then**
9   *Calculate scaling factor* Pr_{NPS}: $\{Pr_{DC}, 2 \cdot Pr_{DC}\} \mapsto \{1, 0.5\}$;
10      $P_{EV,res} = scaling\ factor \cdot P_{EV,res}$;
11   **end**
12    $P_{DC,set} = OCC_{DC} \cdot LUT\ value \cdot P_{EV,res}$;
13 **end**

Algorithm A.2: Price-sensitive case 4

```
// Case 4: Both AC and DC chargers occupied
```
1 **case** $N_{occ,AC} > 0$ **and** $N_{occ,DC} = 1$ **do**
```
   // BESS control
```
2   **if** $Pr_{NPS} < (Pr_{AC} + Pr_{DC}) \cdot 0.5$ **then**
3       $P_{BESS,set} = \max\{-P_{EV,dem}, P_{BESS,dis,avail}, P_{BESS,dis,res}\}$;
4   **else**
5       $P_{BESS,set} = 0$;
6   **end**
```
   // EV charger limitation
```
7   *Calculate* $P_{EV,res}$;
8   **if** $P_{BESS,set} = 0$ **then**
9   *Calculate scaling factor* Pr_{NPS}: $\{(Pr_{AC} + Pr_{DC}) \cdot 0.5, (Pr_{AC} + Pr_{DC})\} \mapsto \{1, 0.5\}$;
10      $P_{EV,res} = scaling\ factor \cdot P_{EV,res}$;
11   **end**
12   **for** $k = 1$ **to** 4 **do**
13      $P_{AC,set}^{k} = OCC_{AC}^{k} \cdot LUT\ value \cdot P_{EV,res}$;
14   **end**
15    $P_{DC,set} = OCC_{DC} \cdot LUT\ value \cdot P_{EV,res}$;
16 **end**
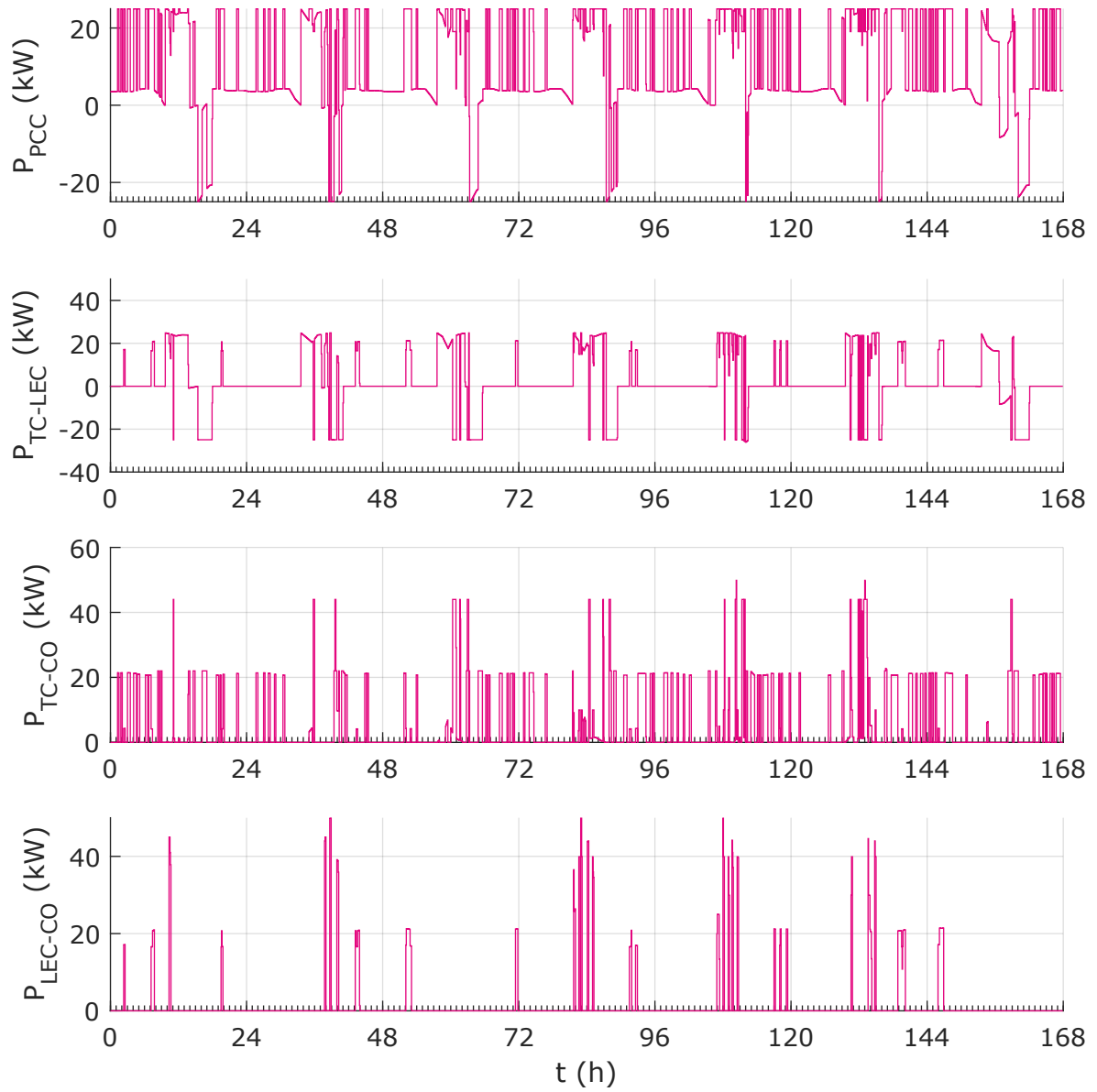
Figure A.7: Power flow at coupling points for baseline strategy in winter
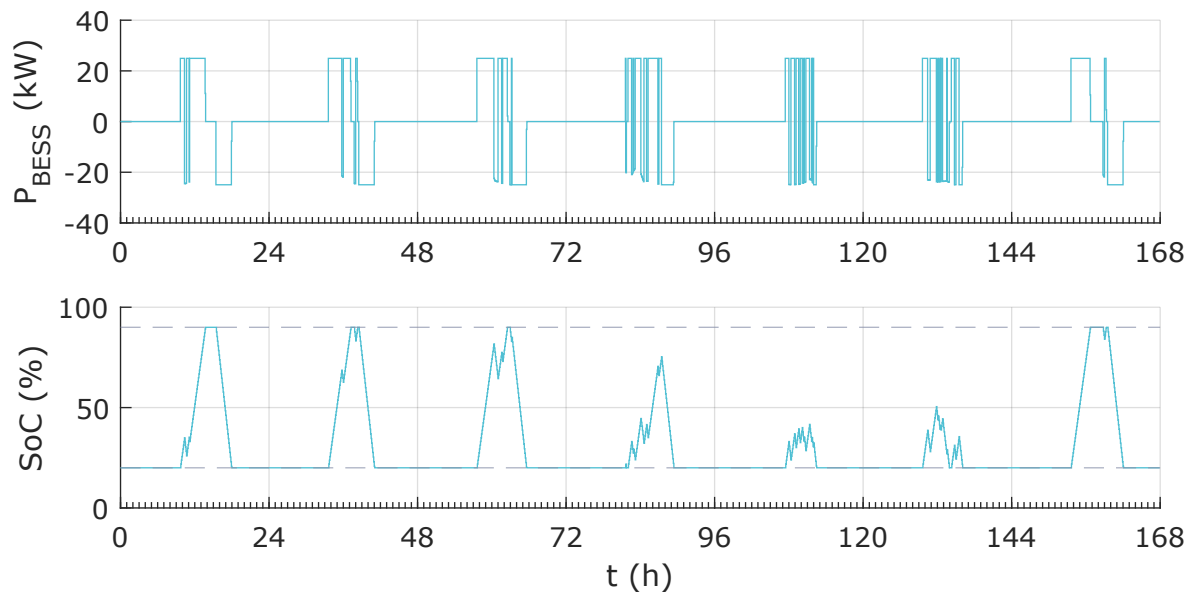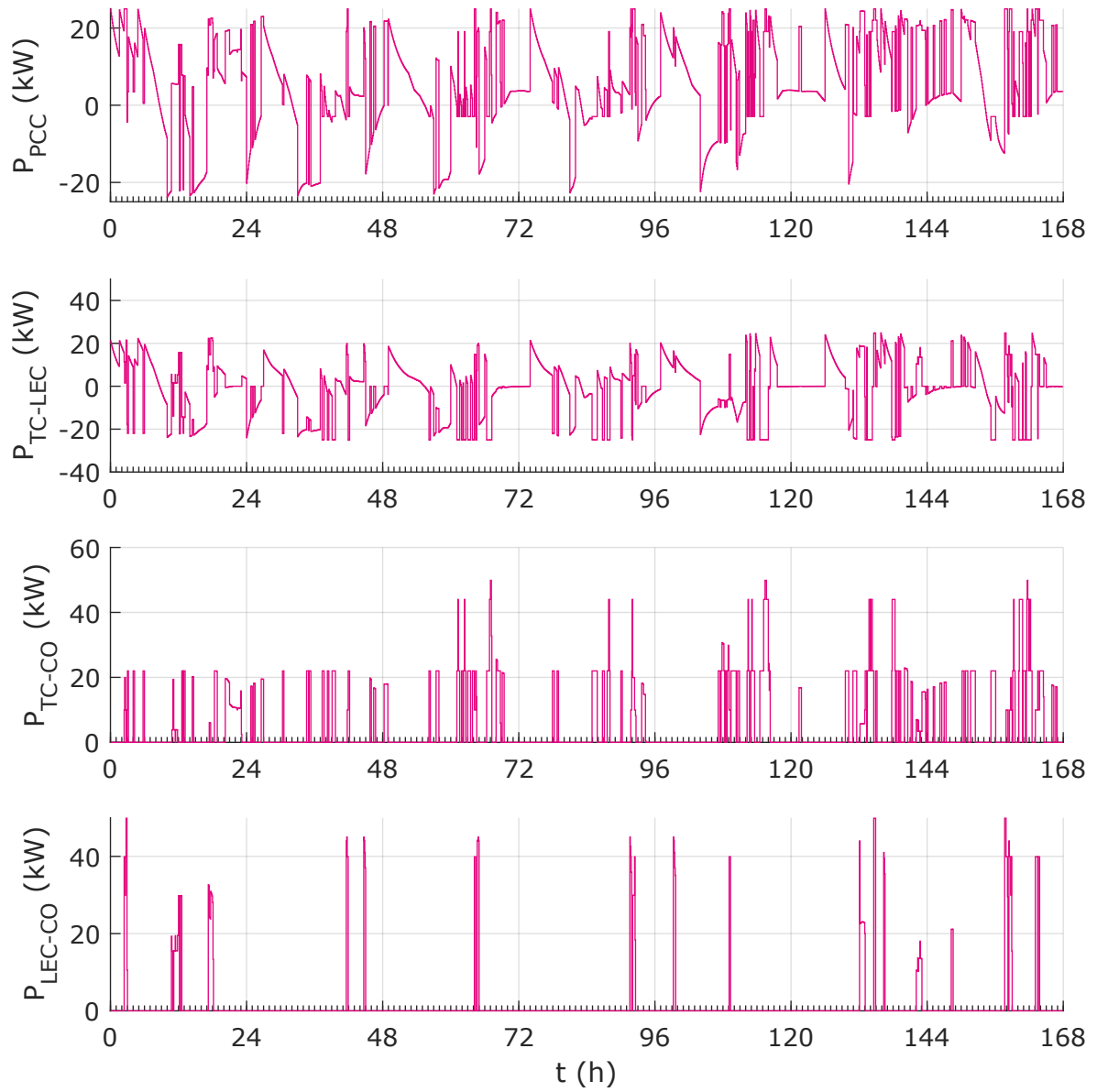
Figure A.8: BESS usage for baseline strategy in winter

Figure A.9: Power flow at coupling points for price-sensitive strategy in summer

Figure A.10: BESS usage for price-sensitive strategy in summer

Figure A.11: Power flow at coupling points for price-sensitive strategy in winter

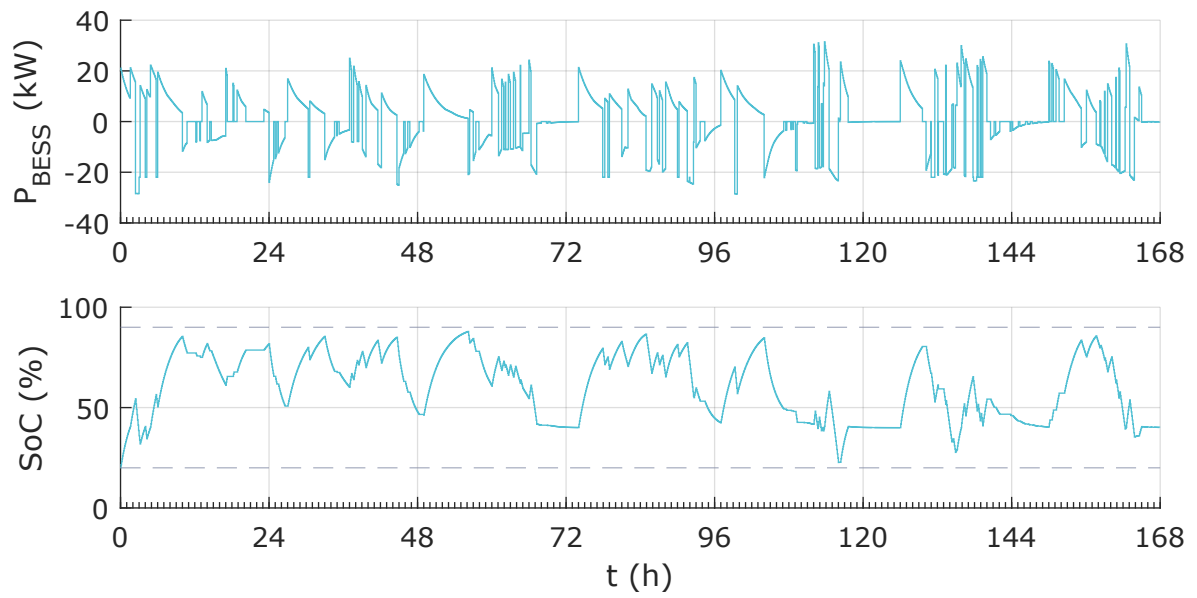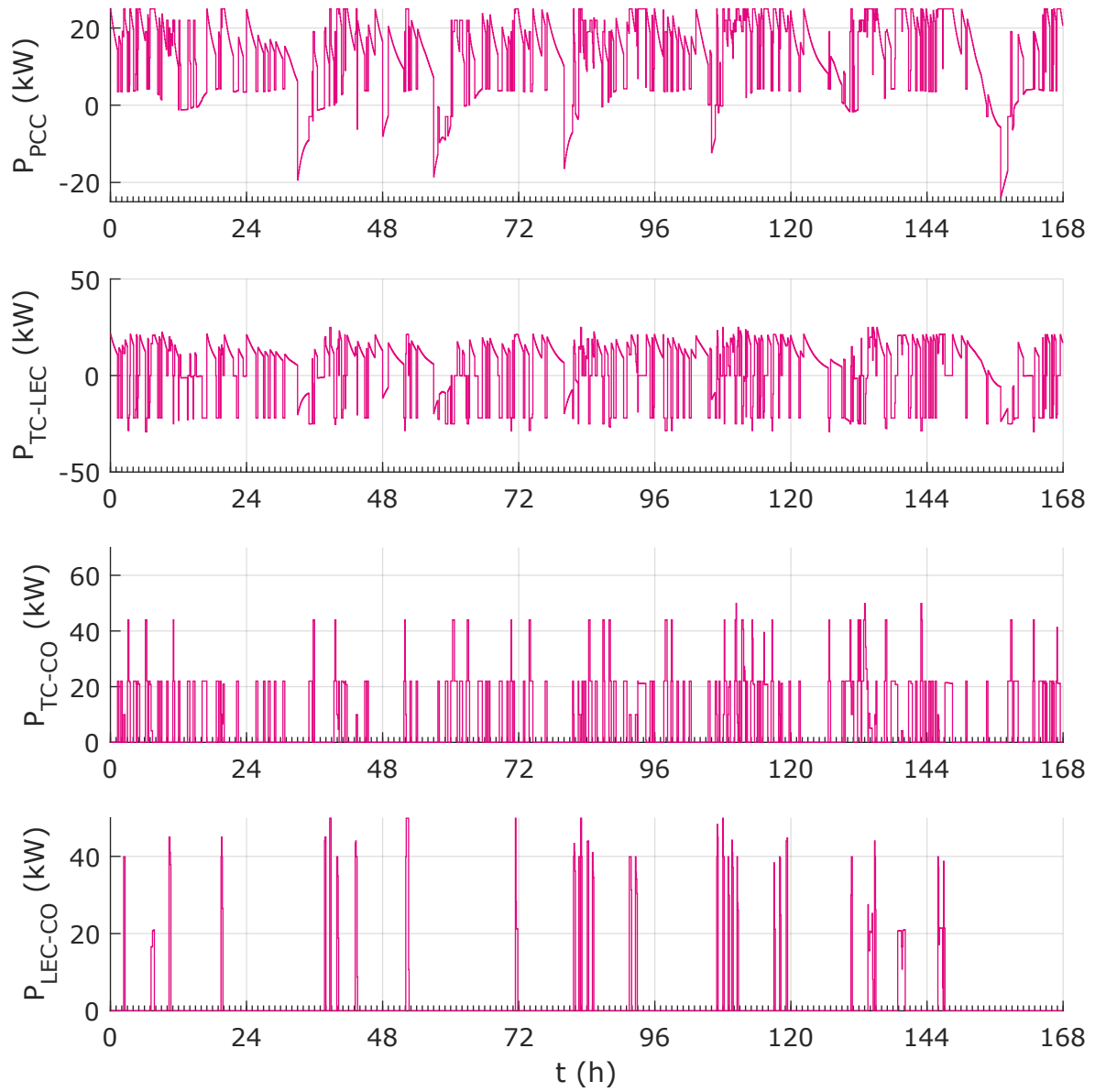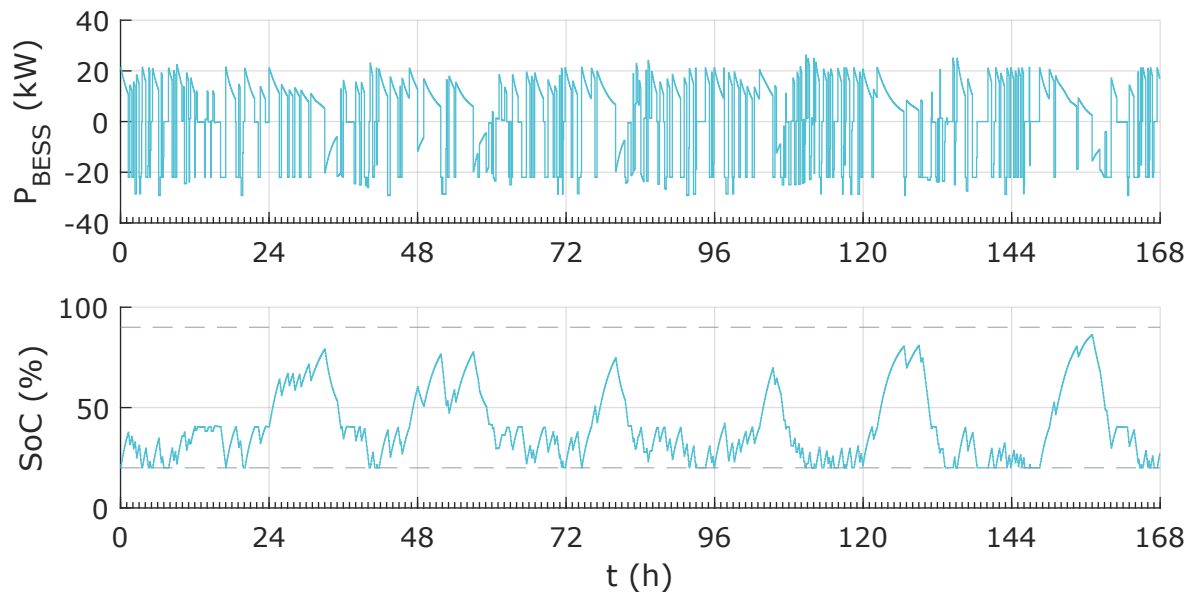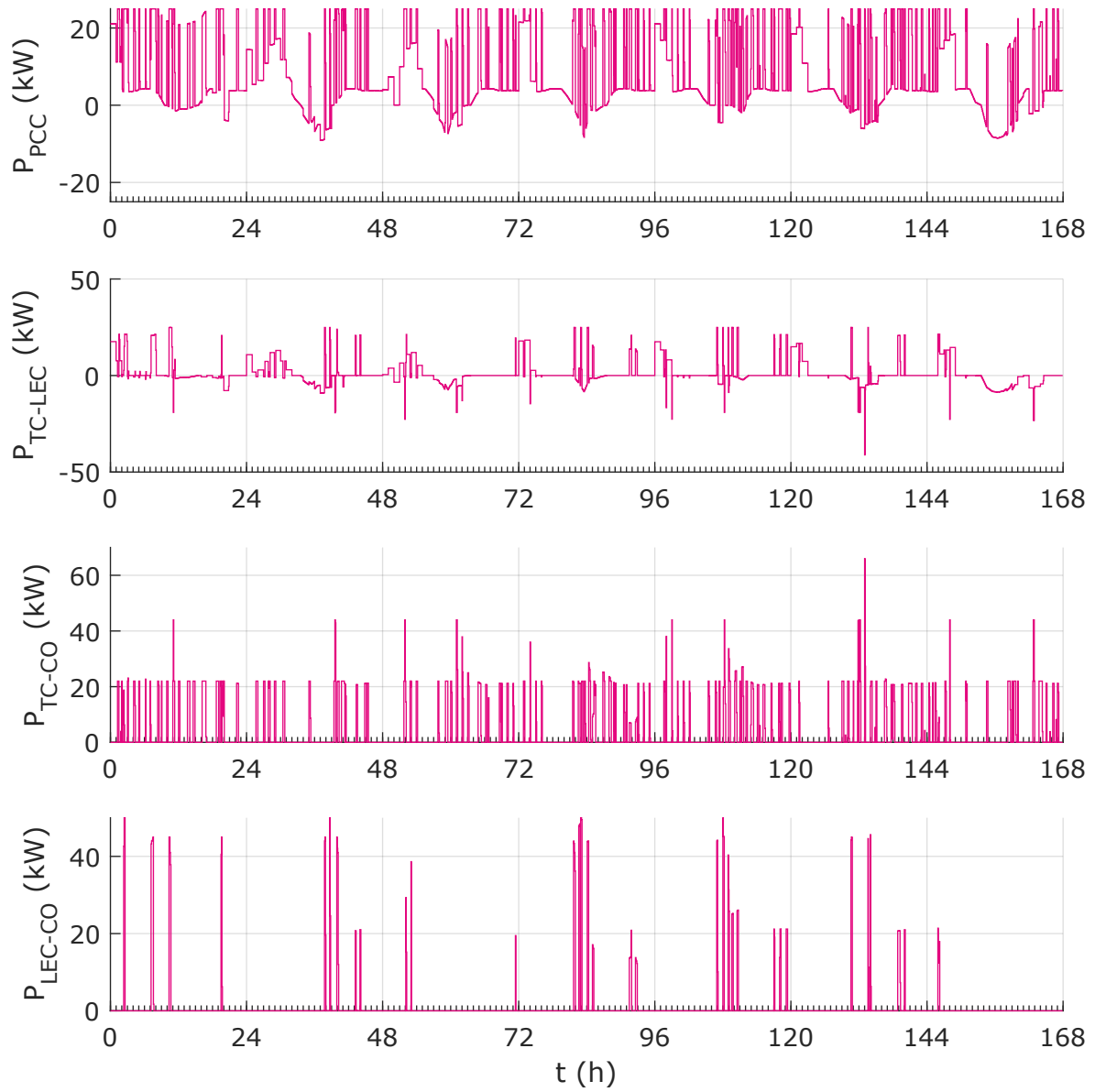Figure A.12: BESS usage for price-sensitive strategy in winter
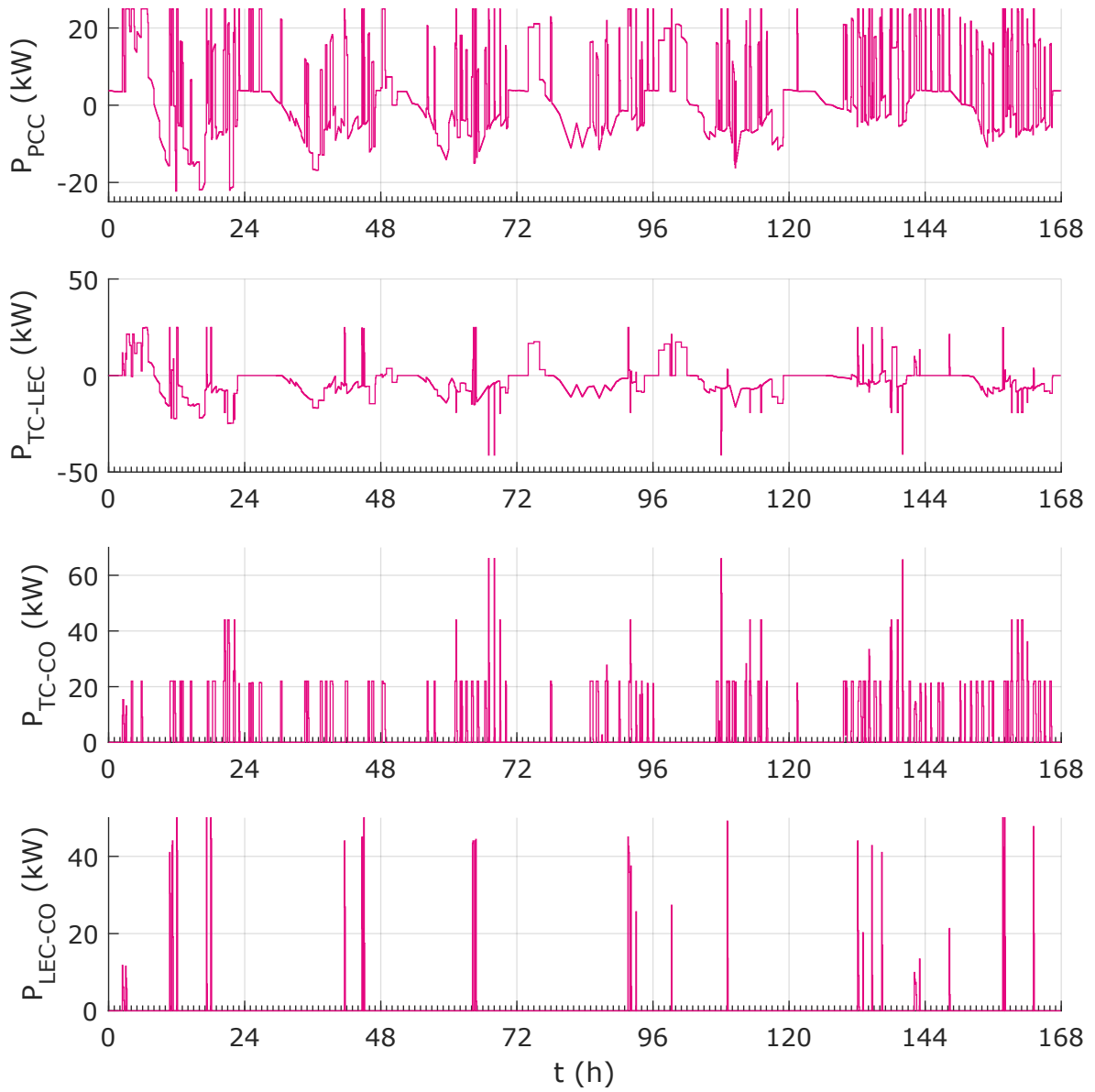
Figure A.13: Power flow at coupling points for scheduling strategy in summer
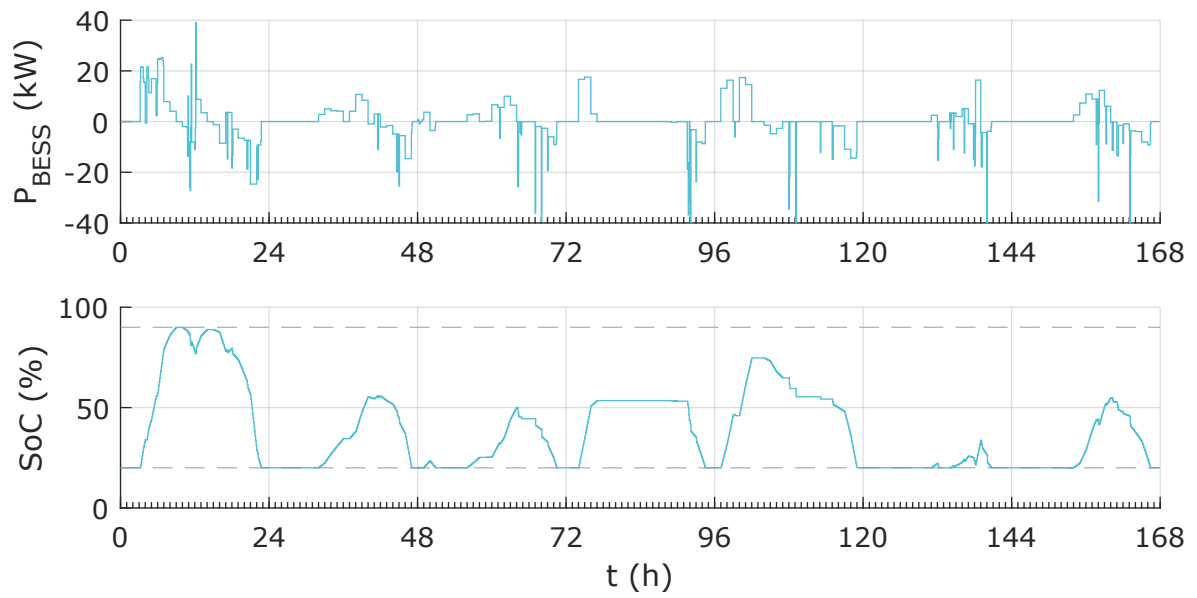
Figure A.14: BESS usage for scheduling strategy in summer

Figure A.15: Power flow at coupling points for scheduling strategy in winter
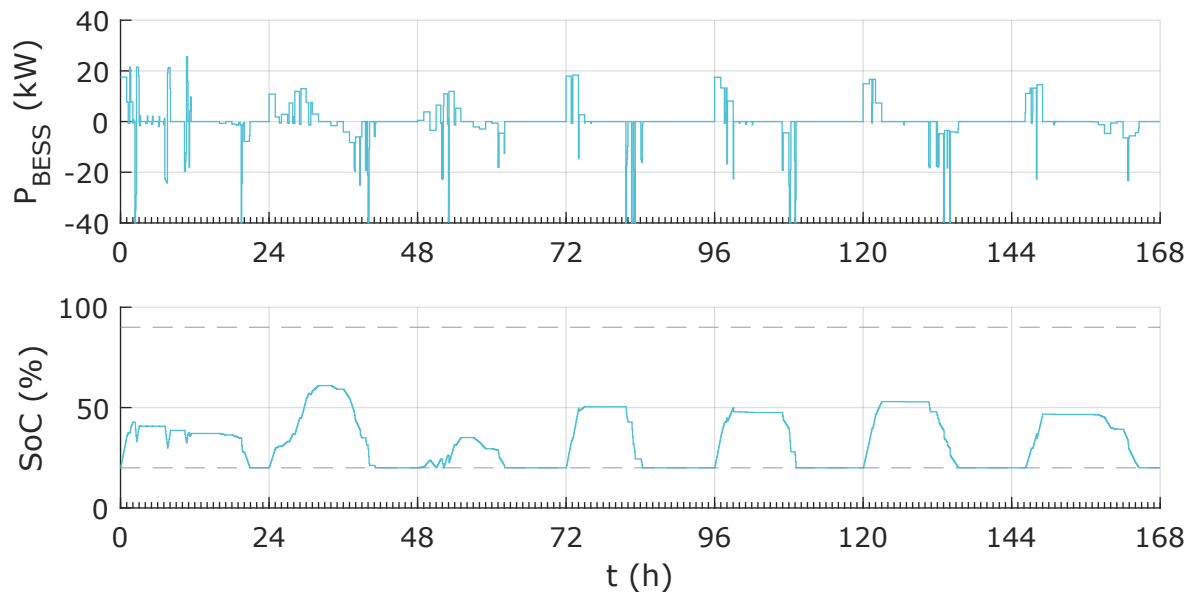
Figure A.16: BESS usage for scheduling strategy in winter

Table A.1: Additional simulation results

Metric	Baseline		Price-sensitive		Scheduling	
	Summer	Winter	Summer	Winter	Summer	Winter
Energy import from main grid (kWh)	1482.70	1988.10	1371.00	2309.60	900.79	1478.70
Energy export to main grid (kWh)	−580.10	−201.93	−443.16	−126.10	−523.24	−105.20
Minimum charging time (h)	58.00	69.67	58.00	69.67	58.00	69.67
Cancelled charging time (h)	1.50	0.83	1.75	0.00	5.83	1.08
Actual charging time (h)	64.00	75.17	63.50	71.67	81.25	82.17
Extended charging time (h)	7.50	6.33	7.25	2.00	29.08	13.58
Cancelled EVs at AC chargers	2/127	2/179	2/127	0/179	10/127	1/179
Cancelled EVs at DC charger	2/ 25	1/ 33	3/ 25	0/ 33	4/ 25	2/ 33